

**NANO-STRUCTURED, DRUG-ELUTING MEDICAL DEVICES FOR  
IMPROVED CLINICAL OUTCOMES**

by  
Kunal S. Parikh

A dissertation submitted to Johns Hopkins University in conformity with the  
requirements for the degree of Doctor of Philosophy

Baltimore, Maryland  
March 2017

© 2017 Kunal S. Parikh  
All Rights Reserved

## Abstract

The biological response to implanted medical devices is critical to the success of surgical procedures. Implantation of foreign devices into the body increases infection risk and may cause inflammation, both of which can result in surgical/device failure. Electrospinning is a promising manufacturing technology due to its capacity to form medical devices composed of nano- and micro-fibers from almost any polymer or polymer/drug combination. This versatility allows for tuning of fiber size and selection of polymer and/or drug to locally modulate the biological response to devices. Here, we investigate the use of electrospinning to manufacture devices with added functionality to improve clinical outcomes.

Although they are associated with vision-threatening eye infections, more than 12 million nylon sutures are used in ocular procedures each year. We demonstrate manufacture, via wet electrospinning, of biocompatible sutures capable of sustained antibiotic release for more than 60 days *in vitro* and activity against *Staphylococcus epidermidis* for at least 1 week *in vitro*.

Next, we engineered a novel system to manufacture and twist together hundreds of drug-loaded nanofibers into a single multifilament suture. To our knowledge, this is the first demonstration of a drug-loaded suture capable of surpassing United States Pharmacopeia strength specifications. Multifilament sutures delivered antibiotic at detectable levels in rat eyes for at least 14 days, and prevented ocular infection against consecutive bacterial inoculations over 1 week in a rat model of bacterial keratitis.

Millions of vascular anastomosis procedures are performed yearly. The inflammatory response to the surgical procedure using sutures leads to neointimal hyperplasia, and resulting vessel stenosis. We demonstrate manufacture of nanofiber-coated sutures capable of sustained anti-proliferative drug release and reduction of neointimal hyperplasia, in comparison to standard nylon sutures, following anastomosis of the rat abdominal aorta.

Finally, we describe the adaptation of our manufacturing platform to glaucoma, which affects over 60 million people, and in which fibrosis is the major cause of surgical treatment failure. We demonstrate manufacture of nano-structured, small lumen glaucoma shunts that are biocompatible and significantly reduce intraocular pressure in normotensive rabbits for at least 27 days. Collectively, these results demonstrate the clinical potential of nano-structured, drug-eluting medical devices.

Advisors: Justin Hanes, Ph.D.; Youseph Yazdi, Ph.D.

Thesis Committee: Justin Hanes, Ph.D.; Youseph Yazdi, Ph.D.; Laura M. Ensign, Ph.D.;  
Peter J. McDonnell, M.D.

## **Acknowledgments**

I am grateful to the many individuals, organizations, and foundations who have supported my doctoral work and provided me with the opportunity to grow as an engineer and as an individual. My PhD tenure has been characterized by unprecedented synchronicity and growth, and my relationships and experiences in Baltimore will continue to influence my life, career, and impact aspirations in the decades to come.

I am particularly thankful to my doctoral advisors, Drs. Justin Hanes and Youseph Yazdi. It is through the Center for Bioengineering Innovation & Design (CBID) that I first learned of the superb biomedical engineering program at Johns Hopkins University, and became compelled to apply. Dr. Yazdi took a chance on me in starting up the CBID PhD program and never wavered in his support of my ambitions, scientific or otherwise. I am honored to have learned the innovation process directly from him, and even more so to have grown in my understanding of what it means to be an engineer and a human being. I will forever treasure our conversations on faith, leadership, innovation, and impact.

I never anticipated that an elevator ride in the Smith Building on the morning of December 4<sup>th</sup>, 2012 would change the course of my PhD, and my career. Since our first encounter on that elevator, Justin has been a tremendous advocate and mentor. I've learned so much simply from being around him and observing the growth of the Center for Nanomedicine. He has constantly encouraged me to think bigger, and always sought to provide me with the resources and experiences to grow my impact. More importantly, he has helped me develop as a scientist capable of critiquing my own research and asking the right questions.



I am grateful to both of them for their confidence and trust, and will seek to pay forward the impact they've had on me.

I am thankful to the additional members of my thesis committee, Drs. Peter McDonnell and Laura Ensign. Dr. McDonnell first identified the need for an antibiotic-eluting suture, which served as the impetus for my doctoral research and has led to additional innovations in vascular and ocular surgery. His insights on the clinical need and translational pathway have been critical to our technology development efforts, and I am grateful for his ardent support and always kind words. Moreover, his leadership, vision, humility, and care for patients sets a high standard for myself and everyone within the Wilmer community. I am grateful to have met Dr. Ensign, a fellow Buckeye, whose life and care for others are both truly inspiring. She has never wavered in her support of our research, or in me, and has been a true advocate in every sense of the word. I will cherish our many interactions and conversations together, and am thankful for her willingness to share her experiences and learnings with me. I consider her a dear friend, mentor, and confidant, and she has my gratitude and help, if she ever needs it, for the remainder of our careers.

I am fortunate to have had tremendous collaborators and partners in innovation in Drs. Ian Pitha, Narutoshi Hibino, and Qingguo Xu. I am grateful for their mentorship, collaboration, and for their continued trust and confidence in me. I admire their motivations, work ethic, and drive to develop better solutions for patients, and hope to continue to work with them in the decades to come.

I am also grateful to my advisors and colleagues within the Center for Nanomedicine (CNM). I am truly privileged to have had the opportunity to work within CNM, and to have had the freedom and resources to invent new technologies with potential for human impact. Almost everyone in the CNM family has helped me in one way or another, but I am particularly grateful to Drs. Himat Patel, Abhijit Date, and Gregg Duncan. Himat has become one of my closest advisors and colleagues who has my utmost trust and respect. Moreover, he and his family have become my Baltimore family. I am grateful to Gregg and Abhijit for being tremendous collaborators and friends. I'm also thankful to Joseph Vargas and Dr. Fareeha Zulfiqar, without whom none of the research in CNM is possible.

I have the utmost appreciation for my team within CNM: Dr. Revaz Omiadze, Aditya Josyula, Richard Shi, Ju Young Ahn, Geoffrey Yoo, Julie Shade, Tom Zhang, and Dr. Takuma Fukunishi. I am grateful to them for their trust in me, for their time, their effort, their enthusiasm, and their sacrifice. My tenure at Johns Hopkins would not have been as fruitful, productive, or enjoyable without them. I am forever indebted to each of them, and will do everything in my power to ensure their success over the remainder of their careers. Thank you.

I'm privileged to have been able to spend my PhD tenure within the Johns Hopkins University ecosystem. The opportunity to work at the intersection of engineering and medicine with some of the brightest minds in the world is one that I truly cherished and did not take lightly. I've learned so much from so many individuals within this community: Drs. Michael Paulaitis, Kannan Rangaramanujam, Seulki Lee, Warren Grayson, Al

Sommer, David Rothstein, Dan Ford, Cinnamon Dornsife, Reza Shadmehr, David Yue, Eliot McVeigh, Soumyadiptya Acharya, Tim Weihs, Kelly Barry, and many more. My career will be more impactful because of my interactions with them. I am particularly grateful to have met David Green and Dr. Eric Rice. Both have treated me as family, candidly shared their own experiences, and have sought to support me in any way possible. They are true role models that have helped shaped me and my future. I'm thankful for my interactions and relationships within The Wilmer Eye Institute with Libby Bell and Drs. Allen Eghrari, David Friedman, Jennifer Thorne, Pradeep Ramulu, Ashvini Reddy, and Amanda Bicket. The Wilmer community has been incredibly welcoming and has taught me so much about ophthalmology and patient care.

I am also grateful to my partners and mentors within the Baltimore community: Amanda Allen, Andrew Rose, Chris Steer, Phil Spector, Rodney Foxworth, Sebastian Segquier, Newt Fowler, JC Weiss, Khoi Le, and Drs. Carrie Nieman and Frank Lin. I am continually inspired by their leadership and drive to create a better Baltimore for all.

I must thank Dr. Gregory Washington who first encouraged me to begin conducting research as a high school senior. He has been a remarkable advocate and advisor ever since. I am also thankful to Dr. David Tomasko who has advocated for me since my earliest days at The Ohio State University and is always willing to help me think through my next steps. I am eternally grateful to Dr. Jessica Winter who afforded me the opportunity to grow as both a researcher and entrepreneur as an undergraduate. I'm also appreciative of Dr. Jed Johnson, who trained me in the art of electrospinning as an undergraduate and has given

me advice on everything from vascular graft fabrication to company formation. I'm thankful for the continued friendship and partnership of Dr. Gang Ruan.

Finally, I would like to thank my family, Sailesh, Sonal, Paras, and Meghi Parikh. My father gave me my faith and taught me what it meant to work hard. My mother has sacrificed so much for our family and taught me to stand up for myself. My brother made sure I never deviated from the right path, and collectively, they taught me the importance of being a good person above all else. I have the utmost respect, gratitude, and admiration for my uncle, Girish Parikh, who first came to the United States in 1960. Without him, I would not have had the freedom or opportunities I'm so grateful for.

I must also thank Michelle and Clarice Smith, and the Robert H. Smith Family Foundation. Their generous donation provided my team with the resources to develop the technologies described in this dissertation. They are a terrific example of the power of philanthropy, and have allowed me to pursue ideas and lines of research that otherwise would not have been possible. I'm thankful to the National Science Foundation whose fellowship allowed me to be independent and pursue my own ideas and hypotheses. I'm grateful to the Roche Foundation and the Metro Washington Chapter of the ARCS Foundation. Their funding has allowed me to invest in my own personal development, and to explore translation of the technologies described within this dissertation. I am particularly grateful to the women of the ARCS Foundation for their unwavering support and kind words. I'm also appreciative of Thomas and Mary Kelly, whose award welcomed me to the Johns Hopkins community and who individually set a terrific example for young scientists.

# Table of Contents

<b>Abstract.....</b>	<b>ii</b>
<b>Acknowledgments .....</b>	<b>iv</b>
<b>List of Tables .....</b>	<b>xiii</b>
<b>List of Figures.....</b>	<b>xiv</b>
<b>1. Introduction.....</b>	<b>1</b>
<b>2. Development of absorbable, antibiotic-eluting sutures for ophthalmic surgery.....</b>	<b>7</b>
<b>2.1. Introduction.....</b>	<b>7</b>
<b>2.2. Materials and Methods.....</b>	<b>9</b>
2.2.1. <i>Microfiber Suture Fabrication</i> .....	9
2.2.2. <i>Suture Characterization</i> .....	10
2.2.2.1. <i>Suture Size and Morphology</i> .....	10
2.2.2.2. <i>Tensile Strength Measurement</i> .....	10
2.2.3. <i>In Vitro Drug Release</i> .....	10
2.2.4. <i>Assessment of Bacterial Inhibition</i> .....	11
2.2.5. <i>Assessment of In Vivo Biocompatibility</i> .....	11
2.2.6. <i>Statistical Analysis</i> .....	12
<b>2.3. Results .....</b>	<b>12</b>
2.3.1. <i>Suture Fabrication and Characterization</i> .....	12
2.3.2. <i>In Vitro Levofloxacin Release</i> .....	13
2.3.3. <i>Inhibition of S. Epidermidis</i> .....	14
2.3.4. <i>In Vivo Performance and Biocompatibility</i> .....	14

<b>2.4. Discussion.....</b>	<b>15</b>
<b>2.5. Conclusion .....</b>	<b>18</b>
<b>3. Ultra-thin, high strength, antibiotic-eluting sutures for prevention of ophthalmic infection.....</b>	<b>24</b>
<b>3.1. Introduction.....</b>	<b>24</b>
<b>3.2. Materials and Methods.....</b>	<b>27</b>
3.2.1. <i>Suture Manufacture .....</i>	27
3.2.2. <i>Suture Characterization .....</i>	28
3.2.2.1. <i>Suture Size .....</i>	28
3.2.2.2. <i>Suture Morphology.....</i>	28
3.2.2.3. <i>Suture Breaking Strength.....</i>	28
3.2.2.4. <i>Suture Strength Retention.....</i>	28
3.2.2.5. <i>Suture Drug Loading.....</i>	29
3.2.3. <i>Animal Studies .....</i>	29
3.2.3.1. <i>In Vivo Biocompatibility.....</i>	29
3.2.3.2. <i>Pharmacokinetic Study.....</i>	30
3.2.3.3. <i>Bacterial Inoculation and Evaluation .....</i>	31
3.2.4. <i>Statistical Analysis.....</i>	32
<b>3.3. Results .....</b>	<b>33</b>
3.3.1. <i>Suture Manufacture and Characterization.....</i>	33
3.3.2. <i>Suture Breaking Strength.....</i>	34
3.3.3. <i>In Vivo Suture Biocompatibility .....</i>	36
3.3.4. <i>Pharmacokinetics of Levofloxacin Delivered from Sutures .....</i>	37

3.3.5. <i>Prevention of Ophthalmic Infection</i> .....	37
<b>3.4. Discussion</b> .....	<b>40</b>
<b>3.5. Conclusion</b> .....	<b>43</b>
<b>4. Rapamycin-eluting, nanofiber-coated sutures for inhibition of neointimal hyperplasia following vascular anastomosis procedures</b> .....	<b>50</b>
<b>4.1. Introduction</b> .....	<b>50</b>
<b>4.2. Materials and Methods</b> .....	<b>53</b>
4.2.1. <i>Suture Fabrication</i> .....	53
4.2.2. <i>Suture Characterization</i> .....	54
4.2.2.1. <i>Suture Size</i> .....	54
4.2.2.2. <i>Suture Morphology</i> .....	54
4.2.2.3. <i>In Vitro Drug Release</i> .....	54
4.2.2.4. <i>Suture Breaking Strength</i> .....	55
4.2.3. <i>Animal Studies</i> .....	55
4.2.3.1. <i>Evaluation of neointimal hyperplasia</i> .....	56
4.2.4. <i>Statistical Analysis</i> .....	56
<b>4.3. Results</b> .....	<b>57</b>
4.3.1. <i>Fabrication and Characterization of Nanofiber-coated Sutures</i> .....	57
4.3.2. <i>In Vitro Release of Rapamycin from Nanofiber-coated Sutures</i> .....	58
4.3.3. <i>Nanofiber-coated Suture Breaking Strength</i> .....	59
4.3.4. <i>Effect of Rapamycin Nanofiber Coating on Post-operative Neointimal Hyperplasia</i> .....	59
<b>4.4. Discussion</b> .....	<b>61</b>

4.5. Conclusion .....	63
<b>5. Reduction of intraocular pressure in rabbits via a nano-structured glaucoma drainage implant .....</b>	<b>70</b>
<b>5.1. Introduction.....</b>	<b>70</b>
<b>5.2. Materials and Methods.....</b>	<b>73</b>
5.2.1. <i>Simulation of Flow through Shunt.....</i>	73
5.2.2. <i>Electrospun Shunt Manufacture .....</i>	73
5.2.3. <i>Shunt Characterization.....</i>	74
5.2.4. <i>Evaluation of In Vitro Fluid Flow through Shunt .....</i>	74
5.2.5. <i>In Vivo Performance and IOP Measurement .....</i>	75
5.2.6. <i>Assessment of In Vivo Biocompatibility.....</i>	76
5.2.7. <i>Statistical Analysis.....</i>	76
<b>5.3. Results .....</b>	<b>77</b>
5.3.1. <i>Simulated Pressure Change.....</i>	77
5.3.2. <i>Shunt Fabrication and Characterization.....</i>	77
5.3.3. <i>In Vitro Performance and Flow through Shunt.....</i>	78
5.3.4. <i>IOP Reduction .....</i>	79
5.3.5. <i>In Vivo Biocompatibility.....</i>	80
<b>5.4. Discussion.....</b>	<b>80</b>
<b>5.5. Conclusion .....</b>	<b>84</b>
<b>6. Summary.....</b>	<b>91</b>
<b>References .....</b>	<b>94</b>
<b>Curriculum Vitae .....</b>	<b>115</b>



## **List of Tables**

**Table 2.1. United States Pharmacopeia specifications for absorbable sutures. .... 19**

**Table 3.1. Levofloxacin concentration in rat corneal tissue and aqueous humor. ... 47**

## List of Figures

Figure 2.1. Wet electrospinning setup and microfiber suture SEM.....	20
Figure 2.2. Suture diameter, tensile strength, and <i>in vitro</i> drug release.....	21
Figure 2.3. <i>In vitro</i> bacterial inhibition. ....	22
Figure 2.4. Histological analysis of suture biocompatibility. ....	23
Figure 3.1. Manufacture of drug-eluting, multifilament sutures. ....	44
Figure 3.2. Breaking strength of PCL sutures in reference to U.S.P. specifications.	45
Figure 3.3. Histological analysis of suture biocompatibility. ....	46
Figure 3.4. Evaluation of ophthalmic infection 2 days after inoculation of <i>S. aureus</i> . .....	48
Figure 3.5. Evaluation of ophthalmic infection following consecutive <i>S. aureus</i> inoculations over the period of 1 week.....	49
Figure 4.1. Manufacturing schematic and SEM images of nanofiber-coated sutures. .....	65
Figure 4.2. Cumulative <i>in vitro</i> release of rapamycin.....	67
Figure 4.3. Breaking strength of nanofiber-coated nylon sutures in reference to U.S.P. specifications. ....	68
Figure 4.4. Evaluation of neointimal hyperplasia following vascular anastomosis..	69
Figure 5.1. Model of pressure change through shunt.....	85
Figure 5.2. Manufacturing system and shunt design.....	86
Figure 5.3. PET shunt characterization.....	87
Figure 5.4. Theoretical and experimental pressure differential with flow of PBS through shunt. ....	88

<b>Figure 5.5. IOP measurements in rabbits following implantation of either closed or open PET shunts. ....</b>	<b>89</b>
<b>Figure 5.6. Glaucoma shunt biocompatibility. ....</b>	<b>90</b>

## 1. Introduction

Drug delivery systems (DDS) capable of local and sustained release provide significant advantages in the treatment of disease.<sup>1</sup> Localized drug delivery has the potential to improve treatment efficacy through site-specific administration, while simultaneously requiring a lower dose of drug, and reducing systemic side-effects.<sup>2</sup> Sustained drug release may preclude issues with medication adherence and patient compliance, and minimize complications by limiting the number of invasive procedures or injections.<sup>1,3</sup> Despite these advantages, FDA approval and successful commercialization of DDS is a lengthy and capital-intensive process, and remains a major challenge.<sup>1,4</sup> Drug-eluting devices are a sub-category of DDS with reduced commercial risk, as they are often regulated as medical devices with a shorter development timeline and approval process than drug products.<sup>4</sup> Thus, medical devices providing local drug delivery in a sustained manner provide a promising avenue for improvement of clinical outcomes across a wide range of surgical procedures and in the treatment of a variety of diseases. As more therapies utilize devices during surgery or indicate implantable devices for treatment, incorporating drug delivery functionality can provide significant additional benefit.<sup>4</sup> Drug-eluting devices can improve patient care through ease of use and therapy compliance, deliver drug locally to eliminate the side-effects and risks of systemic exposure, and/or improve the safety and effectiveness of an existing device or surgical procedure by modulating the local biological response to reduce complications and the need for re-interventions. In the latter case, regulatory approval follows a medical device pathway with the existing device as the predicate.<sup>4</sup> In order to achieve successful clinical translation, drug-eluting devices must be biocompatible, stable for the duration of use, cost-effective, and under ideal circumstances,

are composed of generally regarded as safe (GRAS) materials, deliver a drug already approved for the intended application, fit into the surgical workflow, do not require additional maintenance or removal, and are reimbursable.<sup>1,4,5</sup>

Electrospinning is a promising platform for the manufacture of drug-eluting medical devices. Electrospinning is compatible with almost any natural or synthetic polymer, can incorporate prophylactic or therapeutic moieties, and be realized into a wide range of different morphologies or conformations.<sup>6,7</sup> Devices manufactured via electrospinning are also highly modifiable through coatings, laser cutting, and other processing modifications to tune each aspect of the device, including size, shape, strength, rigidity, porosity, degradability, glidability, and biocompatibility. Moreover, the capacity of electrospinning to produce nanofibers and incorporate them into a medical device provides a substantial advantage. Kam and coworkers have demonstrated that nanoscale features with high aspect ratios decrease expression of growth factors associated with fibrosis.<sup>8</sup> They also showed that these features can reduce protein adsorption which has been implicated in device fouling and can lead to infection or device failure.<sup>9</sup> Here, we describe the use of electrospinning to manufacture medical devices with potential to improve clinical outcomes via nanotopography and/or local drug delivery.

Sutures are used ubiquitously in colon and rectal, general, neurological, obstetrics and gynecological, ocular, oral and maxillofacial, orthopedic, otolaryngological, plastic, thoracic and cardiovascular, and urological surgery.<sup>10</sup> The almost universal use of sutures at the surgical site makes them well-situated for therapeutic, prophylactic, and/or wound

healing interventions. However, attempts to develop drug-eluting sutures have been limited primarily by a lack of sufficient tensile strength.<sup>7,11-22</sup> Drug-coated sutures have been developed to circumvent these shortcomings, but are limited in their capacity to load sufficient drug, control drug release, and/or scale manufacturing.<sup>14,17,23-27</sup> Without the ability to deliver drug in a controlled manner, drug-coated sutures are limited to use in anti-infection applications in general surgery, and to date, there are no market offerings for drug-eluting sutures in ocular or vascular surgery.

Although conventional nylon sutures are associated with vision-threatening microbial keratitis and endophthalmitis, they are used in closure of 2 million corneal wounds per year in the United States, and in more than 12 million ocular procedures per year globally.<sup>28-30</sup> For this reason, it has become routine to prescribe expensive antibiotic drops off-label for prophylactic use after ocular surgery; however, topical eye drops are associated with poor patient compliance.<sup>31</sup> Additionally, properly instilling eye drops is particularly difficult for pediatric patients and for those who are elderly and/or in cognitive decline.<sup>32,33</sup> A potential alternative to frequent topical application is through antibiotic delivery from the surgical suture itself. For this purpose, the suture must: (i) be of suitable size for ocular surgery, (ii) be of high-strength to resist breakage and bacterial colonization, and (iii) provide sustained antibiotic delivery. Chapter 2 describes the manufacture, via wet electrospinning, and evaluation of an absorbable, antibiotic-eluting, monofilament suture for ocular surgery. Chapter 3 details the development of a novel manufacturing process for production of multifilament, ophthalmic-grade, antibiotic-eluting sutures with improved mechanical

properties. Chapter 3 also describes the use of these sutures to prevent infection within a rat model of bacterial keratitis.

Millions of anastomoses, or surgical connections between arteries or veins, are performed in vascular bypass, vascular access, solid organ transplant, and reconstruction procedures each year in the United States.<sup>34</sup> Neointimal hyperplasia, or proliferation and migration of vascular smooth muscles cells into the vessel lumen space, develops immediately post-operatively at the anastomotic site due to the damage and resulting inflammation caused by surgical closure of the anastomosis using sutures.<sup>35</sup> The resulting stenosis, or narrowing of the vessel after the anastomosis, is the main contributor to arterial, venous, and arteriovenous graft failure.<sup>36-40</sup> Depending on the type of procedure, failure rates due to neointimal hyperplasia have been reported up to 50%.<sup>41</sup> Thus, preventing anastomotic stenosis is the key to long-term efficacy of all types of vessel anastomoses. We hypothesized that a drug-coated suture could modulate the post-operative inflammatory response to reduce neointimal hyperplasia while also providing sufficient strength for an extended period of time to allow for sufficient wound healing. Chapter 4 describes the use of the novel manufacturing process detailed in Chapter 3 to uniformly coat a conventional nylon suture with degradable, drug-loaded nanofibers. Chapter 4 also details the use of these nanofiber-coated sutures in a rat model of vascular anastomosis.

We also hypothesized that the novel manufacturing platform described in Chapter 3 could be extended to the manufacture of a broad range of medical devices to improve outcomes in a variety of surgical interventions. Glaucoma is a leading cause of irreversible vision

loss that affected over 60 million people in 2010.<sup>42,43</sup> It is known that intraocular pressure (IOP) reduction prevents development of glaucoma and vision loss from glaucoma.<sup>44,45</sup> While surgery lowers IOP more effectively than eye drop treatment, it is associated with reduced visual acuity, increased cataract formation, and perioperative complications such as hyphema, ptosis, and hypotony (IOP that is too low), which each occur in approximately 10% of cases.<sup>46</sup> Glaucoma surgeries create a vent for fluid to be released from the eye. This vent is either fashioned from the wall of the eye (trabeculectomy) or is created by a glaucoma drainage implant (GDI). These surgeries lose efficacy over time, and the five-year failure rates for trabeculectomy or the Ahmed and Baerveldt<sup>®</sup> GDIs are 25.7%, 39.5%, and 44.7%, respectively.<sup>47,48</sup> The majority of surgical failures occur as a result of scar tissue and fibrosis around the vent following surgery.<sup>49</sup> Alternatively, the surgery can vent pressure too well, thereby causing low IOPs. Hypotony can occur after trabeculectomy (up to 18%) as well as following insertion of GDIs such as the Ahmed or Baerveldt<sup>®</sup>.<sup>47,50,51</sup> Thus, glaucoma surgery would be significantly improved by creating a venting system that both minimizes the fibrotic response and decreases the risk of post-operative hypotony. Chapter 5 describes the adaptation of our novel manufacturing system for production of nano-structured glaucoma shunts, and the evaluation of a non-absorbable, small-lumen glaucoma shunt in a normotensive rabbit model.

Medical devices are used in almost every surgical procedure, and additional functionality via nanotopography and/or local drug delivery can serve to improve therapeutic efficacy and/or reduce complications following surgical intervention. The manufacturing platform described in Chapters 3-5 can be used to provide controlled drug release functionality to



medical devices through direct loading and/or via coating. Moreover, this technology can be implemented within the current surgical workflow, preclude issues with patient compliance, and incorporate a broad range of drugs for a multitude of clinical applications. In total, the results presented here could directly impact the lives of more than 80 million individuals globally.

## **2. Development of absorbable, antibiotic-eluting sutures for ophthalmic surgery**

**Note:** This chapter has been published in *Translational Vision & Science Technology* in which Fabiana Kashiwabuchi and Kunal Parikh are co-first authors.

### **2.1. Introduction**

Interest in the development of drug-eluting sutures for a variety of clinical applications has grown over the past decade.<sup>12,17,52</sup> Drug-eluting sutures may prevent complications and/or serve in a therapeutic role while simultaneously closing wounds and holding tissue together.<sup>53</sup> Sutures are already a part of the surgical workflow, and this next generation of sutures could provide for additional functionality through local and sustained drug release.<sup>12</sup> However, attempts to develop drug-eluting sutures have been limited by lack of sufficient tensile strength, sustained drug release, or scale needed for commercial viability.<sup>7,11-22</sup> Furthermore, drug-eluting sutures thin enough to be used in ophthalmic surgery have not been described in the literature (**Table 2.1.**), where, globally, more than 12 million procedures per year use nylon sutures to close ocular wounds and incisions.<sup>30,54-57</sup> In 2002, Ethicon received approval to market a series of antibiotic-coated sutures; however, none are indicated for ophthalmic use and, to date, there are no market offerings for antibiotic-eluting sutures for ocular surgery.<sup>27,58-60</sup>

Although infections of the eye, such as bacterial keratitis and endophthalmitis, are rare, they can lead to significant negative consequences including corneal ulceration, edema, inflammation, and blindness.<sup>61</sup> It has long been reported that the placement of foreign material into the body reduces the inoculum size of bacteria required for infection, and that the conventional nylon sutures used in ocular procedures can harbor bacteria and potentially facilitate infection.<sup>28,62</sup> This phenomenon is further exacerbated when sutures become loose or break *in situ*. Heaven and coworkers reported that almost 40% of loose or broken nylon corneal sutures were contaminated with bacteria, and *Staphylococcus epidermidis* (*S. epidermidis*) was isolated in more than 80% of cases.<sup>29</sup> For this reason, it has become routine to prescribe expensive antibiotic drops off-label for prophylactic use after ophthalmic surgery; however, topical eye drops are associated with low patient compliance.<sup>31</sup> Additionally, properly instilling eye drops is particularly difficult for pediatric patients and for those who are elderly and/or in cognitive decline.<sup>32,33</sup> A potential alternative to frequent topical application would be to supply antibiotics directly from the surgical suture itself. For this purpose, the suture must: (i) be of suitable size, (ii) be of high-strength to resist breakage and bacterial colonization, and (iii) provide sustained antibiotic delivery. Such a suture might prevent ocular infections while providing convenience for both the patient and the surgeon.

Here, we describe the development of an absorbable suture loaded with levofloxacin, a third-generation fluoroquinolone and broad spectrum antibiotic used to treat ocular infection.<sup>63,64</sup> The suture was manufactured via electrospinning, a simple technique first introduced in the early 1900's that employs electric forces to elongate and simultaneously

decrease the diameter of a viscoelastic polymer stream, allowing for the formation of solid fibers ranging from nanometers to microns in diameter.<sup>6,65</sup> Electrospinning provides a scalable and versatile platform, allowing for the incorporation of almost any polymer, such as the poly(L-lactide) (PLLA) and polyethylene glycol (PEG) used in this work. Both of these polymers are generally regarded as safe (GRAS) and have been used in medical devices approved by the United States Food and Drug Administration.<sup>66</sup> We investigate the size, strength, drug release, bacterial inhibition, and biocompatibility of this new platform.

## **2.2. Materials and Methods**

### *2.2.1. Microfiber Suture Fabrication*

Levofloxacin microfiber sutures were manufactured using the wet electrospinning setup depicted in **Figure 2.1.A** and described by Zhang and coworkers.<sup>67</sup> Briefly, PLLA (221 kDa; Corbion, Amsterdam, Netherlands) at 86-89% (w/w) was mixed with levofloxacin (Sigma Aldrich, St. Louis, MO) at 10 wt% and either PEG (35 kDa, Sigma Aldrich) or Pluronic F127 (BASF, Florham Park, NJ) between 1-4 wt% and dissolved in chloroform (Sigma Aldrich) at room temperature for 24 h. Levofloxacin concentration was held constant and PLLA concentration in chloroform was maintained at 15 wt% in all formulations. Sutures were produced by wet electrospinning the polymer/drug solution in a setup consisting of a high voltage power supply (Gamma High Voltage Research, Ormond Beach, FL), syringe pump (Fisher Scientific, Waltham, MA), and rotating metal collector with hexane (Sigma Aldrich) as the landing solvent. The polymer solution was ejected through a blunted 18G needle (Fisher Scientific) at 13 mL/h with 4.7 kV of applied

voltage 5 cm away from the collector rotating at 40 rpm. Fibers were then collected and desiccated for two days prior to storage at -20°C.

### *2.2.2. Suture Characterization*

#### *2.2.2.1. Suture Size and Morphology*

Sutures were serially dehydrated in ethanol (Sigma Aldrich) and dried prior to sputter coating with 10 nm of Au/Pd. Samples were then imaged via scanning electron microscopy (SEM) at 1-2 kV using a LEO Field Emission SEM (Zeiss, Oberkochen, Germany) and suture diameter measured using ImageJ software (n = 14 for each condition).

#### *2.2.2.2. Tensile Strength Measurement*

Mechanical properties of the sutures were evaluated using a DMA 6800 (TA Instruments, Timonium, MD). 3 cm long samples (n = 7 for each condition) were clamped vertically and force from a 5 N load cell was applied at 0.05 N/min to stretch the sample until breaking.

#### *2.2.3. In Vitro Drug Release*

10 mg of suture (n = 3) was placed into 10 mL of 1x Dulbecco's Phosphate Buffered Saline (PBS, ATCC, Manassas, VA) rotating at 37°C. At each time point, 2 mL aliquots were withdrawn and replaced with fresh PBS. Aliquots were frozen, lyophilized, and resuspended in ultrapure water prior to high performance liquid chromatography (HPLC; Waters Corporation, Milford, MA) analysis. 100 µL samples were injected into a Waters

Symmetry™ 300 C<sub>18</sub> 5 µm column with a mobile phase of 0.1% v/v trifluoroacetic acid (Sigma Aldrich) in water:acetonitrile (75:25 v/v, Fisher Scientific) at a flow rate 1 mL/min. Elution was monitored by a 2998 photodiode array detector to detect levofloxacin with excitation at 290 nm and emission at 502 nm. Drug loading was determined by dissolving a 5 mg sample of suture into a mixture of tetrahydrofuran (Sigma Aldrich):acetonitrile (20:80) and injecting into the column under the same conditions as the release samples.

#### *2.2.4. Assessment of Bacterial Inhibition*

1 cm of suture was placed in 1 mL of PBS and incubated at 37°C for 1, 3, and 6 h and 1, 2, 3, 4, 5, 6, and 7 days (n=6 for each time point). *S. epidermidis* (ATCC) was cultured overnight at 37°C on agar plates produced using nutrient agar (BD, Franklin Lakes, NJ). At each time point, sutures were retrieved and placed on plated cultures in order to investigate bacterial inhibition. Bacterial inhibition zones around the sutures were measured and imaged 24 h after suture placement.

#### *2.2.5. Assessment of In Vivo Biocompatibility*

Animals were cared for and experiments conducted in accordance with protocols approved by the Animal Care and Use Committee of the Johns Hopkins University. Protocols are also in accordance with the ARVO Statement for the Use of Animals in Ophthalmic and Vision Research. 1 mm of 8-0 Ethilon® (nylon), Vicryl® (poly(lactic-co-glycolic acid); PLGA) (Ethicon, Somerville, NJ) and 4% PEG/PLLA/levofloxacin sutures (n=3) were implanted into the corneas of 6-8 weeks old, male Sprague-Dawley rats (Harlan Laboratories, Frederick, MD). Prior to implantation, rats were intraperitoneally

anesthetized with a solution of Ketamine:Xylazine (75:5mg/kg, Sigma Aldrich) and a drop of 0.5% proparacaine hydrochloride ophthalmic solution (Bausch & Lomb Inc., Tampa, FL) was applied to the cornea. Following implantation, the rats were evaluated for signs of infection every day for seven days. The rats were then euthanized and eyes enucleated, fixed in formalin (Sigma Aldrich) for 24 h, embedded in paraffin, cross sectioned, and stained with hematoxylin and eosin for histological evaluation.

#### *2.2.6. Statistical Analysis*

Suture size, strength, and *in vitro* drug release are presented as mean  $\pm$  standard error. Statistical significance was determined via one-way ANOVA followed by Tukey test.

### **2.3. Results**

#### *2.3.1. Suture Fabrication and Characterization*

Several different parameters, including needle gauge, flow rate, applied voltage, distance to collector, lending solvent, and collector rotation speed were optimized in order to manufacture sutures from a wet electrospinning setup described previously (Figure 2.1.A).<sup>67</sup> Electrospinning of a 10 wt% polymer solution with application of 4.7 kV into a collector containing hexane and rotating at 40 rpm allowed for manufacture of a single, uniform, defect-free, cylindrical filament without beading, necking, or pores (**Figure 2.1.B**), which might adversely affect tensile strength and reproducibility. Microfibers manufactured with a collector speed of 40 rpm were thinner than those manufactured at lower speeds, and were more uniform in diameter than those manufactured at higher speeds

where there was also significant fiber loss at the edge of the collector. PLLA and levofloxacin served as the core suture components and the concentration of drug was held constant in the various formulations tested; however, the addition of F127 or different concentrations of PEG modified several suture properties. 4% PEG along with the use of blunted 18G needles and a flow rate of 13 mL/h provided for sutures  $45.1 \pm 7.7 \mu\text{m}$  in diameter (**Figure 2.2.A**). This qualifies as an 8-0 suture suitable for use in ophthalmic surgery, and would be stronger than 9-0 or 10-0 sized sutures manufactured from this setup. Under these conditions, it was possible to produce meters of suture material at a time.

Following suture manufacture, fibers were desiccated and stored at  $-20^{\circ}\text{C}$  preceding use in additional experiments. Prior to tensile testing, sutures were allowed to fully thaw and were cut into 3 cm segments. Tensile strength evaluation determined that the 4% PEG/PLLA/levofloxacin formulation also provided the highest breaking strength of all formulations tested at  $0.099 \pm 0.007 \text{ N}$ . As the concentration of PEG increased from 1% to 4%, by weight, so did the average strength of the sutures (**Figure 2.2.B**), although it was not statistically significant.

### 2.3.2. *In Vitro Levofloxacin Release*

Preliminary studies indicated minimal drug release from PLLA/levofloxacin sutures manufactured via electrospinning. However, the addition of small percentages of F127 and PEG polymers to the formulation resulted in significant and sustained release of levofloxacin *in vitro* (**Figure 2.2.C**). Regardless of the addition to the core polymer formulation, all modified suture formulations demonstrated initial burst release in the first



48 h followed by a slow, sustained, and linear release prior to ultimately reaching a plateau. The 4% PEG/PLLA/levofloxacin suture demonstrated the most significant burst release and also the highest cumulative release of all formulations tested. This suture formulation was found to have 4% drug loading and levofloxacin was detected in release media after more than two months with approximately 65% cumulative release.

### 2.3.3. Inhibition of *S. Epidermidis*

Bacterial inhibition zone experiments were conducted with *S. epidermidis* to determine whether levofloxacin released from sutures was capable of eliminating bacteria in an *in vitro* setting, and how long this effect might last *in vivo*. 4% PEG/PLLA/levofloxacin sutures were cut to 1 cm in length and incubated in 37°C PBS from 1 h up to 7 days. After each time point, the suture was removed from solution and placed in the center of an agar plate that had been cultured with *S. epidermidis* for 24 h. PBS, neat drug, and 4% PEG/PLLA sutures were used as controls (**Figure 2.3.A-C**). As depicted, PBS, and 4% PEG/PLLA did not inhibit bacterial growth, while the 4% PEG/PLLA/levofloxacin suture created a 2 cm inhibition zone after 24 h of drug release in PBS. Further, after 7 days in release media (**Figure 2.3.D**), drug-loaded sutures still provided bacterial inhibition, confirming that biologically active antibiotic was being released from the suture in an amount sufficient to eliminate surrounding bacteria.

### 2.3.4. In Vivo Performance and Biocompatibility

In order to evaluate the potential clinical value of an absorbable, antibiotic-eluting suture, wet electrospun sutures were implanted into the corneal stroma of male Sprague Dawley

rats. 8-0 Ethilon<sup>®</sup>, 8-0 Vicryl<sup>®</sup>, and 8-0 4% PEG/PLLA/levofloxacin sutures of approximately 1 mm in length were compared to each other and untreated controls after 7 days. Notably, 4% PEG/PLLA/levofloxacin sutures remained in the cornea and maintained integrity through the 7 day period, similar to the Ethilon<sup>®</sup> and Vicryl<sup>®</sup> sutures. Rats were monitored daily, and there were no gross signs of infection or inflammation among any of the animals for all sutures tested. Histological analysis (**Figure 2.4.A-D**) showed that the tissue reaction to the electrospun 4% PEG/PLLA/levofloxacin suture was indistinguishable to that of the nylon suture and untreated controls. There were no obvious signs of neovascularization or inflammation in the control, nylon, or antibiotic-eluting suture conditions. However, immune cell infiltration was apparent in each of the rat eyes containing a Vicryl<sup>®</sup> suture.

## **2.4. Discussion**

In this study, we demonstrated the manufacture, via wet electrospinning, of an absorbable, antibiotic-eluting suture composed of PLLA, PEG, and levofloxacin. The drug-eluting sutures provided sustained antibiotic release for more than 60 days *in vitro*, demonstrated activity against *S. epidermidis* for at least 1 week *in vitro*, and demonstrated similar biocompatibility to standard nylon sutures when implanted into rat corneas. To our knowledge, this is the first study to describe ophthalmic-grade antibiotic-eluting sutures prepared by electrospinning. Future studies to further preclinical development will include evaluation of duration of *in vivo* antibiotic release and prevention of ocular infection *in*

*in vivo* using varied suture lengths in the range of lengths typically used for ophthalmic procedures (a few mm to several cm).<sup>68</sup>

Wet electrospinning proved to be a versatile and scalable platform for the manufacture of drug-loaded sutures. Filament size was easily modified by changing equipment parameters such as flow rate, and a single run was able to manufacture several feet of uniform filament material.<sup>67</sup> As with other electrospinning setups, the system is compatible with a wide range of polymer, drug, and solvent combinations.<sup>65</sup> There is potential for this system to be used to tune suture size (2-0 to 10-0), degradation time (weeks to years), and drug release (burst and/or sustained) to allow for myriad clinical applications.

Similar to previous studies using electrospinning to manufacture drug-eluting sutures, the breaking strength of the 8-0 sized 4% PEG/PLLA/levofloxacin was below what is required by USP specifications.<sup>11,12,15,18,69</sup> Although the suture maintained integrity when implanted *in vivo*, additional optimization to further improve the mechanical properties of electrospun sutures is necessary. The literature has shown that voltage and polymer concentration can influence PLLA crystallinity and, therefore, breaking strength.<sup>70</sup> Additionally, it is possible that certain polymer and drug combinations would be stronger than others due to physicochemical interactions. Interestingly, although levofloxacin and PLLA are both hydrophobic, increasing the concentration of hydrophilic PEG did not significantly modify suture tensile strength.<sup>66,71</sup> In addition to varying electrospinning parameters and modifying polymer/drug choice, electrostretching and other post-modifications may serve

to improve tensile strength.<sup>67</sup> Residual solvent may also have reduced the tensile strength of the sutures.<sup>12</sup>

While optimizing tensile strength, consideration must be given to maintaining an ideal drug release profile. In this study, we observed a burst release in the first 48 h followed by sustained release for more than 30 days, which is ideal for eliminating and preventing infection. However, increasing the PLLA molecular weight to improve strength may further slow the second period of drug release to the point where antibiotic release is below the minimum inhibitory concentration.

Of critical importance in this study was the *in vivo* safety profile of the 4% PEG/PLLA/levofloxacin suture. While residual solvent is a concern in the use of electrospinning for biomedical applications, there were no signs of local or systemic toxicity due to any residual chloroform that may have remained in the suture after desiccation. Furthermore, the local inflammation observed via histology was comparable to nylon and clearly less than that of commercially available sutures composed of PLGA. This may be due to the quicker degradation of PLGA into acidic byproducts.<sup>12</sup> PLLA is known to be a biodegradable, biocompatible polymer with good crystallinity and strength, and has been shown not to elicit negative cellular or tissue reactions in other electrospun suture applications.<sup>19</sup>

Nylon sutures can harbor bacteria and lead to post-operative ocular infections that are vision-threatening if not properly cared for. While antibiotic eye drops are effective, they

are rarely used as prescribed. Hermann and coworkers observed topical antibiotic eye drop compliance in patients following cataract surgery and found that no patient followed the protocol exactly. 50% of patients took less than half of the prescribed doses over the course of the study.<sup>31</sup> Lack of compliance with antibiotic drops may not only allow for an infection to occur and to progress, but will also provide for the development of antibiotic resistance.<sup>72</sup> Ophthalmic-grade sutures capable of sustained antibiotic delivery may provide a solution to this significant clinical need.

## **2.5. Conclusion**

This study demonstrated the manufacture of an absorbable, ophthalmic-sized suture capable of sustained *in vitro* release of levofloxacin and inhibition of *S. epidermidis*, a common cause of post-operative ocular infection. The suture composed of PLLA, PEG, and levofloxacin was histologically similar after implantation in the rat cornea to commercially available nylon, whereas Vicryl<sup>®</sup>, a commercially available, absorbable suture composed of PLGA, demonstrated immune cell infiltration. With improved strength, this platform has the potential to prevent post-operative infection and preclude issues with compliance that may result in the development of ulcers, endophthalmitis, and antibiotic resistance.

**Table 2.1. United States Pharmacopeia specifications for absorbable sutures.**

Suture size and strength suitable for ophthalmic surgery are highlighted in green.

\* indicates that tensile strength is measured by straight pull.

USP Size	Limits on Average Diameter ( $\mu\text{m}$ )		Knot-Pull Tensile Strength (N)
	Min.	Max.	
10-0	20	29	0.24*
9-0	30	39	0.49*
8-0	40	49	0.69
7-0	50	69	1.37
6-0	70	99	2.45
5-0	100	149	6.67
4-0	150	199	9.32
3-0	200	249	17.4
2-0	300	339	26.3

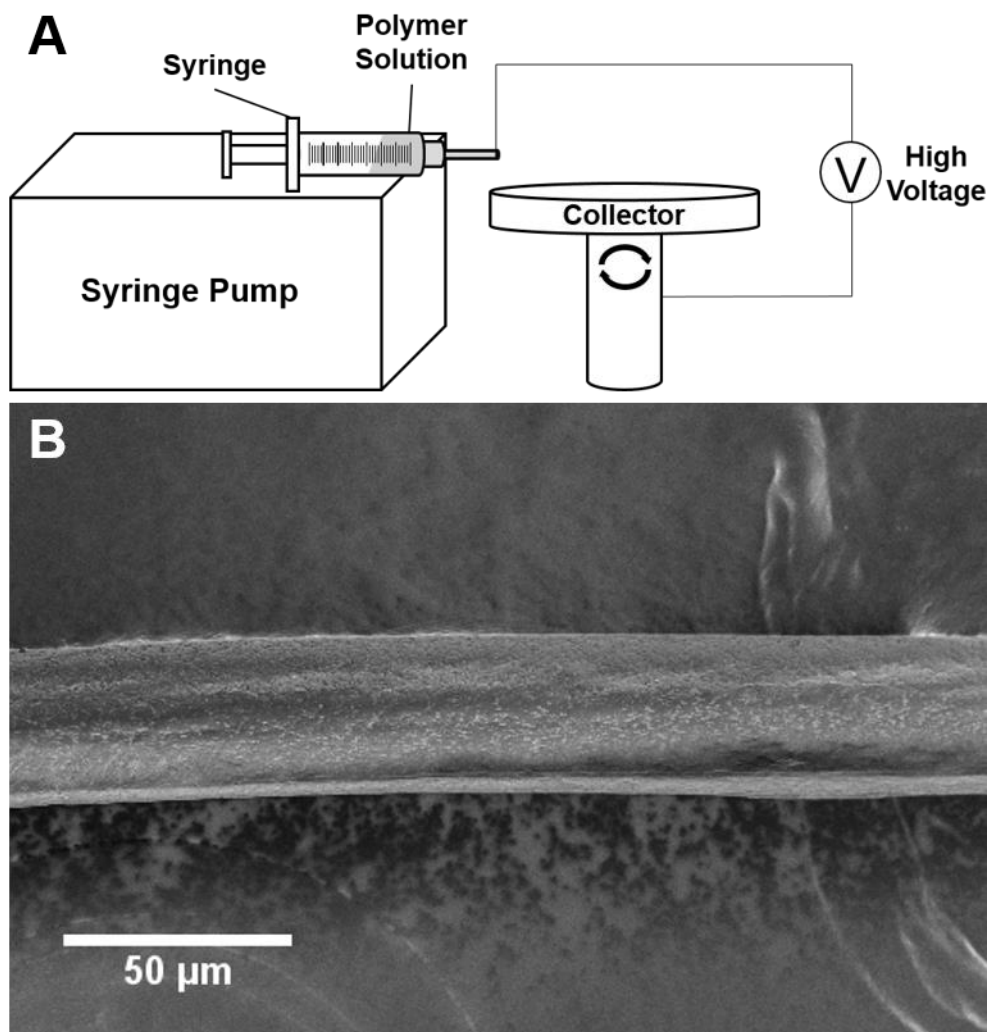


**Figure 2.1. Wet electrospinning setup and microfiber suture SEM.**

(A) Schematic of wet electrospinning setup. Voltage is applied to the polymer or polymer/drug solution which is driven into a rotating, grounded collector containing hexane. This provides for the manufacture of (B) long, uniform, defect-free, and drug-eluting monofilament sutures as shown via SEM.

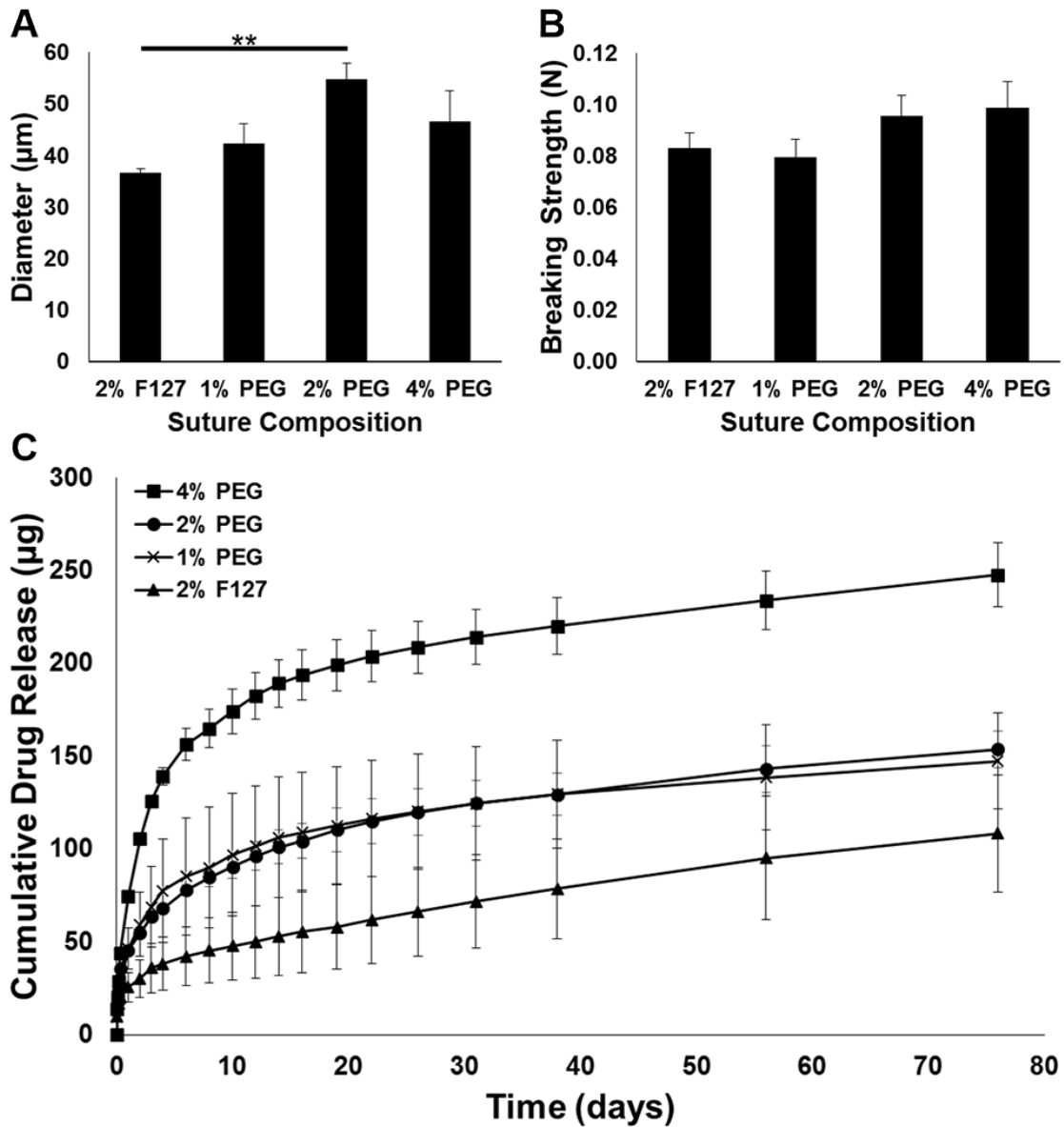


**Figure 2.2. Suture diameter, tensile strength, and *in vitro* drug release.**

Monofilament suture (A) diameter, (B) breaking strength, and (C) *in vitro* drug release with the addition of different polymers to the core PLLA/levofloxacin formulation. 2% F127, 1% PEG, and 4% PEG suture diameters are suitable for ophthalmic use. \*\* indicates  $p < 0.01$ . All formulations provide for sutures of similar strength. All formulations demonstrate sustained release of levofloxacin, while the 4% PEG formulation provides for a more rapid initial and greater overall release.



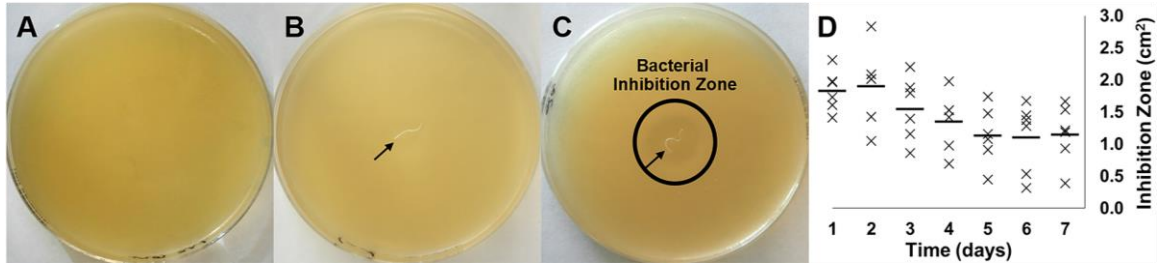


**Figure 2.3. *In vitro* bacterial inhibition.**

*Staphylococcus epidermidis* cultured on agar plates in the presence of (A) PBS, (B) 4% PEG/PLLA suture, (C) 4% PEG/PLLA/levofloxacin suture after 24 h. Black arrow indicates suture location. (D) Inhibition zones were measured for sutures bled for up to 1 week. A bacterial inhibition zone is clearly present surrounding the 4% PEG/PLLA/levofloxacin suture after bleeding for 24 h, and the sutures continue to show activity for at least 1 week.

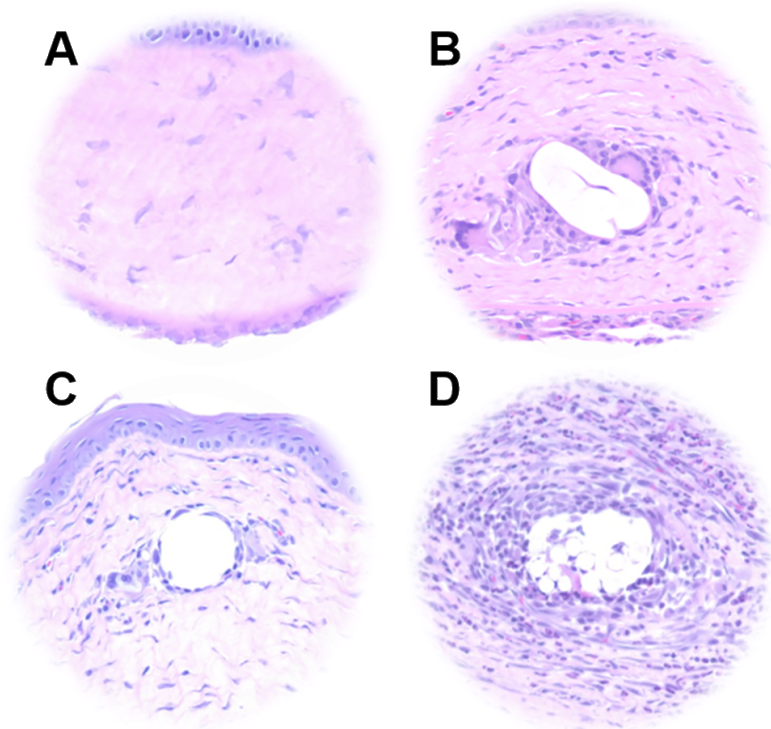


**Figure 2.4. Histological analysis of suture biocompatibility.**

Representative images of hematoxylin and eosin stained sections of (A) untreated corneal tissue and tissue surrounding (B) 4% PEG/PLLA/levofloxacin, (C) 8-0 permanent nylon (Ethilon<sup>®</sup>), and (D) 8-0 absorbable PLGA (Vicryl<sup>®</sup>) sutures following implantation for 1 week in Sprague-Dawley rat corneas. The electrospun suture elicited a tissue reaction comparable to that of nylon, while immune cell infiltration was observed in the vicinity of the Vicryl<sup>®</sup> suture.

### **3. Ultra-thin, high strength, antibiotic-eluting sutures for prevention of ophthalmic infection**

#### **3.1. Introduction**

From the first recorded use of natural fibers as sutures in 3,500 B.C. to the advent of synthetic, absorbable sutures in 1970, advances in material science and surgical practice have sought to develop the perfect suture: one that is sterile, strong, easy to handle, absorbable, and biologically inert to provide the appropriate conditions for wound healing and tissue repair.<sup>18,52,56,73,74</sup> The ideal suture also degrades and loses strength as the surrounding tissue heals and gains strength, and is able to scale to commercial production. We envision a generation of sutures that will meet each of these requirements while also providing sufficient and controlled release of therapeutic moieties, such as small molecule drugs, nucleic acids, and proteins to reduce complications and modulate the biological response to surgery in order to improve clinical outcomes.

Sutures are a promising means of therapeutic delivery directly to the surgical site. However, clinical implementation of such technology has been limited due to the inability of drug-loaded sutures to meet United States Pharmacopeia (U.S.P.) standards for suture strength.<sup>57,75</sup> Conventional suture manufacturing processes are not compatible with most therapeutic moieties, and drug-loaded sutures in preclinical development have demonstrated breaking strength of only one-tenth that the strength required for clinical use.<sup>11,12,18,20,21,69,75-80</sup> Drug-coated sutures have been developed to circumvent these

shortcomings, but are limited in their capacity to load sufficient drug, control drug release, and/or scale manufacturing.<sup>14,17,23-27</sup> Without the ability to deliver drug in a controlled manner, drug-coated sutures are limited to use in anti-infection applications, which are the only current market offerings for drug delivery via sutures. However, these antibacterial coatings are only available in conjunction with absorbable thread, are only indicated for use in general surgery (6-0 – 2-0 U.S.P. classification), and do not meet U.S.P. specifications for diameter.

There is a significant need for an antimicrobial suture in ocular surgery, where, globally, more than 12 million procedures per year use conventional nylon sutures to close ocular wounds and incisions.<sup>30</sup> Non-absorbable nylon sutures are a mainstay of ocular surgery due to their increased biocompatibility in comparison to absorbable sutures, and their capacity to retain strength at the surgical site.<sup>66</sup> Nylon sutures are used in procedures such as penetrating keratoplasty, where sutures may remain in the eye for 12-24 months, and as with other implantable devices, increase the risk of infection following ophthalmic procedures due to their susceptibility to bacterial adhesion, proliferation, and biofilm formation.<sup>28,29,61,81-83</sup> Incidence of infectious keratitis following penetrating keratoplasty has been reported between 1.76% and 12.1%.<sup>84</sup> Suture-related complications are implicated in 20% to more than 50% of these cases, and can have devastating consequences, including poor visual outcomes, re-intervention, and graft failure.<sup>84-87</sup> Thus, it is particularly important to provide for local antibacterial functionality along with implantation of non-absorbable sutures within the eye. Local antibiotic delivery from the suture itself would provide bacterial inhibition at the vulnerable surgical incision and help

to alleviate concerns of non-compliance with topical antibiotic eye drops, which are often prescribed post-operatively. Antibiotic-eluting sutures may also reduce the need for post-operative oral antibiotic prescriptions, the systemic administration of which can lead to emergence of resistant organisms and associated complications such as *Clostridium difficile* infection and life-threatening diarrhea.<sup>72,88</sup> In addition to keratoplasty, glaucoma, retinal detachment, vitrectomy, and cataract surgeries, where nylon sutures have been used, antibiotic-eluting sutures may also decrease the risk of infection associated with concurrent implantation of keratoprotheses, lacrimal stents, orbital plates, glaucoma drainage implants, or other ocular devices.<sup>89-96</sup>

An antibiotic-eluting suture for ophthalmology must be extremely fine (20 – 50  $\mu\text{m}$  in diameter; 10-0 – 8-0 U.S.P. classification) while retaining high strength for the duration of the intended application and providing sufficient release of an antibacterial agent to reduce or prevent ophthalmic infection.<sup>57,75</sup> Here, we describe a novel manufacturing system for production of ultra-thin, high strength, antibiotic-loaded sutures for ophthalmic surgery. The basis for this platform is a well-known and versatile fiber production technique known as electrospinning, which applies high voltage to a polymer solution to draw out fine threads.<sup>6</sup> Although the use of electrospinning in suture manufacture has been previously reported in the literature, to our knowledge, this is the first platform to manufacture and twist individual, highly crystalline, drug-loaded nanofibers into a single, multifilament suture capable of surpassing U.S.P. strength specifications.<sup>11,12,20,69,76</sup> In order to provide an antibacterial alternative to the use of nylon sutures in ophthalmic surgery, we manufactured sutures composed of 80 kDa polycaprolactone (PCL) and levofloxacin

(Levo). Levo is a third-generation fluoroquinolone and broad-spectrum ophthalmic antibiotic indicated for treatment of bacterial conjunctivitis.<sup>97</sup> PCL is a biocompatible polymer capable of long-term degradation that has been used in sutures and other medical devices for more than 30 years.<sup>66,98-100</sup> We maximized fiber crystallinity, and consequently, suture tensile strength by electrospinning nanofibers composed of low molecular weight PCL and subsequently twisting them into a single suture to provide additional compaction and structural reinforcement. We evaluated antibiotic-eluting suture size, breaking strength, drug release, biocompatibility, and efficacy *in vivo* in a rat model of bacterial keratitis.

## **3.2. Materials and Methods**

### *3.2.1. Suture Manufacture*

Polymer solutions were made via dissolution of 80 kDa PCL (Sigma-Aldrich, St. Louis, MO) alone or with drug in hexafluoroisopropanol (Sigma-Aldrich) by shaking overnight at room temperature. PCL concentration was maintained at 10% (w/w) in relation to solvent. Levofloxacin (Sigma-Aldrich), moxifloxacin (LKT Laboratories, St. Paul, MN), bacitracin (Carbosynth, San Diego, CA), and tobramycin (Sigma-Aldrich) were dissolved at either 8%, 16%, 24%, or 40% (w/w) in relation to polymer. Solutions were electrospun via pumping at 450  $\mu\text{L}/\text{h}$  through a 20 G blunt-tip needle with an applied voltage of 17kV, at a distance of 13 cm from a set of parallel grounded collectors to form parallel nanofibers. One collector was then rotated clockwise for a specified number of rotations (twists) prior to removal of the suture from the collectors and storage at  $-20\text{ }^{\circ}\text{C}$ .

### *3.2.2. Suture Characterization*

#### *3.2.2.1. Suture Size*

Suture diameter was determined via light microscopy using the 20x objective of an Eclipse TS100 (Nikon Instruments, Melville, NY) and calibrated Spot 5.2 Basic imaging software (Spot Imaging, Sterling Heights, MI). Each suture was measured at three different locations at least 2 cm apart, and used in additional experimentation only if the average diameter was within  $\pm 0.5 \mu\text{m}$  of the specified diameter.

#### *3.2.2.2. Suture Morphology*

Suture morphology was observed via scanning electron microscopy (SEM) at 1 kV using a LEO Field Emission SEM (Zeiss, Oberkochen, Germany). Prior to imaging, samples were desiccated and then sputter coated with 10 nm of Au/Pd (Desk II, Denton Vacuum, Moorestown, NJ).

#### *3.2.2.3. Suture Breaking Strength*

Sutures ( $n = 3-4$  for each condition) were clamped vertically and then pulled until breaking at a rate of 2.26 mm/min using a DMA 6800 (TA Instruments, Timonium, MD).

#### *3.2.2.4. Suture Strength Retention*

PCL/8% Levo and PCL/16% Levo sutures ( $n = 5$ ) were sectioned into two halves. The breaking strength of one segment was measured as described above, while the other segment was submerged in 1x Dulbecco's Phosphate Buffered Saline (PBS; ATCC,

Manassas, VA) and shaken at 225 rpm at 37 °C for 31 days. Sutures were then dried prior to measuring breaking strength.

#### *3.2.2.5. Suture Drug Loading*

15 mm of PCL/8% Levo and PCL/16% Levo sutures (n = 3) were submerged in a mixture of acetonitrile and tetrahydrofuran (80:20, Fisher Scientific, Waltham, MA) and sonicated for 30 minutes prior to evaluating via high performance liquid chromatography (HPLC). Samples were injected into a Symmetry™ 300 C18 5 µm column (Waters Corporation, Milford, MA) with a mobile phase of 0.1% v/v trifluoroacetic acid (Sigma Aldrich) in water:acetonitrile (75:25 v/v, Fisher Scientific) at a flow rate of 1 mL/min. Levofloxacin was detected at an excitation wavelength of 295 nm and emission wavelength of 496 nm.

#### *3.2.3. Animal Studies*

All animals were cared for and experiments conducted in accordance with protocols approved by the Animal Care and Use Committee of the Johns Hopkins University. Protocols are also in accordance with the ARVO Statement for the Use of Animals in Ophthalmic and Vision Research.

##### *3.2.3.1. In Vivo Biocompatibility*

Three 2 mm long 10-0 nylon, Vicryl® (poly(lactic-co-glycolic acid); PLGA) (Ethicon, Somerville, NJ) and PCL/Levo suture filaments were implanted into the corneas of 6-8 week old, male Sprague Dawley rats (Harlan Laboratories, Frederick, MD). Prior to implantation, rats were intraperitoneally anesthetized with a solution of ketamine:xylazine



(75:5mg/kg, Sigma Aldrich) and a drop of 0.5% proparacaine hydrochloride ophthalmic solution (Bausch & Lomb Inc., Tampa, FL) was applied to the cornea. Following implantation, the rats were evaluated daily for signs of infection, inflammation, or irritation. Two days after implantation, the rats were euthanized and eyes enucleated, fixed in formalin (Sigma Aldrich) for 24 h, embedded in paraffin, cross sectioned, and stained with hematoxylin and eosin (H&E) for histological evaluation.

#### *3.2.3.2. Pharmacokinetic Study*

PCL/8% Levo and PCL/16% Levo sutures were implanted into Sprague Dawley rat corneas as described above (n = 4 for each formulation at each time point). At 15, 60, and 120 min, and at 1, 3, 7, and 14 days, aqueous humor was collected from each eye, followed by removal of implanted sutures and harvesting of the cornea. Tissue and aqueous humor samples were weighed immediately after harvesting. Corneal tissue samples were homogenized in 100  $\mu$ L to 150  $\mu$ L of PBS prior to extraction. The standard curve and quality control samples were prepared in PBS as a surrogate matrix for both aqueous humor and homogenized tissue. Levofloxacin was extracted from 15  $\mu$ L of aqueous humor or tissue homogenate with 50  $\mu$ L of acetonitrile containing 1  $\mu$ g/mL of the internal standard, moxifloxacin-d4 (Toronto Research Chemicals, Canada). After centrifugation, the supernatant was then transferred into autosampler vials for LCMS/MS analysis. Separation was achieved with an Agilent Zorbax XDB-C18 (4.6  $\times$  50 mm, 5  $\mu$ m) column with water/acetonitrile mobile phase (40:60, v:v) containing 0.1% formic acid using isocratic flow at 0.3 mL/min for 3 minutes. The column effluent was monitored using an AB Sciex triple quadrupole™ 5500 mass-spectrometric detector (Sciex, Foster City, CA) using

electrospray ionization operating in positive mode. The spectrometer was programmed to monitor the following MRM transitions: 362.0 → 318.0 for levofloxacin and 406.1 → 108.0 for the internal standard, moxifloxacin-d4. Calibration curves for levofloxacin were computed using the area ratio peak of the analysis to the internal standard by using a quadratic equation with a 1/x<sup>2</sup> weighting function using two different calibration ranges of 0.25 to 500 ng/mL with dilutions up to 1:10 (v:v) and 5 – 5,000 ng/mL.

### 3.2.3.3. *Bacterial Inoculation and Evaluation*

Sprague Dawley rats were anesthetized as described above. The operative eye was then scratched using a 20 G needle (Fisher Scientific) prior to implantation of three 2 mm long nylon (n = 12), Vicryl<sup>®</sup> (n = 4), or PCL/8% Levo (n = 4) suture filaments. 100 μL of 1x10<sup>8</sup> CFU/mL of *S. aureus* was then administered topically over a period of 10 mins. 10 μL of 0.5% levofloxacin solution was administered topically either once post-operatively or three times daily to rat eyes with nylon sutures (n = 4, each). Two days after implantation, gross images were taken of each eye, prior to swabbing the cornea with a cotton-tipped applicator (Fisher Scientific), and streaking onto tryptic soy agar (Fisher Scientific) plates. Plates were stored in an incubator at 37 °C for 24 h and then imaged. After swabbing the eye, eyes were enucleated and either prepared for histological evaluation as described above (n = 3 for each condition) or evaluated for bacterial load (n = 4 for each condition). Briefly, each eye was placed in sterile tryptic soy broth (Fisher Scientific) and homogenized using a Power Gen 125 homogenizer (Fisher Scientific) for 4 min. Samples were then centrifuged at 300 rcf for 5 min, and optical density of the supernatant measured at a wavelength of

600 nm via spectrophotometry. Infection was confirmed by a positive swab culture and bacterial load significantly higher than a control eye.

A long-term study was also performed to evaluate resistance to infection after multiple inoculations. Nylon, PCL/8% Levo, and PCL/16% Levo sutures (n = 8, each) were implanted into rat corneas on day 0, with inoculation of *S. aureus* to only the PCL/Levo suture conditions, as described above. On day 2, rat corneas were swabbed to evaluate infection. On day 5, the corneas of all rats were scratched and inoculated with *S. aureus*. On day 7, swabs were taken of each cornea followed by either histological evaluation, bacterial homogenization, or removal of sutures for examination via SEM (n = 4 for each condition). For the latter experiment, sutures were removed from the cornea and fixed in formalin (Sigma-Aldrich) for 30 min prior to washing with PBS and dehydration with increasing concentrations of ethanol (Fisher Scientific). Sutures were then imaged as described above.

#### 3.2.4. Statistical Analysis

Suture breaking strength, Levo concentration, and bacterial load are presented as mean  $\pm$  standard error. Statistical significance for breaking strength and bacterial load data was determined via one-way ANOVA followed by Tukey test. Statistical significance for the Kaplan-Meier curve of long-term infection prevention was determined via the Mantel-Cox test.

### 3.3. Results

We hypothesized that sutures composed of twisted PCL/Levo nanofibers would provide suitable strength at the surgical site for an extended duration while also delivering antibiotic in a sufficient and controlled manner to prevent post-operative suture colonization and ocular infection.

#### *3.3.1. Suture Manufacture and Characterization*

In order to limit the effect of drug loading on the strength of polymeric matrices, we engineered a novel manufacturing system capable of producing and twisting together hundreds of individual drug-loaded, polymeric nanofibers (**Figure 3.1.A**). As with conventional electrospinning, high voltage is applied to a polymer or polymer/drug solution pumped at a controlled flow rate in order to form polymeric fibers. However, instead of collecting fibers on a rotating drum, fibers are collected in parallel between two grounded collectors situated perpendicularly to the syringe pump. Rotation of one collector results in the twisting of deposited parallel fibers into a single, multifilament suture. The amount of fiber deposition, and consequently, suture diameter can be reproducibly tuned by adjusting spray time.

SEM of multifilament sutures confirmed manufacture of a highly uniform, non-porous, and defect-free thread composed of nanofibers (**Figure 3.1.B**). Notably, individual nanofibers had a flat, ribbon-shaped morphology. Multifilament, drug-loaded sutures were cylindrical in nature and met U.S.P. specifications for 10-0 suture diameter (20-29  $\mu\text{m}$ ), making them

suitable in size for ocular surgery. They were also comparable in both size and shape to commercially available 10-0 Ethilon<sup>®</sup> (nylon) sutures (Figure 3.1.B).

### 3.3.2. Suture Breaking Strength

The key challenge for translation of drug-loaded sutures to the clinic has been an inability to meet U.S.P. specifications for suture strength. Thus, we next examined the impact of fiber conformation, drug concentration, drug type, and diameter on antibiotic-loaded suture breaking strength.

**Figure 3.2.A** illustrates the difference in PCL suture strength with 8% Levo in either a monofilament or twisted multifilament conformation of identical diameter (28  $\mu\text{m}$ ). As may be expected, monofilament PCL suture breaking strength was reduced by more than 50% when Levo was incorporated ( $p < 0.001$ ). In contrast, the multifilament PCL suture breaking strength was not significantly changed with drug loading. Further, the multifilament PCL suture breaking strength increased accordingly with the increase in number of collector rotations (twists). A multifilament PCL suture with 1,575 twists, 8% Levo within the suture formulation, and a diameter of 28  $\mu\text{m}$  surpassed the minimum U.S.P. breaking strength specification for 10-0-sized sutures of 0.24 N.

Next, we explored the amount of drug that could be loaded into multifilament sutures while maintaining U.S.P. strength specifications. We produced 1,575 twist, 28  $\mu\text{m}$  multifilament sutures composed of PCL with no drug or with 8%, 16%, 24%, or 40% Levo within the suture formulation. Sutures with 16% or more Levo had a significantly lower breaking

strength ( $p < 0.05$ ) than PCL sutures alone or with 8% Levo (**Figure 3.2.B**). It was possible to include up to 24% Levo within the multifilament suture formulation while still surpassing clinical strength requirements for a 10-0 suture. Notably, even with inclusion of 40% Levo into the suture formulation, multifilament PCL suture breaking strength was significantly higher ( $p < 0.05$ ) than a monofilament suture with 8% Levo (Figure 3.2.A), and reached 75% of the U.S.P. specification (Figure 3.2.B). Critically, both PCL/8% Levo and PCL/16% Levo sutures maintained their strength and demonstrated minimal degradation *in vitro* over a period of 31 days in PBS.

We next evaluated the compatibility of the multifilament suture platform with various types of small molecule antibiotics indicated for ophthalmic use. We manufactured 1,575 twist, 28  $\mu\text{m}$  sutures composed of PCL and 8% of either moxifloxacin, bacitracin, or tobramycin. Moxifloxacin is a fourth generation fluoroquinolone that has shown superior potency to Levo, while bacitracin and tobramycin are from the polypeptide and aminoglycoside antibiotic classes, respectively.<sup>72</sup> Although these antibiotics have different physicochemical properties owing to their varying molecular structures, there was no significant difference in breaking strength of multifilament PCL sutures loaded with any of these molecules (**Figure 3.2.C**). Importantly, all drug-loaded sutures met both size and strength specifications for a 10-0 suture for ocular surgery.

9-0 (30-39  $\mu\text{m}$ ) and 8-0 (40-49  $\mu\text{m}$ ) sutures are also commonly used in ocular surgery. We evaluated the capacity for this manufacturing platform to scale to larger diameter sutures with correspondingly improved breaking strength by increasing electrospinning spray time

to manufacture 1,575 twist PCL/8% Levo sutures that were 38  $\mu\text{m}$  (9-0) and 48  $\mu\text{m}$  (8-0) in diameter. In order to understand the effect of suture diameter on breaking strength, we also evaluated the breaking strength of 21  $\mu\text{m}$  diameter PCL/8% Levo sutures manufactured in a similar fashion (**Figure 3.2.D**). Varying suture diameter significantly affected breaking strength in all cases ( $p < 0.05$ ). Decreasing suture diameter from 28 to 21  $\mu\text{m}$  decreased breaking strength more significantly than increasing Levo concentration from 8% to 40% (Figure 3.2.B), demonstrating the importance of suture diameter in the resulting breaking strength of multifilament sutures. 38  $\mu\text{m}$  PCL/8% Levo multifilament sutures surpassed U.S.P. specifications for 9-0 sutures and were 64% stronger than 28  $\mu\text{m}$  sutures. 48  $\mu\text{m}$  PCL/8% Levo sutures, also measured via straight pull, demonstrated a 61% increase in tensile strength in comparison to 38  $\mu\text{m}$  sutures.

### *3.3.3. In Vivo Suture Biocompatibility*

In order to evaluate the use of electrospun, multifilament sutures as a potential alternative to nylon or other commercially available sutures, we assessed the tissue reaction to 10-0 nylon, Vicryl<sup>®</sup>, PCL, PCL/8% Levo, and PCL/16% Levo sutures following implantation into the rat corneal stroma for 2 days. There were no gross signs of irritation, inflammation, or infection among any of the treated or control groups for the duration of the study. Histological analysis (**Figure 3.3.**) revealed that implantation of PCL or PCL/Levo sutures did not cause neovascularization, and that the tissue reaction was comparable to commercially available nylon sutures. Notably, a small ring of cells was observed surrounding implanted absorbable Vicryl<sup>®</sup> sutures.

#### 3.3.4. Pharmacokinetics of Levofloxacin Delivered from Sutures

In order to determine the duration and concentration of Levo delivery from sutures *in vivo*, we conducted a pharmacokinetic study by implanting three 2 mm lengths of 28  $\mu\text{m}$  PCL/8% Levo and PCL/16% Levo sutures into rat corneas. Analysis of Levo concentration in harvested aqueous humor and corneas revealed a burst release of antibiotic following suture implantation and for multiple hours afterwards (**Table 3.1**). The Levo release profiles were similar in eyes implanted with either 8% or 16% Levo sutures. However, eyes with PCL/16% Levo sutures contained higher concentrations of Levo in both the aqueous humor and cornea at almost all time points. Sutures maintained their location and macroscopic structure throughout the course of the study, and in both 8% and 16% Levo conditions, Levo was detected in the cornea and aqueous humor 14 days after implantation. HPLC analysis of dissolved sutures revealed Levo loading of 80 and 161  $\mu\text{g}/\text{m}$ , respectively, for 8% and 16% Levo sutures.

#### 3.3.5. Prevention of Ophthalmic Infection

We assessed the potential clinical utility of PCL/Levo sutures by evaluating their capacity to prevent infection following one or two consecutive inoculations of *Staphylococcus aureus* (*S. aureus*). Rat eyes were scratched, three 2 mm lengths of 10-0 nylon, Vicryl<sup>®</sup>, or PCL/Levo sutures were implanted into the cornea, and *S. aureus* was administered. Rats receiving implantation of nylon sutures were divided into three groups: (1) no post-operative treatment, (2) topical administration of a single drop of 0.5% Levo immediately after inoculation, and (3) topical administration of 0.5% Levo three times daily beginning immediately after inoculation. Implantation of Vicryl<sup>®</sup> and nylon sutures without post-



operative treatment resulted in severe infections characterized by a bacterial load 3.4 – 4.3 times higher than that of a healthy, control cornea (**Figure 3.4.A**). The eyes were highly inflamed and red, with a whitish hue likely indicating bacterial colonization and proliferation surrounding the sutures themselves (**Figure 3.4.B**). Healthy, control corneas contained a small amount of endogenous bacteria, the amount of which was not significantly different than corneas implanted with PCL/8% Levo sutures or corneas implanted with nylon sutures receiving three daily drops of Levo. A single drop of Levo following implantation of nylon sutures significantly decreased the bacterial load in comparison to a nylon suture alone ( $p < 0.05$ ), but was not sufficient to prevent infection (**Figure 3.4.A**). These findings are further confirmed by histological and bacterial culture analysis. H&E staining revealed substantial inflammation and cellular infiltration within the corneas of rats receiving implantation of Vicryl<sup>®</sup> or nylon sutures without post-operative administration of Levo (**Figure 3.4.C**). Notably, the concentration of cells was greatest within the immediate vicinity of implanted sutures, providing another indication that the suture itself may be the nidus of infection and location of bacterial adherence. Cells were also concentrated around nylon sutures implanted in rat eyes receiving a single post-operative dose of Levo. However, there was no sign of infection or inflammation in the corneal tissue surrounding PCL/8% Levo sutures or nylon sutures in rats receiving three daily doses of Levo, and the tissue resembled that of a healthy control. Culture of bacterial swabs on agar plates similarly confirmed the presence of infection in rats with implantation of Vicryl<sup>®</sup> or nylon sutures, or nylon sutures followed by a single dose of Levo administered topically.

We also evaluated the capacity of 10-0 PCL/Levo multifilament sutures to continue to prevent ocular infection following the immediate post-operative period. PCL/8% Levo and PCL/16% Levo sutures were implanted into rat corneas with administration of *S. aureus* immediately following implantation and again 5 days after implantation. Eyes containing nylon sutures were only inoculated once 5 days after implantation. In congruence with the results of the short-term infection study, eyes containing PCL/Levo sutures, at either concentration of Levo, did not become infected after the initial *S. aureus* inoculation. However, 7 days after implantation, 25% of eyes implanted with PCL/8% Levo sutures displayed a minor infection confirmed by bacterial swab and homogenization (Figure S2, Supporting Information). Notably, 0% of rat eyes containing 10-0 PCL/16% Levo sutures showed signs of infection (**Figure 3.5.A**). These results are significantly different ( $p < 0.01$ ) than the outcomes observed for eyes containing nylon sutures of which 100% became infected after a single bacterial inoculation 5 days after suture implantation. SEM images of sutures removed from rat corneas 7 days after implantation further confirmed these results (**Figure 3.5.B**). High magnification images revealed the presence of *S. aureus* on all nylon sutures with vast amounts of biofilm formation. *S. aureus* was also detected on PCL/8% Levo sutures collected from infected eyes, although biofilm formation was less apparent. *S. aureus* colonization was not apparent on PCL/16% Levo sutures collected 7 days after implantation, and after two consecutive bacterial inoculations.

### 3.4. Discussion

Commercially available sutures are known to be associated with vision-threatening microbial keratitis and endophthalmitis.<sup>66,84-87,101</sup> Suture-related complications are implicated in up to more than 50% of infections following penetrating keratoplasty procedures.<sup>84-87</sup> Although sutures are employed in a lower percentage of cataract surgeries, after three years, more than 65% of sutures have been reported to become loose or broken. Upon removal, cultures reveal that almost 40% of such sutures demonstrate bacterial contamination.<sup>29</sup> In addition, implantation of devices such as keratoprotheses in conjunction with sutures has demonstrated post-operative infection rates of more than 17%.<sup>102</sup> An antibiotic-eluting suture offers an opportunity to prevent suture-related post-operative infections, and to reduce the risk of infection following ocular device implantation; however, there are currently no market offerings for drug-eluting sutures in ophthalmology.

We designed a novel electrospinning system for manufacture of nano-structured, drug-eluting sutures, and evaluated its potential for development of antibiotic-eluting sutures for ocular surgery. Degradable, multifilament sutures manufactured using this platform met or exceeded U.S.P. specifications for size and strength suitable for ophthalmic use. Further, these sutures surpassed breaking strength specifications when loaded with a wide range of antibiotics of different physicochemical properties. The multifilament sutures demonstrated biocompatibility comparable to conventional nylon sutures, and delivered levofloxacin at detectable levels in rat eyes for at least 14 days. Moreover, Levo-eluting,

multifilament sutures manufactured utilizing this platform prevented ocular infection against multiple bacterial challenges for a period of 1 week *in vivo*, and were significantly more effective than a single post-operative antibiotic drop at decreasing bacterial load within the eye.

To our knowledge, this is the first manufacturing platform to produce drug-loaded sutures that surpass U.S.P. breaking strength specifications.<sup>12,18,20,69,76</sup> Similar to prior reports in the literature, micron-sized, electrospun PCL monofilament sutures lost more than 50% of their strength with inclusion of Levo. In contrast, twisted, multifilament nanofiber sutures did not lose strength with inclusion of an equivalent amount of Levo. Both the composition of the sutures and the manufacturing process likely contributed to these outcomes. PCL is a semi-crystalline, hydrophobic, and biodegradable polymer.<sup>99</sup> It has been shown that the process of electrospinning alone alters the molecular orientation of PCL to improve crystallinity and that PCL nanofibers increase in tensile strength with reduced diameter due to molecular confinement.<sup>103</sup> This phenomenon is not observed in PCL fibers produced via the melt flow extrusion process used to manufacture commercially available sutures today.<sup>103</sup> Further, PCL crystallinity increases along with a decrease in molecular weight.<sup>99</sup> We maximized fiber crystallinity, and consequently suture strength, by electrospinning nanofibers composed of low molecular weight PCL. Moreover, twisting of individual nanofibers into a multifilament suture provides additional structural reinforcement, resistance to breakage, and knot security.<sup>57</sup> The flat, ribbon-shaped morphology of the individual nanofibers suggests that the twisting process led to stretching of nanofibers, which has also been shown to improve fiber crystallinity and tensile strength.<sup>104</sup> Increased

twisting also resulted in a more compact nanofiber bundle, illustrated by the increased spray time necessary to manufacture sutures of an equivalent diameter at a higher number of twists. Thus, increasing the number of twists allowed for incorporation of a greater number of nanofibers into a single suture, thereby amplifying breaking strength and increasing drug loading capacity. Collectively, these factors contributed to manufacture of drug-loaded, multifilament PCL sutures with unprecedented strength.

The highly crystalline and hydrophobic nature of PCL nanofibers manufactured through this process likely partitions the drug and polymer.<sup>12,103</sup> This may explain the equivalent strength of multifilament PCL sutures without drug and with inclusion of 8% Levo or other antibiotics with disparate molecular structures. This might also lead to the burst release of Levo observed following implantation of drug-loaded sutures into rat eyes. Although a burst release of antibiotic is critical for prevention of immediate post-operative infection when wounds or surgical incisions are healing and most vulnerable to bacterial infiltration, sutures are susceptible to bacterial colonization for as long as they remain *in vivo*.<sup>29,62,81,84,85,87,101,102,105,106</sup> Given the small diameter of sutures utilized in ophthalmic procedures, it is unlikely that antibiotic-coated sutures could provide sufficient drug delivery over this duration.<sup>14,17</sup> However, local antibiotic delivery from drug-loaded sutures may preclude issues of poor patient compliance with topical eye drops, prevent suture-related infections that lead to treatment failure and re-intervention, reduce the need for oral antibiotic use, decrease the risk of infection associated with implantable ocular devices, and serve as an alternative to the more than 12 million nylon sutures used in ocular procedures each year.<sup>30,72,84,87,102,107</sup>

### **3.5. Conclusion**

Implantation of sutures or other devices into the eye increases the risk of potentially sight-threatening ophthalmic infection. The surfaces of these devices are vulnerable to bacterial colonization and proliferation, and biofilm formation. We have developed a novel platform for manufacture of high strength, nano-structured, drug-loaded sutures capable of meeting U.S.P specifications for suture diameter and strength. This platform is compatible with several ophthalmic antibiotics of varying physicochemical properties, and can surpass clinical strength requirements while delivering sufficient levels of antibiotic locally. Multifilament nanofiber sutures manufactured utilizing this platform demonstrated biocompatibility and prevention of ophthalmic infection following multiple inoculations of *S. aureus* over a period of one week. This platform for suture manufacture is highly tunable, and may have potential to improve clinical outcomes across a broad spectrum of surgical procedures.

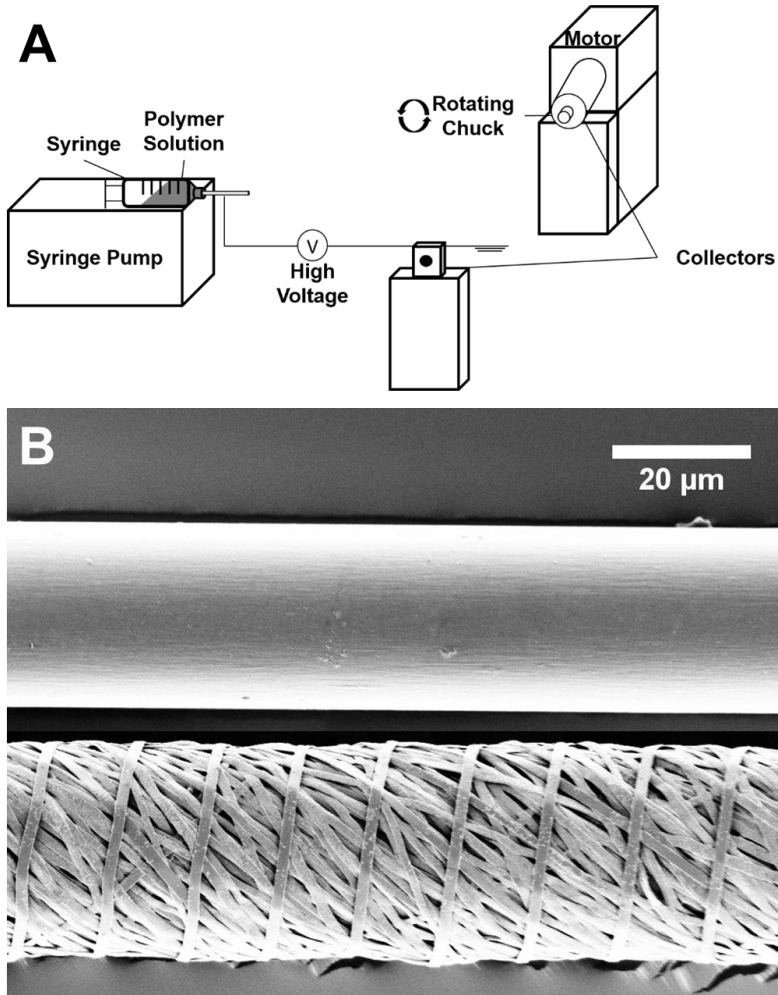


**Figure 3.1. Manufacture of drug-eluting, multifilament sutures.**

(A) Schematic of suture manufacturing system: high voltage is applied to a polymer or polymer/drug solution pumped at a controlled rate perpendicular to two grounded collectors. One collector is motorized, allowing for twisting of hundreds of parallel nanofibers into a single, multifilament suture. (B) SEM images of a conventional 10-0 nylon suture (top) and 10-0 multifilament PCL/Levo suture (bottom).

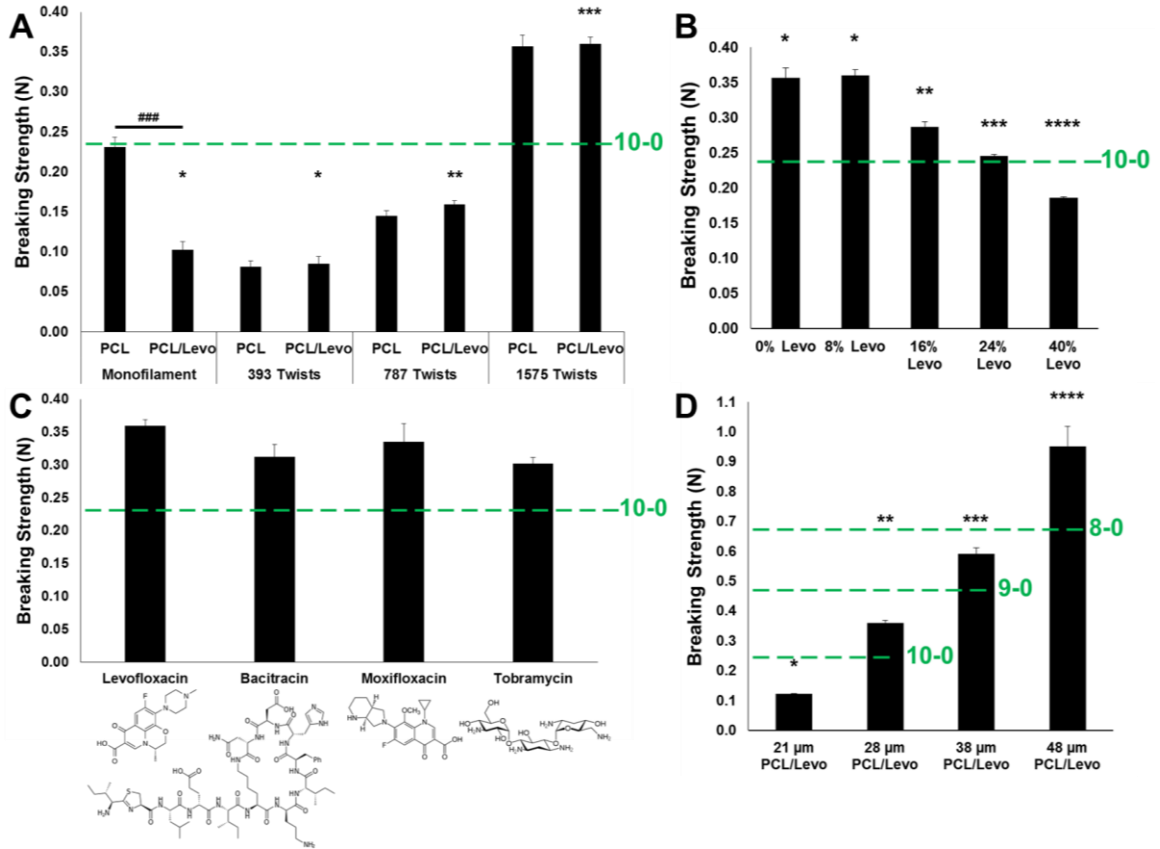


**Figure 3.2. Breaking strength of PCL sutures in reference to U.S.P. specifications.**

(A) Comparison of breaking strength of 28 μm PCL/8% Levo monofilaments vs 28 μm PCL/8% Levo multifilaments at varying levels of twisting. (B) Breaking strength of 28 μm multifilament sutures at 1,575 twists composed of PCL and 8% of different ophthalmic antibiotics. (C) Breaking strength of 28 μm PCL/Levo multifilament sutures at 1,575 twists at a range of Levo concentrations. (D) Breaking strength of PCL/8% Levo multifilament sutures at 1,575 twists at a range of diameters suitable for ophthalmic surgery. Note that all sutures were measured by straight pull. Difference in number of \* indicates statistical significance at  $p < 0.05$ . ### indicates statistical significance at  $p < 0.001$ .



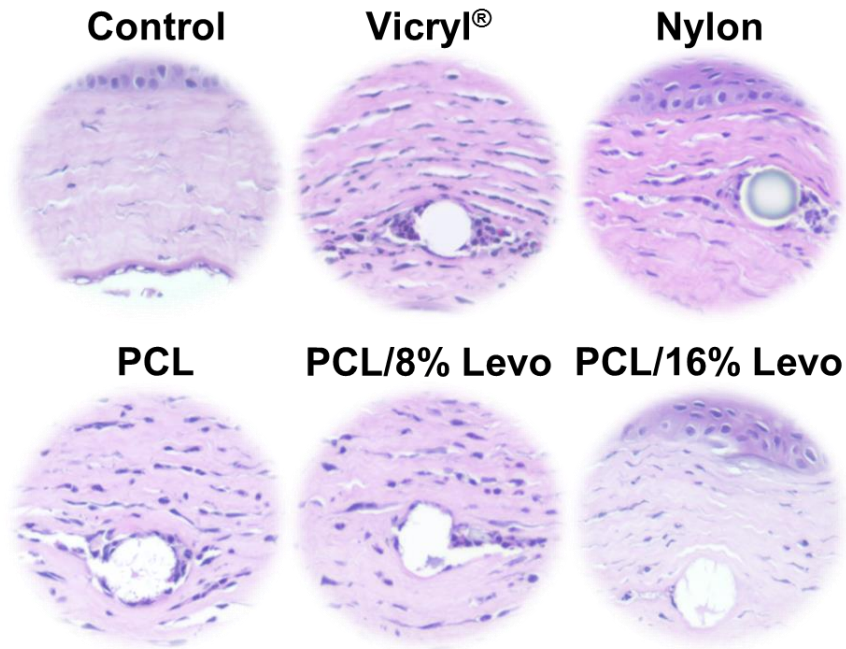


**Figure 3.3. Histological analysis of suture biocompatibility.**

Representative images of H&E-stained tissue surrounding Vicryl<sup>®</sup>, Nylon, PCL, PCL/8% Levo, and PCL/16% Levo sutures implanted into rat corneas for 2 days. Control indicates healthy, untreated corneal tissue.

**Table 3.1. Levofloxacin concentration in rat corneal tissue and aqueous humor.**

Concentration of levofloxacin within rat cornea and aqueous humor following implantation of three 2 mm segments of either 10-0 PCL/8% Levo or PCL/16% Levo sutures.

Time (hr)	PCL/8% Levo		PCL/16% Levo	
	Aqueous Humor (ng/mL)	Cornea (ng/g)	Aqueous Humor (ng/mL)	Cornea (ng/g)
<b>0.25</b>	4,125 ± 153	23,167 ± 5,714	4,650 ± 596	40,676 ± 1,875
<b>1</b>	3,503 ± 433	20,937 ± 2,398	5,145 ± 444	27,998 ± 3,690
<b>2</b>	1,877 ± 172	8,793 ± 1,528	4,144 ± 485	26,048 ± 4,518
<b>24</b>	54.5 ± 16	261 ± 47	122 ± 41	627 ± 214
<b>72</b>	12.3 ± 2.8	8.2 ± 0.6	33.8 ± 21	14.5 ± 5.6
<b>168</b>	133.9 ± 105	87.9 ± 58	210.9 ± 150	93.1 ± 63
<b>336</b>	2.1 ± 1.5	5.3 ± 0.6	3.3 ± 2.0	3.0 ± 0.4

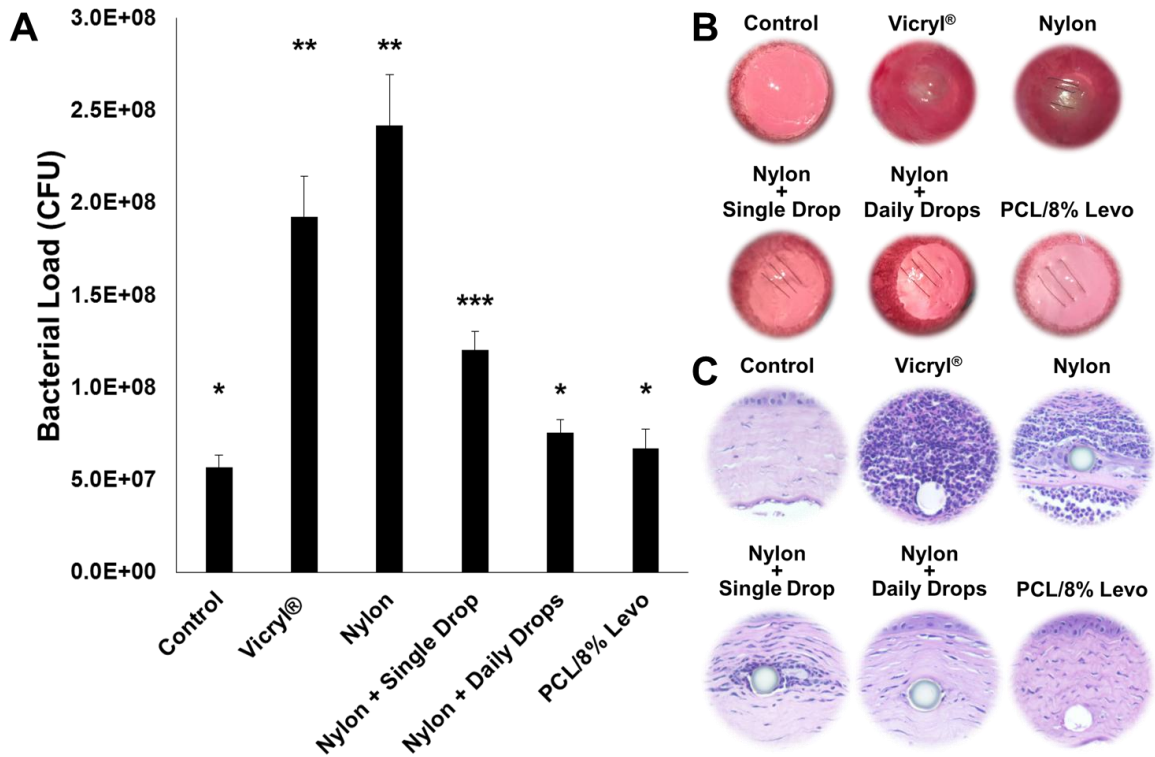


**Figure 3.4. Evaluation of ophthalmic infection 2 days after inoculation of *S. aureus*.**

(A) Concentration of bacteria in healthy control rat corneas or inoculated corneas containing either Vicryl®, Nylon, or PCL/8% Levo sutures. Nylon sutures were evaluated alone, with treatment of a single post-operative topical drop of 0.5% Levo, or with treatment of 3 daily drops of 0.5% Levo. Representative images of (B) healthy control and experimental eyes 2 days after bacterial inoculation, and (C) H&E stained tissue surrounding sutures 2 days after bacterial inoculation.

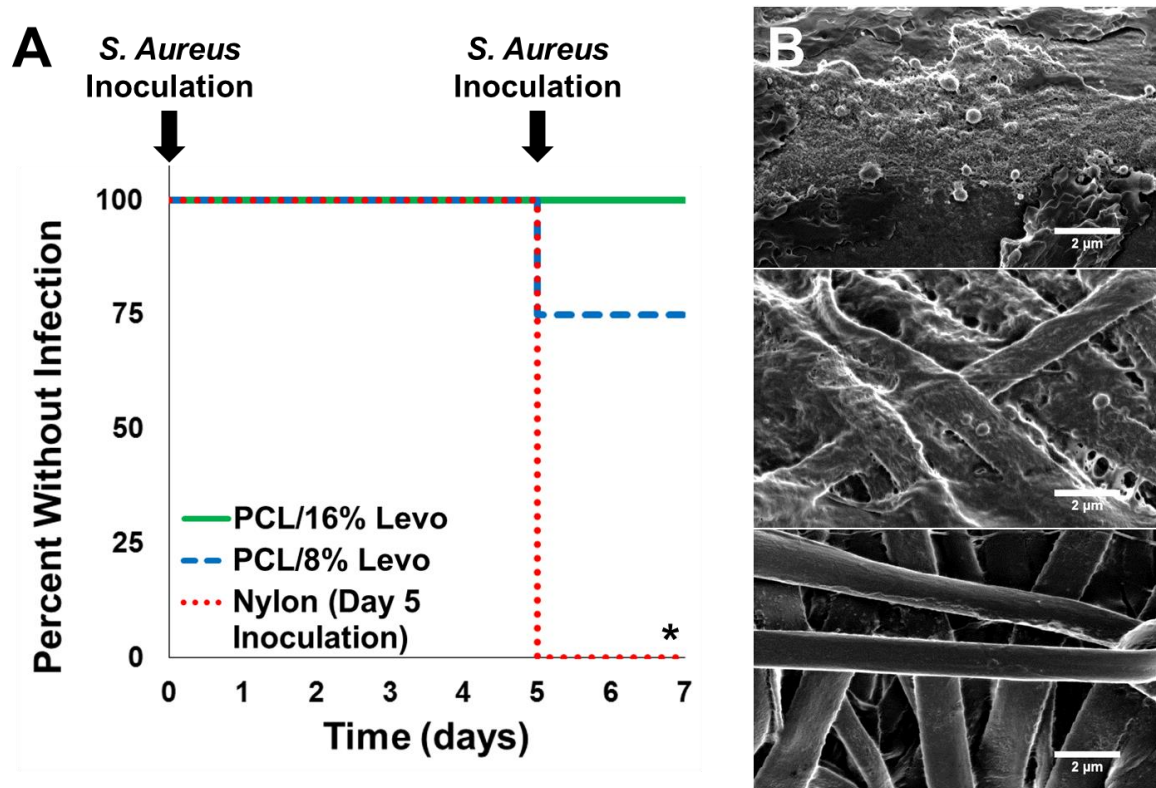


**Figure 3.5. Evaluation of ophthalmic infection following consecutive *S. aureus* inoculations over the period of 1 week.**

(A) Kaplan-Meier curve indicating prevention of ophthalmic infection following inoculation of on day 0 and day 5 of Sprague Dawley rat corneas implanted with either PCL/8% Levo or PCL/16% Levo sutures. Note that all sutures were implanted on day 0 and that corneas containing nylon sutures were only inoculated once, on day 5. \* indicates statistical significance at  $p < 0.01$ . (B) High magnification SEM images of nylon (top), PCL/8% Levo (middle), or PCL/16% Levo (bottom) sutures removed from rat corneas on day 7 following one or two bacterial inoculations.

## **4. Rapamycin-eluting, nanofiber-coated sutures for inhibition of neointimal hyperplasia following vascular anastomosis procedures**

### **4.1. Introduction**

Vascular anastomoses, or surgical connections between arteries and/or veins, are one of the most common surgical procedures involved in millions of vascular bypass, vascular access, solid organ transplant, and reconstruction procedures each year.<sup>108-112</sup> In each case, damage to the vessel walls during the surgical procedure, most often using sutures, leads to deposition of platelets which release inflammatory chemokines and platelet-derived growth factor.<sup>113-115</sup> This cascade signals the inward migration and proliferation of smooth muscle cells, or neointimal hyperplasia, resulting in thickening of the vessel wall.<sup>114,115</sup> The resulting stenosis, or narrowing of the vessel lumen, is the major cause of arterial, venous, arteriovenous, and prosthetic graft failure.<sup>36-40,116,117</sup> Approximately 30% of all arterial bypass grafts and 50% of venous grafts fail due to neointimal hyperplasia.<sup>115</sup> Permanent vascular access is critical for patients with chronic kidney disease or end-stage renal undergoing hemodialysis; however, failure rates are reported as high as 50%, and vascular access complications are responsible for 20% of patient hospitalizations.<sup>111,117,118</sup> There is a significant and unmet clinical need for anastomotic closure with reduced complications, particularly with regard to neointimal hyperplasia.

Several less-invasive closure technologies have been developed over the past few decades, including clips, adhesives, lasers, sleeves, rings, stents, and other devices;

however, each has its own limitations for use and/or complications, such as toxicity, leakage, occlusion, loss of strength, or the need to implant multiple devices.<sup>113,119-126</sup>

Thus, non-absorbable nylon sutures remain the gold standard for anastomotic closure due to their convenience, reliability, flexibility, and capacity to provide strength at the anastomotic site for an extended period of time.<sup>113</sup>

Local delivery of anti-proliferative drugs such as rapamycin (Rap) or paclitaxel may provide an alternative to changes in surgical procedure. The Cypher<sup>®</sup> rapamycin-eluting coronary stent first demonstrated the clinical benefit of local anti-proliferative delivery by preventing hyperplasia, and unlike oral delivery of rapamycin, demonstrated superiority to bare metal coronary stents for an extended period of time at a lower drug dosage.<sup>127-132</sup>

Over the past decade, interest in the development of drug-eluting sutures has grown with the objective of providing local drug delivery at the surgical site to prevent complications and/or enhance wound healing. Literature reports have demonstrated delivery of a wide range of prophylactic and therapeutic moieties, including antibiotics, growth factors, anesthesia, and even tacrolimus for prevention of neointimal hyperplasia.<sup>7,11-22,75</sup>

However, clinical translation of such technologies has been curtailed due to an inability to meet United States Pharmacopeia (U.S.P.) specifications for suture size and strength, provide sufficient and sustained drug delivery, and/or scale to commercial viability.<sup>12,14,17,75</sup> Thus, to date, the only market offerings are triclosan-coated sutures indicated for anti-infection applications in general surgery, and there are no drug-eluting sutures available for use in vascular surgery.<sup>27,58-60</sup>

In order to provide for successful anastomotic closure while also preventing neointimal hyperplasia, a suture must: (1) surpass U.S.P. specifications for suture strength, and maintain strength at the anastomotic site for an extended period of time; (2) meet size requirements for sutures used in vascular surgery (U.S.P. sizes 9-0 – 7-0; 30-69  $\mu\text{m}$  in diameter); (3) provide sufficient delivery of an appropriate drug; (4) have potential to scale its manufacturing.<sup>133</sup> Here, we investigate the use of a novel electrospinning system to produce highly tunable, drug-eluting, nanofibrous coatings for sutures. Electrospinning is an adaptable, well-understood process in which high voltage can be applied to a polymer or polymer/drug solution to draw out solid nanofibers and microfibers.<sup>6</sup> Specifically, we describe the manufacture of an 8-0-sized, non-absorbable suture with a nylon core and nanofiber coating composed of rapamycin, poly(L-lactide) (PLLA), and polyethylene glycol (PEG). Originally used as an anti-fungal agent, rapamycin has been shown to be a potent anti-proliferative and anti-inflammatory drug which inhibits the mammalian target of rapamycin (mTOR) pathway.<sup>134</sup> PLLA and PEG are generally regarded as safe polymers (GRAS) that have been widely utilized in drug delivery applications, and are already incorporated in medical devices approved by the United States Food and Drug Administration.<sup>66</sup> We investigate suture morphology, breaking strength, drug release, and capacity for anastomotic closure and inhibition of neointimal hyperplasia in a rat model of vascular anastomosis.

## 4.2. Materials and Methods

### 4.2.1. Suture Fabrication

Polymer solutions were made via dissolution of PLLA (221 kDa; Corbion, Amsterdam, Netherlands), PEG (35 kDa; Sigma Aldrich, St. Louis, MO), and rapamycin (LC Laboratories, Woburn, MA) in hexafluoroisopropanol (Sigma-Aldrich) by shaking overnight at room temperature. Polymer to solvent concentration was maintained at 10.8% and PEG to PLLA concentration was maintained at 3.9% for all formulations. Rapamycin concentration was 20%, 40%, or 80% in regard to PLLA for the 20% Rap/PLLA/PEG, 40% Rap/PLLA/PEG, and 80% Rap/PLLA/PEG formulations, respectively. Prior to electrospinning, the non-needled end of a 10-0 nylon suture (Ethicon, Somerville, NJ or AROSurgical Instruments, Newport, CA) was placed into the rotational collector. The needled end was driven through the hole in the opposing collector and allowed to hang loosely. Rap/PLLA/PEG solutions were then pumped through a 20 G blunt-tip needle at 1 mL/h with an applied voltage of 15 kV at a distance of 17 cm from the parallel, grounded collectors. The collector containing the non-needled end of the suture was then rotated clockwise for five minutes at 150 rpm and counter-clockwise for 30 s at an identical speed. The suture was then removed from the collectors and stored at -20 °C.



#### *4.2.2. Suture Characterization*

##### *4.2.2.1. Suture Size*

Suture diameter was determined via light microscopy (Eclipse TS100, Nikon Instruments, Melville, NY) and calibrated imaging software (Spot 5.2 Basic, Spot Imaging, Sterling Heights, MI). Each suture was measured at four different locations at least 2 cm apart, and used in further experimentation only if the average diameter was between 46 and 49  $\mu\text{m}$ , qualifying as an 8-0 suture.

##### *4.2.2.2. Suture Morphology*

Nylon and nanofiber-coated suture morphology were observed via scanning electron microscopy (SEM) at 1 kV using a LEO Field Emission SEM (Zeiss, Oberkochen, Germany). Prior to SEM, sutures were sputter coated with 10 nm of Au/Pd (Desk II, Denton Vacuum, Moorestown, NJ).

##### *4.2.2.3. In Vitro Drug Release*

20, 40, and 80% Rap/PLLA/PEG formulations were electrospun and twisted into 20  $\mu\text{m}$  diameter fiber bundles ( $n = 4$  for each condition). Fibers were cut to 15 mm in length and submerged in 200  $\mu\text{L}$  of 1x Dulbecco's Phosphate-Buffered Saline (PBS, Fisher Scientific, Waltham, MA) containing 0.5% (w/vol) Tween-20 (Fisher Scientific). Samples were placed on an orbital shaker at 37  $^{\circ}\text{C}$ , with the release medium collected and replenished with fresh media at 4 h, and at 1, 3, 5, 8, 11, and 14 days. Rapamycin concentration within the release media was measured via high performance liquid

chromatography (HPLC; Waters Corporation, Milford, MA) analysis. Samples were injected into a Symmetry™ 300 C18 5 µm column (Waters Corporation) with a mobile phase of water and methanol (30:70 v/v, Fisher Scientific) at a flow rate 0.8 mL/min for 30 min. Rapamycin elution was detected at a wavelength of 278 nm.

#### *4.2.2.4. Suture Breaking Strength*

Nylon sutures were coated with 20 and 40% Rap/PLLA/PEG nanofibers (n = 4 for each condition) and tied into a surgeon's knot, clamped vertically, and pulled until breaking at a rate of 16 mm/min using an 5966 Dual Column Tabletop Testing System (Instron, Norwood, MA).

#### *4.2.3. Animal Studies*

All animals were cared for and experiments conducted in accordance with protocols approved by the Animal Care and Use Committee of the Johns Hopkins University, and in compliance with the National Institutes of Health guidelines for the Care and Use of Laboratory Animals.

Briefly, female Lewis rats (Hilltop Lab Animals, Scottsdale, PA and Harlan Laboratories, Frederick, MD) were anesthetized via intraperitoneal injection of ketamine (50mg/kg) and xylazine (5mg/kg), and kept under anesthesia with 2% isoflurane in oxygen during the procedure. A portion of the infrarenal abdominal aorta was exposed and cross-clamped, after which three-quarters of the circumference of the aorta was sectioned. The sectioned aorta was then repaired via interrupted suturing using 8-0 nylon (Ethicon), 20%

Rap/PLLA/PEG/Nylon, or 40% Rap/PLLA/PEG/Nylon sutures (n = 6 for each condition). The patency of the anastomosis and ensuing hemostasis were confirmed prior to closure of the abdomen. Animals were monitored daily for 14 days for signs of infection or irritation, after which the abdominal aorta was harvested and fixed in formalin (Sigma Aldrich) for 24 h.

#### *4.2.3.1. Evaluation of neointimal hyperplasia*

Harvested tissue was embedded in paraffin, cross-sectioned, and stained with hematoxylin and eosin (H&E). Only sections containing sutures, indicating the anastomotic region, were utilized for evaluation of neointimal hyperplasia. Two measurements of neointimal hyperplasia thickness were taken for each section and then averaged. The individual sections at the anastomotic site were then averaged together for each replicate for each suture condition.

#### *4.2.4. Statistical Analysis*

Suture breaking strength, suture drug release, and neointimal hyperplasia are presented as mean  $\pm$  standard error. Statistical significance for suture breaking strength was determined via Student's *t*-test. Statistical significance for neointimal hyperplasia was determined via one-way ANOVA followed by Tukey test.

## 4.3. Results

### 4.3.1. Fabrication and Characterization of Nanofiber-coated Sutures

We hypothesized that coating a non-absorbable, nylon suture with absorbable, rapamycin-loaded nanofibers would simultaneously provide for sufficient drug release and sustained strength at the anastomotic site in order to provide for appropriate wound healing with reduced post-operative complications.

In order to coat a standard nylon suture in a uniform, reproducible, and highly tunable manner, we adapted the novel manufacturing system described in Chapter 3 consisting of a syringe pump with a polymer/drug solution perpendicular to a pair of grounded collectors, one of which is capable of rotation. The non-needled end of the nylon suture was attached to the collector capable of rotation, and the needled end of the suture was placed through the opposing collector (**Figure 4.1.A**). 20, 40, and 80% Rap/PLLA/PEG solutions were electrospun into nanofibers which deposited between the two parallel, grounded collectors, and were then twisted around the nylon suture by rotating the collector attached to the non-needled end of the suture.

Several electrospinning parameters, such as flow rate, applied voltage, and distance to collectors were optimized in order to manufacture nanofibers composed of rapamycin, PLLA, and PEG. **Figure 4.1.B** depicts a 10-0 nylon suture before (bottom) and after (top) coating with rapamycin-loaded nanofibers. Notably, coating thickness is reproducibly tunable and can be adjusted in a facile manner by modifying spray time. SEM images

displayed manufacture of non-porous, defect-free nanofibers wound tightly around the nylon thread core to form a nanofiber-coated suture. Thin and short polymeric fibers were also dispersed around the outside of the coating. **Figure 4.1.C** depicts both the nylon suture and coated nylon suture at a lower magnification, demonstrating the uniformity of the coating along the length of the suture.

The major challenge in the translation of drug-eluting sutures has been the inability to simultaneously surpass U.S.P. requirements for suture breaking strength while also providing sufficient and sustained drug delivery. Thus, we next examined the drug release profiles and breaking strength of Rap/PLLA/PEG/Nylon sutures.

#### *4.3.2. In Vitro Release of Rapamycin from Nanofiber-coated Sutures*

Previous studies in the literature have suggested that the addition of a small percentage of a hydrophilic moiety such as PEG can improve the release kinetics of a hydrophobic drug from a similarly hydrophobic polymeric matrix.<sup>75</sup> 20, 40, and 80% Rap/PLLA/PEG nanofibers each demonstrated continued rapamycin release *in vitro* for at least 14 days (**Figure 4.2.**). However, the release profiles of each nanofiber formulation varied drastically. The 20 and 40% formulations both demonstrated sustained release of rapamycin *in vitro*. However, as the concentration of drug within the formulation increased, a more pronounced burst effect was observed. A burst release profile was observed for both the 40 and 80% suture formulations with the majority of the rapamycin release occurring within the first 24 h in the case of the 80% rapamycin formulation.

#### 4.3.3. Nanofiber-coated Suture Breaking Strength

Based on the results of the *in vitro* drug release study, 20 and 40% Rap/PLLA/PEG coating formulations were chosen as lead candidates due to their capacity for sustained release. We next evaluated the breaking strength of 10-0 nylon sutures coated with either 20 or 40% Rap/PLLA/PEG nanofibers. According to the U.S.P., synthetic sutures resistant to the action of living mammalian tissue with a coating that adds significantly to suture diameter, but not to suture strength, are classified as Class II, non-absorbable surgical sutures.<sup>133</sup> The coating process used in this study increased the size of a standard 10-0 nylon suture to between 46 and 49  $\mu\text{m}$ , thus decreasing the U.S.P. size to 8-0.<sup>133</sup> The minimum average knot-pull tensile strength requirement for an 8-0, non-absorbable, Class II suture is 0.39 N.<sup>133</sup> As shown in **Figure 4.3.**, both 20 and 40% Rap/PLLA/PEG/Nylon sutures surpassed U.S.P. specifications for suture breaking strength by more than 30%. Moreover, because suture strength is derived from the nylon core, doubling the concentration of rapamycin within the coating formulation did not significantly affect suture strength

#### 4.3.4. Effect of Rapamycin Nanofiber Coating on Post-operative Neointimal Hyperplasia

Finally, we evaluated the potential clinical utility of rapamycin nanofiber-coated nylon sutures by determining their capacity to maintain an anastomotic site and decrease local neointimal hyperplasia. Following sectioning of the rat abdominal aorta, the vessel was anastomosed via interrupted suturing using 8-0 nylon, 20% Rap/PLLA/PEG/Nylon, or 40% Rap/PLLA/PEG/Nylon sutures. No suture-related complications were observed during any of the procedures. The nanofiber-coated nylon sutures were able to pass

through the tissue several times and suture the vessel appropriately without any peeling or loss of the coating. Further, vessel patency and hemostasis were confirmed immediately post-operatively in all cases. No anti-platelet or anti-coagulation therapy, or any other kind of therapy was provided in the 14 day post-operative period, and there was no operative or suture-related infection or mortality at any time under any condition.

After 14 days, rat abdominal aortas were harvested and evaluated grossly and via histology. In all cases, the sutures remained in place, and there was no leakage observed at the anastomotic site. H&E staining of tissue sections at the anastomosis confirmed the presence of neointimal hyperplasia within the inner lumen of vessels sutured using nylon (**Figure 4.4.A**), 20% Rap/PLLA/PEG/Nylon (**Figure 4.4.B**), and 40% Rap/PLLA/PEG/Nylon (**Figure 4.4.C**) sutures, indicated by a highly inflamed, pink-colored tissue region often adjacent to the sutures themselves. However, there was a significant reduction in neointimal hyperplasia thickness in tissues anastomosed using rapamycin-eluting sutures (**Figure 4.4.D**). Vessels anastomosed using either of the drug-eluting sutures displayed significantly lower ( $p < 0.01$ ) neointimal hyperplasia thickness in comparison to vessels sutured using the standard nylon suture. Further, 40% Rap/PLLA/PEG/Nylon sutures significantly decreased ( $p < 0.01$ ) neointimal hyperplasia in comparison to 20% Rap/PLLA/PEG/Nylon sutures, and reduced neointimal hyperplasia by 25% in comparison to the gold standard 8-0 nylon suture.

#### 4.4. Discussion

The local vascular smooth muscle cell population is multiplied up to five times in the 14 days following vascular anastomoses.<sup>114</sup> This post-operative inflammatory response contributes to 90% of the ultimate neointimal hyperplasia, and the resulting stenosis can have devastating consequences, including re-operation, graft/transplant failure, and death.<sup>111,114,116,118</sup> Thus, it is critical to modulate the local, post-operative biological response in order to improve the outcomes of arterial, venous, arteriovenous, and prosthetic graft procedures.

We developed a new method to endow conventional sutures with drug delivery functionality via a nanofiber coating, and evaluated its potential for use in vascular anastomosis procedures. Rapamycin-eluting, nanofiber coatings demonstrated uniformity along the length of the suture and remained intact while suturing *in vivo*. Further, this coating method allowed for facile tuning of nanofiber coating thickness and rapamycin release profile. Importantly, Rap/PLLA/PEG/Nylon sutures met or exceeded U.S.P. specifications for 8-0 suture diameter and strength, and reduced neointimal hyperplasia in comparison to a standard 8-0 nylon suture following anastomosis of the abdominal aorta in rats.

Rapamycin was chosen for this study due its extensive use, well-known mechanism of action, and demonstrated ability to reduce neointimal hyperplasia and stenosis in both experimental models and in the clinic.<sup>114,119,122,128,129</sup> However, there has been a concern



that while the anti-proliferative activity of rapamycin may inhibit neointimal hyperplasia, it may also inhibit appropriate endothelialization and healing at the anastomotic site.<sup>15</sup> In this study, both rapamycin-eluting suture conditions demonstrated a significant reduction in neointimal hyperplasia while also maintaining the vascular anastomosis through the duration of the study. Thus, it appears that the capacity of the nanofiber coatings to deliver low levels of drug in a sustained manner may provide sufficient modulation of the post-operative inflammatory response while also allowing for appropriate vessel healing. Further, major advantages of this platform are the versatility of electrospinning to incorporate almost any polymer and/or drug, and that the nanofiber coating is not required to contribute to suture strength.<sup>65</sup> Thus, almost any polymer/drug formulation can be implemented to achieve the appropriate release of the active agent in a manner that both significantly reduces neointimal hyperplasia and stenosis while promoting long-term vascular health. The use of this highly versatile and tunable coating platform as a research tool may help to further elucidate the types of drugs and release profiles that are conducive to realizing both objectives.

Another advantage of this coating method is its potential to incorporate multiple types of fibers into a single, tightly wound coating. For example, a coating composed of both short- and long-term degradation fibers could be used to provide early- and extended-term drug release to prevent both immediate- and late-stage complications. Our studies demonstrated that an initial burst release of rapamycin may improve outcomes; however, extended release of rapamycin will be useful in conjunction with non-absorbable sutures which are a source of inflammation as long as they are present at the anastomotic site.<sup>113-</sup>

<sup>115</sup> Additionally, the nanofiber coating could be designed to release an anti-proliferative drug to reduce neointimal hyperplasia and an antibiotic to prevent infection, which is another leading cause of prosthetic graft failure.<sup>111,117</sup>

Although the nanofiber-coated nylon sutures described in this study surpassed U.S.P. requirements for suture strength and maintained the anastomotic site for at least 14 days, it is important to note that the U.S.P. only specifies a minimum average suture breaking strength. Prior to clinical studies, it will be important to evaluate the durability of nanofiber-coated sutures in larger animal models and in different types of anastomoses for a longer duration to ensure that they maintain the anastomosis. If they are successful, nanofiber-coated sutures may have significant potential for use in vascular anastomosis procedures due to their capacity to reduce neointimal hyperplasia without changing the surgical procedure or clinical workflow.

#### **4.5. Conclusion**

This study demonstrated the manufacture of a nanofiber-coated, nylon suture capable of meeting U.S.P. specifications for suture size and strength for vascular surgery, providing sustained release of rapamycin, maintaining the anastomotic site, and reducing post-operative neointimal hyperplasia in a rat model of vascular anastomosis. The coating is composed of GRAS materials, and did not peel or disintegrate during the surgical procedure. This platform has the potential to reduce post-operative complications and improve the clinical outcomes following vascular bypass and vascular access surgeries,

which present a significant economic and health burden, without modifying the current surgical workflow.

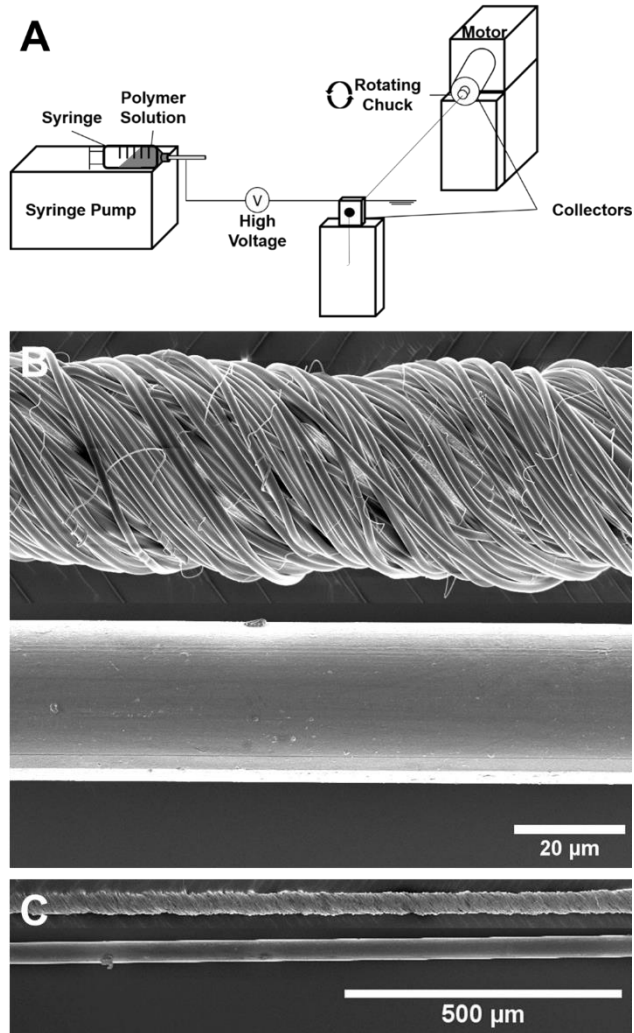


**Figure 4.1. Manufacturing schematic and SEM images of nanofiber-coated sutures.**

(A) Schematic of suture coating system: high voltage is applied to the nozzle of a syringe containing a volatile polymer/drug solution which is pumped at a controlled rate.

Electrospun fibers are deposited between two parallel grounded collectors surrounding a standard suture attached to one collector and driven through the opposing collector.

Following fiber deposition, one collector is mechanically rotated to twist deposited fibers into a uniform coating around the suture. (B) High magnification SEM image of a 10-0 nylon suture (bottom) and a 10-0 nylon suture coated with Rap/PLLA/PEG nanofibers

(top). (C) Low magnification SEM image of a highly uniform nanofiber-coated 10-0 nylon suture (top) and 10-0 nylon suture (bottom).

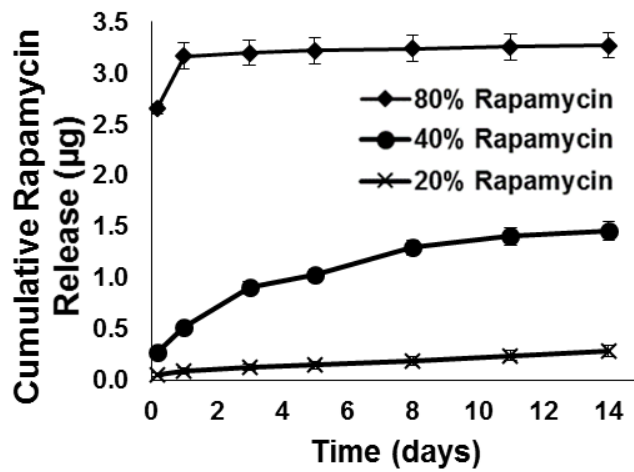


**Figure 4.2. Cumulative *in vitro* release of rapamycin.**

*In vitro* release profiles of rapamycin from PLLA/PEG nanofibers containing different amounts of rapamycin within the coating formulation.

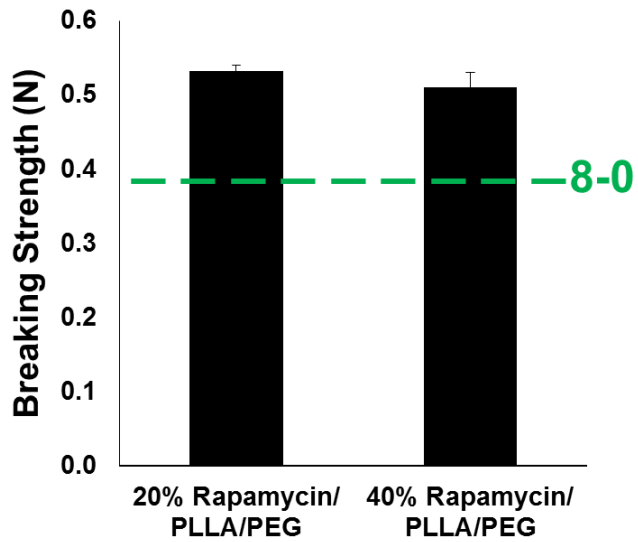


**Figure 4.3. Breaking strength of nanofiber-coated nylon sutures in reference to U.S.P. specifications.**

Comparison of knot-pull breaking strength of 8-0-sized Rap/PLLA/PEG/Nylon sutures containing 20% or 40% rapamycin within the coating formulation. Sutures are classified as a Class II non-absorbable surgical suture by the U.S.P.

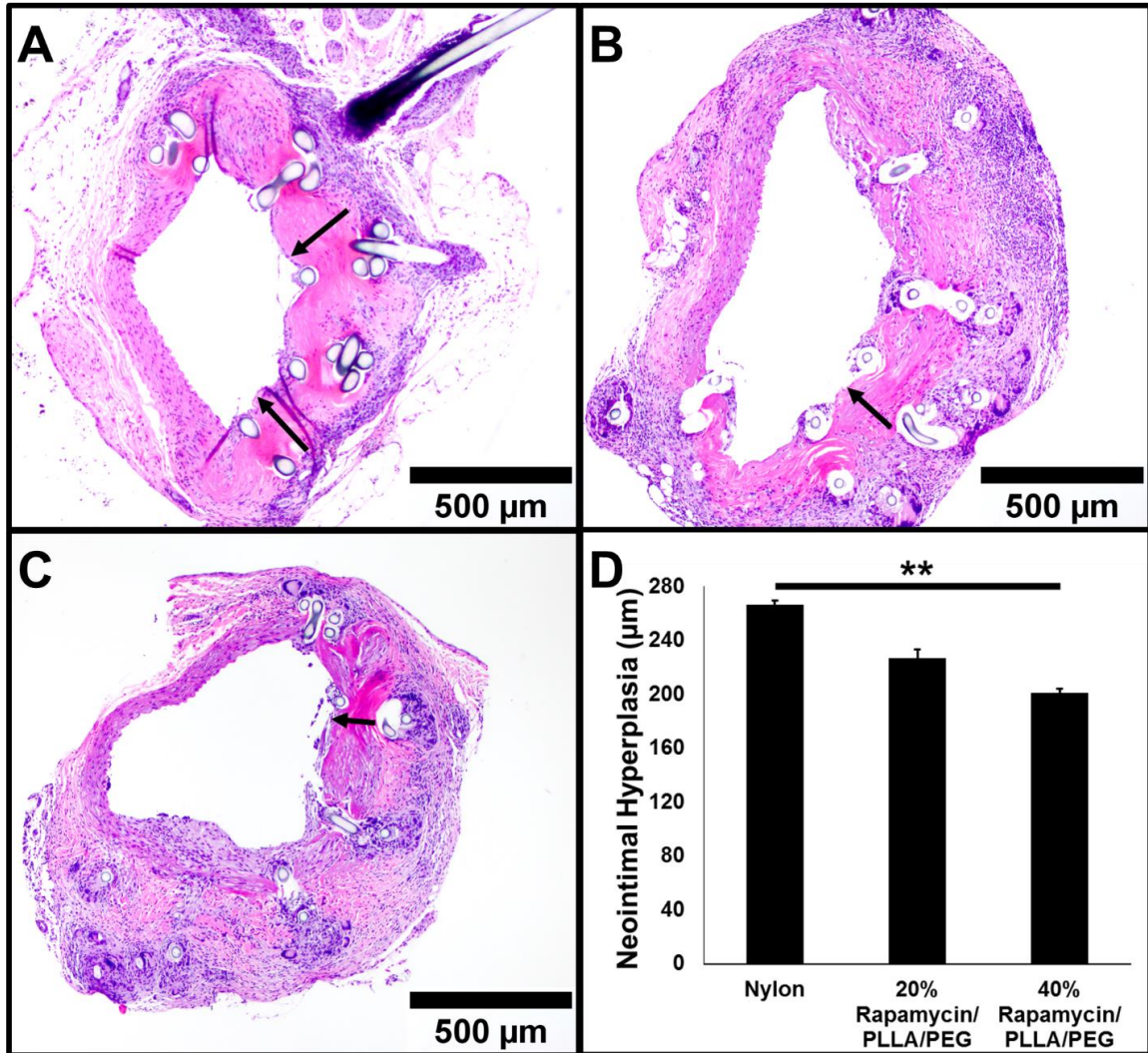


**Figure 4.4. Evaluation of neointimal hyperplasia following vascular anastomosis.**

Representative images of H&E-stained tissue sections of rat abdominal aorta 14 days after anastomosis procedure using (A) nylon suture (8-0), (B) 20%

Rap/PLLA/PEG/Nylon suture (8-0), and (C) 40% Rap/PLLA/PEG/Nylon suture (8-0).

Black arrows indicate regions of neointimal hyperplasia. (D) Quantification of neointimal hyperplasia. Data are calculated as means  $\pm$  SEM. \*\* denotes  $p < 0.01$ .



## **5. Reduction of intraocular pressure in rabbits via a nano-structured glaucoma drainage implant**

### **5.1. Introduction**

Glaucoma is a leading cause of irreversible vision loss and a growing worldwide problem. Over 60 million people were affected by this vision threatening disease in 2010, and this number is predicted to almost double by 2040.<sup>42,43</sup> Approximately 8 million people were bilaterally blind due to glaucoma in 2010 and it is predicted that this number will rise to more than 12 million in 2020.<sup>42</sup> Intraocular pressure (IOP) reduction prevents the development of glaucoma and vision loss from glaucoma.<sup>44,45</sup> Clinically, physicians use medications, laser procedures, and/or incisional surgeries to lower IOP. Topical medications are the first-line therapy as they can effectively reduce IOP while avoiding the risks associated with more invasive procedures and surgeries. However, topical medications do not always lower IOP sufficiently to halt disease progression, are associated with poor patient adherence, and can cause symptomatic eye surface irritation and redness.<sup>135</sup>

The greater risk associated with surgical approaches to IOP reduction is partly attributed to a lack of standardization correlated with post-operative complications.<sup>46,50</sup> The most frequently performed IOP-lowering surgeries create a vent to release pressure from the eye.<sup>136</sup> The specific IOP at which these vents function is often determined by *ad hoc* interventions performed by the surgeon that are at risk for variability from surgeon to

surgeon and by individual surgeons from procedure to procedure. The trabeculectomy is the most commonly performed incisional glaucoma surgery, and was performed in 23,877 Medicare beneficiaries in 2012.<sup>137</sup> Fluid flow through the venting region of a trabeculectomy is regulated by the tension created by sutures that secure a flap of scleral tissue. This process leads to inconsistent outcomes, as sutures often need to be cut in the post-operative period due to inadequate IOP reduction, and the frequency of post-operative hypotony can exceed 10%.<sup>47,51</sup> Hypotony – a term that describes IOPs that are too low – most commonly occurs at IOPs lower than 5 mmHg and can be associated with blurry vision, macular folds, choroidal detachments, and anterior chamber shallowing.<sup>138</sup>

Aqueous tube shunts that drain to subconjunctival reservoirs offer an alternate surgical approach to IOP reduction that has increased in popularity over the past decade. Tube shunt insertion in Medicare beneficiaries increased from 6,307 in 2002 to 12,021 in 2012.<sup>137</sup> However, these devices are still susceptible to post-operative complications, and surgeons have had to devise a number of strategies to minimize post-operative hypotony. The Baerveldt® glaucoma drainage implant (GDI) requires formation of a fibrotic capsule around the implant in order to prevent hypotony, but this process does not occur until several weeks following surgery. Thus, the tube must be occluded or tied off for a period of 4-6 weeks in the post-operative period prior to capsule formation.<sup>139</sup> This strategy either allows for no IOP reduction in the immediate post-operative period or requires the surgeon to create venting incisions in the tube that can lead to inconsistent outcomes.<sup>140,141</sup> The Ahmed GDI contains a valve that is designed to vent above IOPs of 7 mmHg; however, pre-implantation testing of Ahmed valves revealed that 16% of valves did not meet this

specification (either vented bellow 7 mmHg or above 15 mmHg).<sup>142</sup> These cases highlight the need for a more standardized, safer approach to glaucoma surgery.

More recently developed GDIs standardize venting IOP and reduce the risk of post-operative hypotony by utilizing dimensions modeled by the Hagen-Poiseuille equation (HPE):

$$\Delta P = \frac{8\mu LQ}{\pi r^4} \quad (1)$$

The HPE calculates resistance of an incompressible, Newtonian fluid in laminar flow through a cylindrical tube.<sup>143</sup> When applied to IOP reduction in the eye, the venting resistance ( $\Delta P$ ) to fluid outflow is inversely proportional to radius raised to the fourth power ( $r^4$ ) and directly proportional to tube length ( $L$ ), aqueous humor volumetric flow rate ( $Q$ ), and aqueous humor viscosity ( $\mu$ ). The XEN45 microfistula implant has an internal diameter of 45  $\mu\text{m}$  and a length of 6 mm.<sup>143-145</sup> Fluid flowing through this device at a physiological flow rate of 180  $\mu\text{l/h}$  creates a pressure differential of 6.28 mmHg, theoretically avoiding IOPs associated with the complications of hypotony.<sup>143</sup> The dimensions of the InnFocus Microshunt<sup>®</sup> (inner luminal diameter of 70  $\mu\text{m}$ , length of 8.5 mm) are similarly designed to maintain an IOP greater than 5 mmHg.<sup>146,147</sup>

In addition to device design and dimension, material composition can also affect GDI effectiveness.<sup>148</sup> The ideal material must provide flexibility to conform to the contours of the eye, strength to remain patent *in vivo*, and be non-immunogenic.<sup>143,147,149</sup> Electrospinning is a promising platform for the development of shunts for glaucoma surgery, as it allows for incorporation of almost any polymer and prophylactic or

therapeutic moiety into nano or microfibers which can be configured into devices of various dimensions and conformations.<sup>6,65</sup> To date, this approach has been used widely in tissue engineering, and more recently, in the manufacture of medical devices, such as sutures.<sup>150</sup> Here, we describe an electrospinning platform that can create small lumen cylindrical shunts and explore whether these devices are suitable for use as GDIs.

## **5.2. Materials and Methods**

### *5.2.1. Simulation of Flow through Shunt*

Modeling of pressure differential through the shunt was accomplished through use of MATLAB<sup>®</sup> (Mathworks, Natick, MA) and according to the HPE equation by varying flow rate, shunt diameter, and shunt length. The viscosity (0.72 cP) and average flow rate (150  $\mu\text{L/h}$ ) of human aqueous humor at physiological conditions were input for the values of  $\mu$  and  $Q$ , respectively.<sup>143</sup>

### *5.2.2. Electrospun Shunt Manufacture*

PET shunts were manufactured through electrospinning by utilizing a grounded collector consisting of a drill chuck (McMaster-Carr, Elmhurst, IL) and parallel collector stand positioned perpendicular to the polymer jet. Stainless steel wire with a diameter of 50  $\mu\text{m}$  (McMaster-Carr) was inserted through a 25 G, 3.81 cm long, blunt tip needle (Nordson EFD, Westlake, OH) which was then placed into the head of the drill chuck. PET (gift from Nanofiber Solutions, Columbus, OH) was dissolved in 1,1,1,3,3,3-hexafluoro-2-propanol (Sigma Aldrich, St. Louis, MO) at 10 wt% by stirring at 45 °C for 24 h. The polymer

solution was then electrospun onto the wire rotating clockwise at 175 rpm by applying 15 kv of voltage from a power supply (Glassman High Voltage, High Bridge, NJ) to a 20 G blunt tip needle (Nordson EFD) with the polymer solution flowing at a controlled rate of 1.5 mL/h using a programmable syringe pump (New Era Pump Systems, Farmingdale, NY). The shunt was then heated in an oven (Sheldon Manufacturing, Cornelius, OR) for 24 h at 100 °C prior to cooling to RT.

### *5.2.3. Shunt Characterization*

Outer shunt diameter was measured via optical microscopy using an Eclipse TS100 (Nikon Instruments, Melville, NY). Inner lumen diameter and shunt morphology were examined via scanning electron microscopy (SEM) at 1 kv with a LEO Field Emission SEM (Zeiss, Oberkochen, Germany) following desiccation for at least 24 h and sputter coating with 10 nm of Au/Pd. Imaging was conducted prior to removal of the template wire, after removal of the wire, and following *in vitro* fluid flow studies.

### *5.2.4. Evaluation of In Vitro Fluid Flow through Shunt*

PET Shunts were cut to 5, 6, or 7 mm in length (n = 3 for each length), after which the template wire was removed. The shunt was then connected in circuit to a syringe pump and manometer (NETECH, Farmingdale, NY) via the 25 G needle. All flow studies were conducted at RT. 1x Dulbecco's Phosphate Buffered Saline (PBS, ATCC, Manassas, VA) was pumped through the shunt at 50, 100, and 200  $\mu$ L/h. Prior to flow studies, PBS was pumped through a 25 G needle at the specified flow rate and the resulting pressure measurement was subtracted from the pressure observed with attachment of the PET shunt.

Pressure measurements were recorded at least 30 min after a change in flow rate and only if the pressure remained constant for more than 5 min. Long-term flow studies (n = 3) were conducted by flowing PBS through a 6 mm shunt at 150  $\mu$ L/h for 7 days. Theoretical pressure estimates were obtained from the HPE with tube diameter of 50  $\mu$ m and 25 °C PBS viscosity of 0.9 cP.<sup>151</sup>

#### *5.2.5. In Vivo Performance and IOP Measurement*

All animals involved in these studies were cared for in accordance with protocols approved by the Johns Hopkins University Animal Care and Use Committee. Protocols are also in accordance with the ARVO Statement for the Use of Animals in Ophthalmic and Vision Research. New Zealand White rabbits (Robinson Services, Mocksville, NC) were sedated by subcutaneous injection of Ketamine:Xylazine (75:5 mg/kg, Sigma Aldrich). A drop of 0.5% proparacaine hydrochloride ophthalmic solution (Bausch & Lomb, Tampa, FL) followed by a drop of 5% betadine solution (Alcon, Fort Worth, TX) was administered to the operative eye. After placement of an 8-0 silk, stay suture (Ethicon, Somerville, NJ) in the superotemporal limbus, a two-clock hour, fornix-based peritomy was created superotemporally, and the conjunctiva was dissected posteriorly. A 25 G needle (Fisher Scientific, Waltham, MA) was used to create a 2 mm long scleral tunnel prior to entering the anterior chamber. The shunt was gently guided through this tunnel. Once the shunt was in position, the template wire was removed and a 10-0 nylon cross-stitch (Ethicon) was placed at the site of tube entry to prevent fluid leakage around the tube. Balanced saline solution (BSS, Alcon) was irrigated in the anterior chamber using a 30 G needle (Fisher Scientific) to validate shunt patency. The conjunctiva was approximated to the limbus

using two 10-0 nylon sutures and, again, BSS was irrigated into the anterior chamber to ensure that a water-tight bleb had formed. The stay suture was then removed and topical antibiotic ointment was administered to the eye. In this manner, 3 open lumen and 3 closed lumen (containing the template wire) PET shunts were implanted. All shunts were 6 mm in length. Rabbits were monitored daily for signs of infection, inflammation, or irritation, and were monitored periodically through the duration of the experiment. IOP was measured and calibrated as previously reported.<sup>152</sup> Briefly, IOP was measured at 1, 4, 7, 11, 14, 21, and 27 days using a TonoVet (iCare, Vantaa, Finland) rebound tonometer in awake, restrained rabbits without topical anesthesia.

#### *5.2.6. Assessment of In Vivo Biocompatibility*

Following IOP measurement 27 days after implantation, rabbits were euthanized and eyes enucleated, fixed in formalin (Sigma Aldrich), embedded in paraffin, cross-sectioned, and stained with hematoxylin and eosin for histological evaluation.

#### *5.2.7. Statistical Analysis*

Results are presented as mean  $\pm$  SE. IOP data were analyzed using a Student's t-test, and differences between parameters were considered statistically significant for p values  $< 0.05$ .

### 5.3. Results

#### 5.3.1. Simulated Pressure Change

Under physiological conditions, aqueous humor is an incompressible, Newtonian fluid.<sup>143</sup> Thus, by utilizing the HPE and physiological values of aqueous humor viscosity and flow rate, it is possible to determine the dimensions of a non-valved, cylindrical shunt capable of providing IOP reduction while also providing sufficient resistance to flow to prevent hypotony (**Figure 5.1.A**). Through variation of shunt diameter with flow rate held constant at 150  $\mu\text{L/h}$ , simulations revealed that a cylindrical shunt with inner diameter  $\geq 75 \mu\text{m}$  will lead to hypotony at any physiologically relevant shunt length (**Figure 5.1.B**). However, a shunt with a 50  $\mu\text{m}$  inner diameter and greater than 4 mm in length may provide sufficient resistance to flow to maintain IOP above 5 mmHg. In order to achieve significant IOP reduction while simultaneously avoiding hypotony, 5-6 mm long shunts may be ideal. Through variation of shunt length with inner diameter held constant at 50  $\mu\text{m}$ , our simulation confirmed that a 6 mm long shunt is likely to avoid IOPs associated with hypotony, even if aqueous humor flow rate were to fall below its physiological average of 150  $\mu\text{L/h}$  (**Figure 5.1.C**).

#### 5.3.2. Shunt Fabrication and Characterization

Based on the modeling of aqueous humor flow through a cylindrical shunt at physiological conditions, non-absorbable, nano-structured shunts were manufactured using the electrospinning setup depicted in **Figure 5.2.A** with the cross-sectional dimensions shown in **Figure 5.2.B**. 15 kV of voltage was applied to a 10 wt% solution of PET in HFIP flowing



at 1.5 mL/h perpendicular to a rotating, grounded, stainless steel wire. This provided for a dense and uniform coating of PET nanofibers onto the template wire with low wall porosity following heat treatment (**Figure 5.3.A**). In order to achieve high strength and maintain lumen integrity *in vivo*, shunts were manufactured with a wall thickness of  $354 \pm 15 \mu\text{m}$ , and composed of nanofibers, which demonstrate a higher tensile modulus than larger diameter electrospun fibers.<sup>103</sup> 5, 6, and 7 mm long shunts were manufactured with an internal lumen diameter of  $50 \mu\text{m}$  formed via removal of a  $50 \mu\text{m}$  template wire. Prior to *in vitro* flow studies, the shunt was cut to the appropriate size, and the template wire (**Figure 5.3.B**) was removed from the inner lumen (**Figure 5.3.C**).

### 5.3.3. *In Vitro* Performance and Flow through Shunt

Electrospun shunts were evaluated *in vitro* to determine if they are leak-proof, durable, and provide the resistance to flow predicted by the HPE. PBS was pumped through 6 mm long PET shunts at a flow rate of  $150 \mu\text{L/h}$  for a period of one week to evaluate shunt integrity and durability. As shown in **Figure 5.3.D**, the lumen of the shunt remained patent and maintained its size after one week of continuous flow. The inner surface of the shunt was composed of aligned nanofibers showing no degradation or breaking. Moreover, leakage of PBS through the shunt wall was not observed through the duration of the study.

Pressure was also monitored as PBS was pumped through 5, 6, and 7 mm long shunts at physiologically relevant flow rates of 50, 100, and  $200 \mu\text{L/h}$ . Fluid flow studies demonstrated that resistance to flow increased with increased flow rate and increased shunt length (**Figure 5.4.A-C**). At each shunt length, there was a strong correlation between the

experimental measurements and theoretical pressure values predicted by the HPE. This correlation became stronger as shunt length, and therefore, entrance length increased. The percent difference between the slope of the linear trendline of experimental values and slope of the theoretical values was 22%, 8%, and 0%, respectively, for 5, 6, and 7 mm long shunts.

#### *5.3.4. IOP Reduction*

6 mm long PET shunts with either an open or closed lumen were implanted in normotensive rabbit eyes for 27 days via an ab externo procedure designed to vent aqueous humor via subconjunctival outflow. Procedure time ranged from 8-12 min for both types of shunts, and no complications were observed during the procedure or during the immediate post-operative period. The lowest average IOP for rabbits with either open or closed PET shunts was observed 24 h post-operatively, indicating that the procedure itself may have contributed to IOP reduction in the immediate post-operative period (**Figure 5.5.A-B**). However, hypotony and flattening of the anterior chamber were not observed in the immediate, early, intermediate, or late post-operative period. The IOP of operated rabbit eyes containing closed PET shunts was not significantly different than that of the respective control contralateral eye. The decrease in IOP ranged from -4% to 25% on individual days following implantation, with the maximum decrease observed immediately post-operatively. Operated rabbit eyes containing open PET shunts demonstrated a statistically significant decrease in IOP in comparison to the control contralateral eye. IOP reduction ranged from 24% to 57% on individual days following implantation. The IOP of operated

eyes containing open PET shunts was also significantly lower than that of operated eyes containing closed PET shunts.

#### 5.3.5. *In Vivo* Biocompatibility

Nano-structured PET shunts were well-tolerated by rabbit eyes. Implanted shunts did not migrate into the anterior chamber during the course of the study, and there were no gross signs of infection, hyphema, or inflammation due to open or closed shunt implantation. Histological analysis of control subconjunctival tissue and tissue surrounding implanted shunts revealed the migration of cells to the periphery, and into the wall of PET shunts (**Figure 5.6.A-C**). Neovascularization was not observed in the immediate vicinity of either open or closed PET shunts. Notably, tissue sections also reveal that open PET shunts maintain their original inner and outer diameter (data not shown) for at least 27 days following *in vivo* implantation.

### 5.4. Discussion

There is a need for glaucoma drainage devices with reduced post-operative complications, decreased reliance on ad hoc surgical “fixes,” and improved long-term outcomes. Here, we described the manufacture and evaluation of an electrospun tube shunt with dimensions derived from the HPE to preclude post-operative hypotony. Fluid flow through the nanofiber PET shunt obeys the HPE, and the shunt is strong, leak-proof, and durable. The shunt is biocompatible and significantly decreases IOP for at least 27 days in a normotensive rabbit model.

To our knowledge, this is the first study to utilize electrospinning in the manufacture of a glaucoma drainage implant.<sup>153,154</sup> Electrospinning is a simple and versatile platform for the manufacture of medical devices. It is compatible with almost any natural or synthetic polymer, can incorporate prophylactic or therapeutic moieties, and be realized into a wide range of different morphologies or conformations.<sup>6,7</sup> Devices manufactured via electrospinning are also highly modifiable through coatings, laser cutting, and other processing modifications to tune almost every aspect of the device, including size, shape, strength, rigidity, porosity, degradability, glidability, and biocompatibility. For example, nanofibers have been shown to demonstrate increased strength and decreased porosity in comparison to microfibers.<sup>103,155</sup> In this study, the use of nanofibers to construct glaucoma shunts likely contributed to maintenance of an intact shunt lumen *in vivo* and prevention of leaking during flow studies *in vitro*. Heat treatment can be used to further increase shunt strength by aligning polymer chains and enhancing crystallinity, and if necessary, spray time can be modified to change wall thickness and modulate shunt flexibility.<sup>156</sup>

Electrospinning and its versatility seem especially pertinent to the treatment of glaucoma with drainage devices, where the use of slightly inflammatory materials such as polypropylene can lead to device failure, and where scar formation and fibrosis cause significant complications.<sup>148,157</sup> PET was chosen in this application because it is generally regarded as safe, has excellent biostability, a well-understood fibrotic response, and has been used in medical devices for over 50 years.<sup>158</sup> However, should PET have not provided the appropriate strength, flexibility, or biological response, electrospinning permits facile interchange of polymer and/or modification of the manufacturing process to tailor the shunt

to fit the clinical need. Moreover, the capacity of electrospinning to manufacture nanofibers and incorporate them into a medical device, is a substantial advantage in glaucoma treatment. In their natural environment, cells interact with nanoscale architecture and cues within the surrounding extracellular matrix. These cues can affect cell migration, morphology, orientation, and even gene regulation. Kam and coworkers have demonstrated that nanoscale features with high aspect ratios decrease expression of several growth factors associated with fibrosis.<sup>8</sup> Their experiments revealed that these features can also reduce protein adsorption, which has been implicated in glaucoma device fouling and can lead to infection, increase in IOP, or device failure.<sup>9</sup> The methods used to manufacture marketed drainage devices, such as the iStent<sup>®</sup>, MicroShunt<sup>®</sup>, or XEN Gel Stent are limited in their capacity to achieve these effects through manufacturing alone.<sup>159</sup> However, it is important to note that the porosity of nanofibrous devices make them vulnerable to cell and/or tissue ingrowth over the long-term.<sup>158</sup>

While electrospinning may be a suitable platform for manufacture of glaucoma shunts, the safety and efficacy of shunts designed using HPE is still under investigation in humans. The XEN Gel Stent was also designed using the HPE, but is vulnerable to hypotony and anterior chamber shallowing in the immediate post-operative period at inner diameter dimensions of 63 or 140  $\mu\text{m}$ .<sup>144</sup> Due to the small lumen of the XEN Gel Stent with a 45  $\mu\text{m}$  inner diameter, fouling could theoretically affect its function over the long-term.<sup>149</sup> Venting resistance is inversely proportional to  $r^4$ , thus, small variations in shunt diameter can have a considerable effect on venting IOP. Moreover, the HPE may not be able to accurately predict the performance of shunts *in vivo*, as the shunts are curved to suit ocular

anatomy. Additionally, *in vitro* fluid flow studies demonstrated that shorter PET shunts demonstrated a weaker correlation with the HPE. This may be due to the entrance length required to transition into stable, laminar flow, and is another factor to consider in the HPE-driven design of glaucoma shunts.<sup>160</sup>

Although the long-term efficacy of HPE-designed MIGS in humans is still under investigation, the performance of nano-structured PET shunts in healthy, normotensive rabbits in this study is promising. Open PET shunts maintained their inner diameter and significantly decreased IOP for at least 27 days in comparison to the non-operated contralateral eye. This is in stark contrast to previously conducted trabeculectomy and drainage implant procedures in healthy New Zealand White rabbits. Trabeculectomy procedures in these rabbits fail within 7 days without the use of an antifibrotic or antimetabolite agent.<sup>161</sup> In a prospective, non-randomized study of fourteen patients, the MicroShunt<sup>®</sup> demonstrated a 49.8% reduction in IOP in conjunction mitomycin C after 3 years; however, prior studies in New Zealand White rabbits demonstrated no significant change in IOP in comparison to non-operated eyes or to implantation of silicone tubing with an inner diameter of 300  $\mu\text{m}$ .<sup>162,163</sup> This suggests that open PET shunts may be able to vent significantly more aqueous humor in comparison to a healthy drainage system alone. Additional longer-term studies and studies in diseased animal models may help to better understand this result, and to evaluate its potential clinical utility.

## 5.5. Conclusion

This study demonstrated the manufacture of a high strength, non-absorbable, minimally invasive glaucoma drainage implant via electrospinning. The shunt was designed through simulation of the HPE under physiological conditions in order to promote long-term IOP reduction while preventing hypotony. *In vitro* studies revealed that the PET shunt is leak-proof and durable, and that fluid flow through the shunt behaves according to the HPE. *In vivo* experiments reveal that the shunt maintains its inner diameter and significantly decreases IOP for at least 27 days in normotensive rabbit eyes. This versatile fabrication platform could be used to manufacture next generation glaucoma shunts composed of almost any material and capable of additional functionality, including drug delivery.

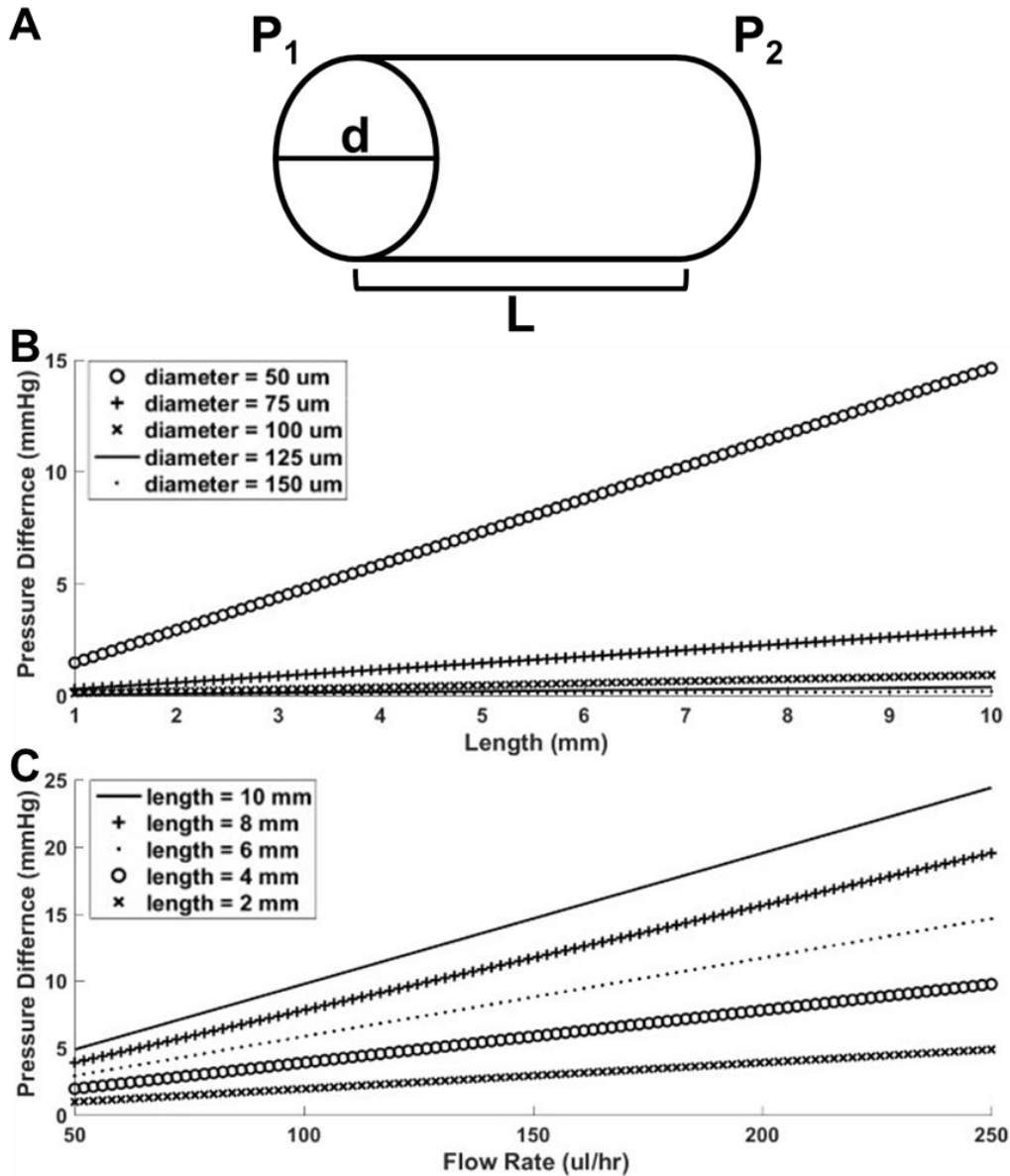


**Figure 5.1. Model of pressure change through shunt.**

(A) Example shunt modeled using the HPE. (B) Change in pressure difference with change in shunt length at a flow rate of 150  $\mu\text{L/h}$ . (C) Change in pressure difference with change in flow rate for a 50  $\mu\text{m}$  diameter shunt. A 6 mm long shunt with a 50  $\mu\text{m}$  diameter is expected to provide significant IOP reduction under physiologically relevant flow rates.



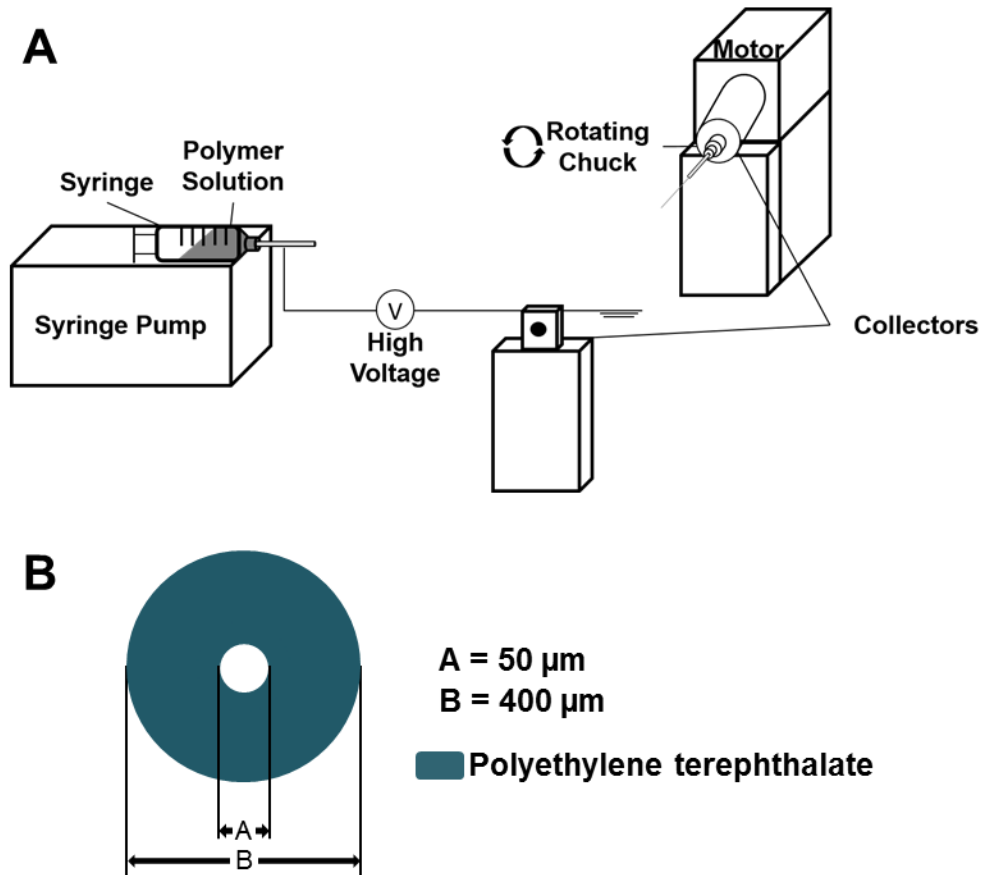


**Figure 5.2. Manufacturing system and shunt design.**

(A) Schematic of electrospinning setup: high voltage is applied to the polymer solution which is then spun into a fiber coating around the template wire. (B) Design of PET shunt. Inner lumen size is dictated by the size of the template wire.

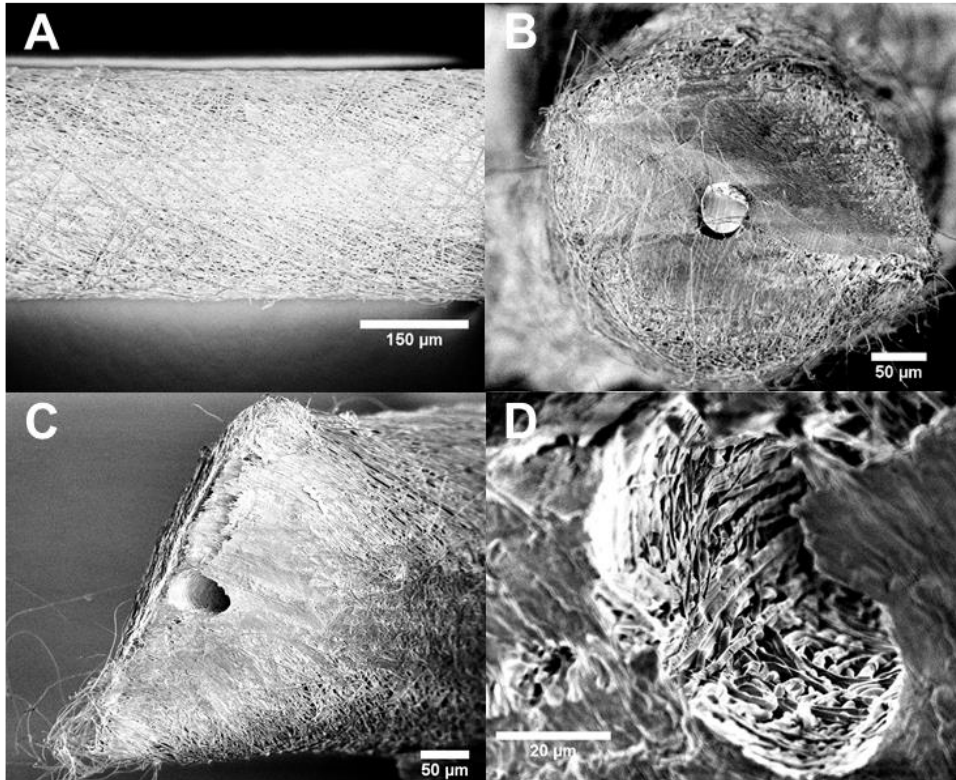


**Figure 5.3. PET shunt characterization.**

(A) Exterior of PET stent composed of nanofibers and revealing minimal porosity. (B) Cross-section of PET shunt with 50  $\mu\text{m}$  diameter template wire and (C) cross-section without template wire. (D) Cross-section of PET shunt following one week of continuous fluid flow demonstrating no signs of degradation or change in diameter.

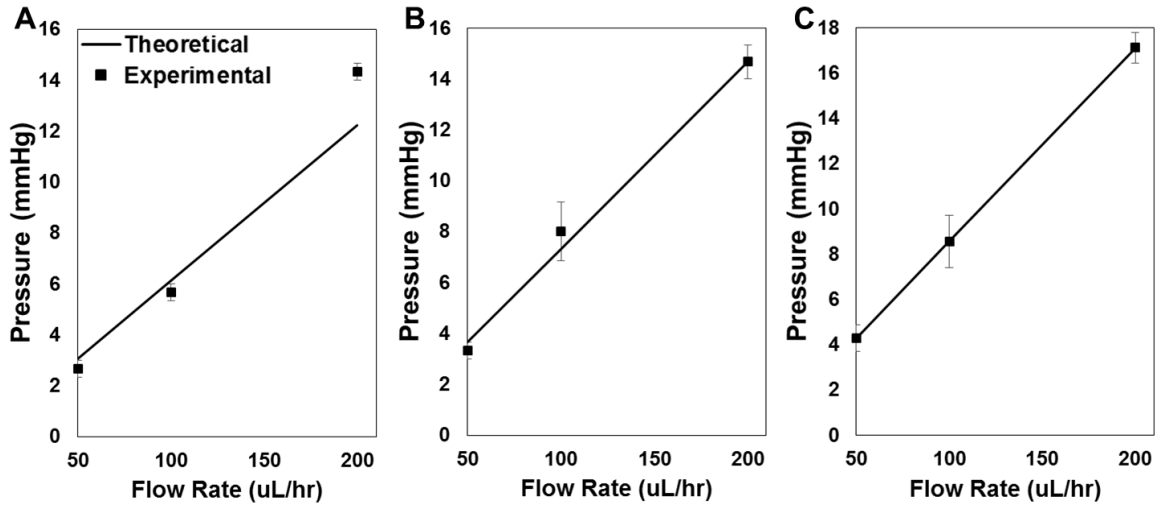


**Figure 5.4. Theoretical and experimental pressure differential with flow of PBS through shunt.**

PET shunts have a 50  $\mu$ m diameter and are (A) 5 mm, (B) 6 mm, or (C) 7mm in length.

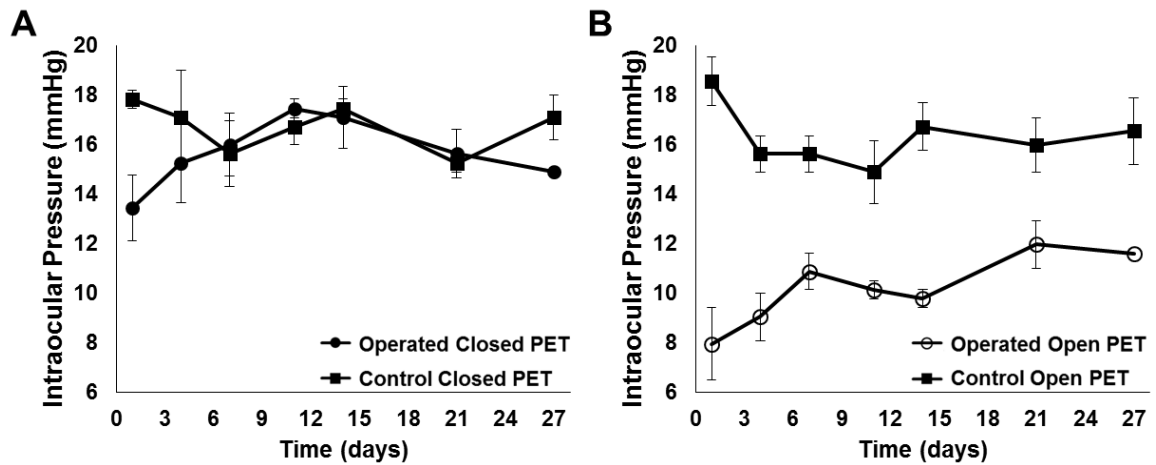


**Figure 5.5. IOP measurements in rabbits following implantation of either closed or open PET shunts.**

IOP was measured in both the operated and the contralateral control eyes of rabbits implanted with either a closed or open PET shunt. (A) Rabbit eyes implanted with a closed PET shunt demonstrated no significant change in IOP in comparison to the contralateral control eye ( $P = 0.08$ ). (B) Rabbit eyes implanted with an open PET shunt demonstrated a significant decrease in IOP in comparison to the contralateral control eye ( $P < 0.0001$ ). Rabbit eyes containing an open PET shunt demonstrated a significant decrease in IOP in comparison to rabbit eyes containing a closed PET shunt ( $P < 0.0001$ ).

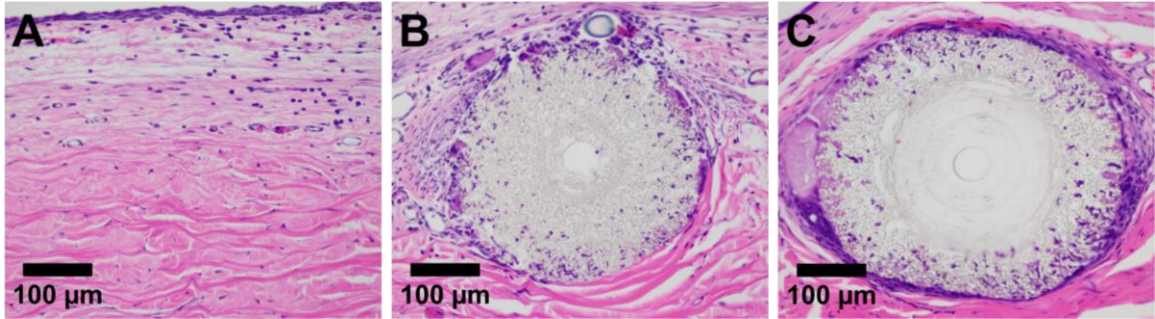


**Figure 5.6. Glaucoma shunt biocompatibility.**

Representative images of (A) untreated subconjunctival rabbit tissue, (B) tissue surrounding an implanted, open PET shunt, and (C) tissue surrounding an implanted, closed PET shunt following hematoxylin and eosin staining. The template wire became dislodged from the closed shunt during sectioning.

## 6. Summary

The biological response to surgical/device intervention is a key leverage point for improvement of clinical outcomes in ocular and vascular surgery, and beyond. Thus, medical devices capable of directly modulating the local biological response without requiring systemic drug administration or a change to the surgical practice carry significant translational potential. We detailed the design, development, and evaluation of medical devices capable of modulating the post-operative biological response through nanotopography and/or drug delivery, while simultaneously serving their originally intended function.

In Chapter 2, we describe the manufacture and evaluation of what is, to our knowledge, the first literature report of an antibiotic-loaded suture prepared by electrospinning at a diameter suitable for ocular surgery. Absorbable, antibiotic-eluting, monofilament sutures composed of PLLA, PEG, and levofloxacin were manufactured via wet electrospinning. Sutures provided sustained antibiotic release for more than 60 days *in vitro*, demonstrated activity against *S. epidermidis* for at least 1 week *in vitro*, and demonstrated similar biocompatibility to standard nylon sutures when implanted into rat corneas. However, the breaking strength of these sutures was below the minimum average breaking strength specified by the U.S.P.

In Chapter 3, we hypothesized that by manufacturing hundreds of highly crystalline, drug-loaded nanofibers and twisting them into a single multifilament suture, we could surpass

suture breaking strength requirements while also providing sufficient antibiotic delivery. To that end, we engineered a novel electrospinning system composed of two grounded collectors (one of which can rotate mechanically) positioned in parallel, allowing for deposition and twisting of nanofibers into a single, high strength, multifilament suture. Antibiotic-loaded, multifilament sutures manufactured using this platform met or exceeded U.S.P. specifications for size and strength suitable for ophthalmic use. To our knowledge, this is the first report of a drug-loaded suture with breaking strength surpassing U.S.P specifications. Further, no strength loss was observed when an equivalent amount of the levofloxacin used in the monofilament suture formulation in Chapter 2 was added to the multifilament suture formulation in Chapter 3. Multifilament sutures demonstrated biocompatibility comparable to conventional nylon sutures, and delivered levofloxacin at detectable levels in rat eyes for at least 14 days. Moreover, levofloxacin-eluting, multifilament sutures prevented ocular infection against consecutive bacterial inoculations for a period of 1 week in a rat model of bacterial keratitis.

In Chapter 4, we utilized the manufacturing platform designed in Chapter 3 to coat conventional nylon sutures with drug-loaded, electrospun nanofibers in order to both surpass suture strength requirements and achieve sustained drug release. We established the uniformity of the nanofiber coating along the length of the suture and demonstrated tuning of rapamycin loading and release from nanofibers without compromising suture breaking strength. In addition, rapamycin-eluting, nanofiber-coated sutures demonstrated successful anastomosis of the rat abdominal aorta, and significantly reduced post-operative neointimal hyperplasia in comparison to a gold standard nylon suture.

In Chapter 5, we extended the use of the manufacturing platform described in Chapter 3 to the manufacture of medical devices other than sutures. We hypothesized that a nano-structured, small lumen glaucoma drainage implant could significantly decrease intraocular pressure while also preventing hypotony. Nanofibrous glaucoma shunts were durable and leak-proof through extended periods of *in vitro* fluid flow, and fluid flow through the shunts behaved according to the Hagen-Poiseuille Equation. Moreover, shunts demonstrated biocompatibility and prevention of hypotony, and significantly decreased intraocular pressure in comparison to the contralateral control eye for at least 27 days when implanted into normotensive rabbits with the proximal end in the anterior chamber and the distal end in the subconjunctival space. This versatile fabrication platform could be used to manufacture next generation glaucoma shunts composed of almost any material and capable of additional functionality, including drug delivery, to improve glaucoma treatment.

Collectively, the results described in this dissertation demonstrate the clinical potential of nano-structured, drug-eluting medical devices in ocular and vascular surgery, and beyond.



## References

1. Anselmo AC, Mitragotri S. An overview of clinical and commercial impact of drug delivery systems. *J Control Release*. Sep 28 2014;190:15-28.
2. Tibbitt MW, Dahlman JE, Langer R. Emerging Frontiers in Drug Delivery. *Journal of the American Chemical Society*. 2016/01/27 2016;138(3):704-717.
3. Park K. Controlled drug delivery systems: past forward and future back. *J Control Release*. Sep 28 2014;190:3-8.
4. Luk A, Junnarkar G. Critical challenges to the design of drug-eluting medical devices. *Therapeutic Delivery*. 2013/04/01 2013;4(4):471-477.
5. Dash AK, Cudworth GC, 2nd. Therapeutic applications of implantable drug delivery systems. *J Pharmacol Toxicol Methods*. Jul 1998;40(1):1-12.
6. Bhardwaj N, Kundu SC. Electrospinning: a fascinating fiber fabrication technique. *Biotechnol Adv*. May-Jun 2010;28(3):325-347.
7. Joseph J, Nair SV, Menon D. Integrating Substrateless Electrospinning with Textile Technology for Creating Biodegradable Three-Dimensional Structures. *Nano Letters*. 2015/08/12 2015;15(8):5420-5426.
8. Kam KR, Walsh LA, Bock SM, Ollerenshaw JD, Ross RF, Desai TA. The effect of nanotopography on modulating protein adsorption and the fibrotic response. *Tissue Eng Part A*. Jan 2014;20(1-2):130-138.
9. Harake RS, Ding Y, Brown JD, Pan T. Design, Fabrication, and In Vitro Testing of an Anti-biofouling Glaucoma Micro-shunt. *Ann Biomed Eng*. Oct 2015;43(10):2394-2405.

10. GlobalData. Surgical Sutures - Global Opportunity Assessment, Competitive Landscape and Market Forecasts to 2018. May 1, 2012 2012:70.
11. Wen Hu, Zheng-Ming Huang, Liu X-Y. Development of braided drug-nanofiber sutures. *Nanotechnology*. 2010;21:1-11.
12. Weldon CB, Tsui JH, Shankarappa SA, et al. Electrospun drug-eluting sutures for local anesthesia. *J. Control. Release*. Aug 10 2012;161(3):903-909.
13. Pasternak B, Rehn M, Andersen L, et al. Doxycycline-coated sutures improve mechanical strength of intestinal anastomoses. *Int J Colorectal Dis*. 2008/03/01 2008;23(3):271-276.
14. Obermeier A, Schneider J, Wehner S, et al. Novel high efficient coatings for anti-microbial surgical sutures using chlorhexidine in fatty acid slow-release carrier systems. *PLoS One*. 2014;9(7):e101426.
15. Morizumi S, Suematsu Y, Gon S, Shimizu T. Inhibition of Neointimal Hyperplasia With a Novel Tacrolimus-Eluting Suture. *Journal of the American College of Cardiology*. 7/19/ 2011;58(4):441-442.
16. Mack BC, Wright KW, Davis ME. A biodegradable filament for controlled drug delivery. *J Control Release*. Nov 3 2009;139(3):205-211.
17. Lee JE, Park S, Park M, et al. Surgical suture assembled with polymeric drug-delivery sheet for sustained, local pain relief. *Acta Biomater*. Sep 2013;9(9):8318-8327.
18. Hu W, Huang ZM, Liu XY. Development of braided drug-loaded nanofiber sutures. *Nanotechnology*. Aug 6 2010;21(31):315104.

19. Hu W, Huang Z-M. Biocompatibility of braided poly(L-lactic acid) nanofiber wires applied as tissue sutures. *Society of Chemical Industry*. 2010;59:92-99.
20. He CL, Huang ZM, Han XJ. Fabrication of drug-loaded electrospun aligned fibrous threads for suture applications. *J Biomed Mater Res A*. Apr 2009;89(1):80-95.
21. Catanzanoa O, Aciernob S, Russo P, et al. Melt-spun bioactive sutures containing nanohybrids for local delivery of anti-inflammatory drugs. *Materials Science and Engineering: C*. 1 October 2014 2014;43:300–309.
22. Choudhury AJ, Gogoi D, Chutia J, et al. Controlled antibiotic-releasing Antheraea assama silk fibroin suture for infection prevention and fast wound healing. *Surgery*. Aug 29 2015.
23. Lee D-H, Kwon T-Y, Kim K-H, et al. Anti-inflammatory drug releasing absorbable surgical sutures using poly(lactic-co-glycolic acid) particle carriers. *Polymer Bulletin*. 2014;71(8):1933-1946.
24. Janiga P, Elayarajah B, Rajendran R, Rammohan R, Venkatrajah B, Asa S. Drug-eluting silk sutures to retard post-operative surgical site infections. *Journal of Industrial Textiles*. October 1, 2012 2012;42(2):176-190.
25. Ming X, Rothenburger S, Nichols MM. In vivo and in vitro antibacterial efficacy of PDS plus (polidioxanone with triclosan) suture. *Surg Infect (Larchmt)*. Aug 2008;9(4):451-457.
26. Bigalke C, Luderer F, Wulf K, et al. VEGF-releasing suture material for enhancement of vascularization: development, in vitro and in vivo study. *Acta Biomater*. Dec 2014;10(12):5081-5089.

27. Ming X, Rothenburger S, Yang D. In vitro antibacterial efficacy of MONOCRYL plus antibacterial suture (Poliglecaprone 25 with triclosan). *Surg Infect (Larchmt)*. Apr 2007;8(2):201-208.
28. Katz S, Izhar M, Mirelman D. Bacterial adherence to surgical sutures. A possible factor in suture induced infection. *Ann Surg*. Jul 1981;194(1):35-41.
29. Heaven CJ, Davison CR, Cockcroft PM. Bacterial contamination of nylon corneal sutures. *Eye (Lond)*. 1995;9 ( Pt 1):116-118.
30. Grinstaff MW. Designing hydrogel adhesives for corneal wound repair. *Biomaterials*. 12// 2007;28(35):5205-5214.
31. Hermann MM, Ustundag C, Diestelhorst M. Compliance With Topical Therapy After Cataract Surgery Using a New Microprocessor–Controlled Eye Drop Monitor. *Investigative Ophthalmology & Visual Science*. 2005;46(13):3832-3832.
32. Winfield AJ, Jessiman D, Williams A, Esakowitz L. A study of the causes of non-compliance by patients prescribed eyedrops. *British Journal of Ophthalmology*. August 1, 1990 1990;74(8):477-480.
33. Burns E, Mulley GP. Practical Problems with Eye-drops Among Elderly Ophthalmology Outpatients. *Age and Ageing*. May 1, 1992 1992;21(3):168-170.
34. Browning MB, Dempsey D, Guiza V, et al. Multilayer vascular grafts based on collagen-mimetic proteins. *Acta biomaterialia*. Mar 2012;8(3):1010-1021.
35. Hosono M, Ueda M, Suehiro S, et al. Neointimal formation at the sites of anastomosis of the internal thoracic artery grafts after coronary artery bypass grafting in human subjects: an immunohistochemical analysis. *The Journal of thoracic and cardiovascular surgery*. Aug 2000;120(2):319-328.

36. Ogus TN, Basaran M, Selimoglu O, et al. Long-term results of the left anterior descending coronary artery reconstruction with left internal thoracic artery. *The Annals of thoracic surgery*. Feb 2007;83(2):496-501.
37. Souza DS, Johansson B, Bojo L, et al. Harvesting the saphenous vein with surrounding tissue for CABG provides long-term graft patency comparable to the left internal thoracic artery: results of a randomized longitudinal trial. *The Journal of thoracic and cardiovascular surgery*. Aug 2006;132(2):373-378.
38. Mack MJ, Osborne JA, Shennib H. Arterial graft patency in coronary artery bypass grafting: what do we really know? *The Annals of thoracic surgery*. Sep 1998;66(3):1055-1059.
39. Roy-Chaudhury P, Kelly BS, Zhang J, et al. Hemodialysis vascular access dysfunction: from pathophysiology to novel therapies. *Blood purification*. 2003;21(1):99-110.
40. Kapadia MR, Popowich DA, Kibbe MR. Modified prosthetic vascular conduits. *Circulation*. Apr 8 2008;117(14):1873-1882.
41. Han J, Lelkes PI. *Drug-eluting vascular grafts*2014.
42. Quigley HA, Broman AT. The number of people with glaucoma worldwide in 2010 and 2020. *Br J Ophthalmol*. Mar 2006;90(3):262-267.
43. Tham YC, Li X, Wong TY, Quigley HA, Aung T, Cheng CY. Global prevalence of glaucoma and projections of glaucoma burden through 2040: a systematic review and meta-analysis. *Ophthalmology*. Nov 2014;121(11):2081-2090.
44. Kass MA, Heuer DK, Higginbotham EJ, et al. The Ocular Hypertension Treatment Study: a randomized trial determines that topical ocular hypotensive

- medication delays or prevents the onset of primary open-angle glaucoma. *Arch Ophthalmol*. Jun 2002;120(6):701-713; discussion 829-730.
45. Heijl A, Leske MC, Bengtsson B, et al. Reduction of intraocular pressure and glaucoma progression: results from the Early Manifest Glaucoma Trial. *Arch Ophthalmol*. Oct 2002;120(10):1268-1279.
  46. Jampel HD, Musch DC, Gillespie BW, et al. Perioperative complications of trabeculectomy in the collaborative initial glaucoma treatment study (CIGTS). *Am J Ophthalmol*. Jul 2005;140(1):16-22.
  47. Solus JF, Jampel HD, Tracey PA, et al. Comparison of limbus-based and fornix-based trabeculectomy: success, bleb-related complications, and bleb morphology. *Ophthalmology*. Apr 2012;119(4):703-711.
  48. Budenz DL, Barton K, Gedde SJ, et al. Five-year treatment outcomes in the Ahmed Baerveldt comparison study. *Ophthalmology*. Feb 2015;122(2):308-316.
  49. Freedman J. TGF-beta(2) antibody in trabeculectomy. *Ophthalmology*. Jan 2009;116(1):166.
  50. Gedde SJ, Herndon LW, Brandt JD, Budenz DL, Feuer WJ, Schiffman JC. Surgical complications in the Tube Versus Trabeculectomy Study during the first year of follow-up. *Am J Ophthalmol*. Jan 2007;143(1):23-31.
  51. Olayanju JA, Hassan MB, Hodge DO, Khanna CL. Trabeculectomy-related complications in Olmsted County, Minnesota, 1985 through 2010. *JAMA Ophthalmol*. May 2015;133(5):574-580.
  52. Neligan PC. Bioactive Sutures. *Plast. Reconstr. Surg*. 2006;118:1645- 1647.

53. Casalini T, Masi M, Perale G. Drug eluting sutures: A model for in vivo estimations. *International Journal of Pharmaceutics*. 6/15/ 2012;429(1–2):148-157.
54. Kronenthal R P, Blaydes JE M. *Sutures Materials in Cataract Surgery*. Vol 11984.
55. Skilbeck CJ. Sutures, ligatures and knots. *Surgery (Oxford)*. 2// 2011;29(2):63-66.
56. Pillai CK, Sharma CP. Review paper: absorbable polymeric surgical sutures: chemistry, production, properties, biodegradability, and performance. *J Biomater Appl*. Nov 2010;25(4):291-366.
57. Pruitt LA, Chakravartula AM. Mechanics of biomaterials: Fundamental principles for implant design. *MRS Bulletin*. 2012/007/001 2012;37(7):698.
58. Fernando Marco, Raquel Vallez, Pablo Gonzalez, Luis Ortega, Jose De La Lama, Lopez-Duran L. Study of the Efficacy of Coated Vicryl Plus® Antibacterial Suture in an Animal Model of Orthopedic Surgery\*. *Surg Infect (Larchmt)*. 2007;8:359- 365.
59. Ming X, Nichols M, Rothenburger S. In vivo antibacterial efficacy of MONOCRYL plus antibacterial suture (Poliglecaprone 25 with triclosan). *Surg Infect (Larchmt)*. Apr 2007;8(2):209-214.
60. Xintian Ming, Stephen Rothenberger, Nichols M. In Vivo and In Vitro Antibacterial Efficacy of PDS\* Plus (Polidioxanone with Triclosan) Suture. *Surg Infect (Larchmt)*. 2008;9:451-458.

61. Brian J. Lee M, Scott D. Smith M, MPH BHJ, MD. Suture-related corneal infections after clear corneal cataract surgery. *J Cataract Refract Surg.* 2009;35:939-942.
62. Leaper D, McBain AJ, Kramer A, et al. Healthcare associated infection: novel strategies and antimicrobial implants to prevent surgical site infection. *Ann R Coll Surg Engl.* Sep 2010;92(6):453-458.
63. Diren Sarisaltik, Teksin ZS. Bioavailability File: Levofloxacin. *J. Pharm. Sci.* 2007;32:197-208.
64. Raizman MB, Rubin JM, Graves AL, Rinehart M. Tear concentrations of levofloxacin following topical administration of a single dose of 0.5% levofloxacin ophthalmic solution in healthy volunteers. *Clinical Therapeutics.* 9// 2002;24(9):1439-1450.
65. Li D, Xia Y. Electrospinning of Nanofibers: Reinventing the Wheel? *Advanced Materials.* 2004;16(14):1151-1170.
66. Ulery BD, Nair LS, Laurencin CT. Biomedical Applications of Biodegradable Polymers. *Journal of polymer science. Part B, Polymer physics.* 2011;49(12):832-864.
67. Zhang S, Liu X, Barreto-Ortiz SF, et al. Creating polymer hydrogel microfibrils with internal alignment via electrical and mechanical stretching. *Biomaterials.* Mar 2014;35(10):3243-3251.
68. Dunn JP, Langer PD, Ophthalmology AAo. *Basic Techniques of Ophthalmic Surgery:* American Academy of Ophthalmology; 2009.



69. Chuan-Long He, Zheng-Ming Huang, Han X-J. Fabrication of drug-loaded electrospun aligned fibrous threads for suture applications. *Journal of Biomedical Materials Research Part A*. 2008:80-95.
70. Ero-Phillips O, Jenkins M, Stamboulis A. Tailoring Crystallinity of Electrospun Plla Fibres by Control of Electrospinning Parameters. *Polymers*. 2012;4(3):1331.
71. Aeschlimann JR, Dresser LD, Kaatz GW, Rybak MJ. Effects of NorA Inhibitors on In Vitro Antibacterial Activities and Postantibiotic Effects of Levofloxacin, Ciprofloxacin, and Norfloxacin in Genetically Related Strains of *Staphylococcus aureus*. *Antimicrobial Agents and Chemotherapy*. February 1, 1999 1999;43(2):335-340.
72. Bremond-Gignac D, Chiambaretta F, Milazzo S. A European perspective on topical ophthalmic antibiotics: current and evolving options. *Ophthalmol Eye Dis*. 2011;3:29-43.
73. Snyder CC. On the history of the suture. *Bull. Hist. Dent*. Oct 1977;25(2):79-84.
74. Spotnitz WD, Falstrom JK, Rodeheaver GT. The Role of Sutures and Fibrin Sealant in Wound Healing. *Surg. Clin. North Am.* . 1997 1997;77(3):651- 669.
75. Kashiwabuchi F, Parikh KS, Omiadze R, et al. Development of Absorbable, Antibiotic-Eluting Sutures for Ophthalmic Surgery. *Translational Vision Science & Technology*. 2017;6(1):1-1.
76. Padmakumar S, Joseph J, Neppalli MH, et al. Electrospun Polymeric Core–sheath Yarns as Drug Eluting Surgical Sutures. *ACS Applied Materials & Interfaces*. 2016/03/23 2016;8(11):6925-6934.

77. Serrano C, Garcia-Fernandez L, Fernandez-Blazquez JP, et al. Nanostructured medical sutures with antibacterial properties. *Biomaterials*. Jun 2015;52:291-300.
78. Chang HI, Lau YC, Yan C, Coombes AG. Controlled release of an antibiotic, gentamicin sulphate, from gravity spun polycaprolactone fibers. *J Biomed Mater Res A*. Jan 2008;84(1):230-237.
79. Valarezo E, Stanzione M, Tammaro L, Cartuche L, Malagon O, Vittoria V. Preparation, characterization and antibacterial activity of poly(epsilon-caprolactone) electrospun fibers loaded with amoxicillin for controlled release in biomedical applications. *J Nanosci Nanotechnol*. Mar 2013;13(3):1717-1726.
80. Champeau M, Thomassin J-M, Tassaing T, Jerome C. Drug Loading of Sutures by Supercritical CO2 Impregnation: Effect of Polymer/Drug Interactions and Thermal Transitions. *Macromolecular Materials and Engineering*. 2015;300(6):596-610.
81. Charles E Edmiston PhD, Gary R Seabrook MD, Michael P Goheen MS, Candace J Krepel MS, MD JBT. Bacterial Adherence to Surgical Sutures: Can antibacterial-Coated Sutures Reduce the Risk of Microbial Contamination? *J Am Col Surg*. 2006;203:481- 489.
82. Christopher T. Hood M, Brian J. Lee M, Bennie H. Jeng M. Incidence, Occurrence Rate, and Characteristics of Suture-Related Corneal Infections After Penetrating Keratoplasty. *Cornea*. 2011;30:624-628.
83. Masini BD, Stinner DJ, Waterman SM, Wenke JC. Bacterial adherence to suture materials. *J Surg Educ*. Mar-Apr 2011;68(2):101-104.

84. Lin IH, Chang Y-S, Tseng S-H, Huang Y-H. A comparative, retrospective, observational study of the clinical and microbiological profiles of post-penetrating keratoplasty keratitis. *Scientific Reports*. 09/02/online 2016;6:32751.
85. Moorthy S, Graue E, Jhanji V, Constantinou M, Vajpayee RB. Microbial Keratitis After Penetrating Keratoplasty: Impact of Sutures. *American Journal of Ophthalmology*. 8// 2011;152(2):189-194.e182.
86. Christo CG, van Rooij J, Geerards AJM, Remeijer L, Beekhuis WH. Suture-related Complications Following Keratoplasty: A 5-Year Retrospective Study. *Cornea*. 2001;20(8):816-819.
87. Hood CT, Lee BJ, Jeng BH. Incidence, Occurrence Rate, and Characteristics of Suture-Related Corneal Infections After Penetrating Keratoplasty. *Cornea*. 2011;30(6):624-628.
88. Prevention CfDca. Antibiotic resistance threats in the United States. 2013.
89. Srikumaran D, Munoz B, Aldave AJ, et al. Long-term Outcomes of Boston Type 1 Keratoprosthesis Implantation: A Retrospective Multicenter Cohort. *Ophthalmology*. 11// 2014;121(11):2159-2164.
90. Kim MJ, Yu F, Aldave AJ. Microbial Keratitis after Boston Type I Keratoprosthesis Implantation: Incidence, Organisms, Risk Factors, and Outcomes. *Ophthalmology*. 11// 2013;120(11):2209-2216.
91. Ahmad S, Mathews PM, Lindsley K, et al. Boston Type 1 Keratoprosthesis versus Repeat Donor Keratoplasty for Corneal Graft Failure: A Systematic Review and Meta-analysis. *Ophthalmology*. 1// 2016;123(1):165-177.

92. Samimi DB, Ediriwickrema LS, Bielory BP, Miller D, Lee W, Johnson TE. Microbiology and Biofilm Trends of Silicone Lacrimal Implants: Comparing Infected Versus Routinely Removed Stents. *Ophthalmic plastic and reconstructive surgery*. Nov/Dec 2016;32(6):452-457.
93. Samimi DB, Bielory BP, Miller D, Johnson TE. Microbiologic trends and biofilm growth on explanted periorbital biomaterials: a 30-year review. *Ophthalmic plastic and reconstructive surgery*. Sep-Oct 2013;29(5):376-381.
94. Nguyen QH, Budenz DL, Parrish Ii RK. Complications of Baerveldt glaucoma drainage implants. *Archives of Ophthalmology*. 1998;116(5):571-575.
95. Al-Torbak AA, Al-Shahwan S, Al-Jadaan I, Al-Hommadi A, Edward DP. Endophthalmitis associated with the Ahmed glaucoma valve implant. *British Journal of Ophthalmology*. April 1, 2005 2005;89(4):454-458.
96. Gedde SJ, Scott IU, Tabandeh H, et al. Late endophthalmitis associated with glaucoma drainage implants. *Ophthalmology*. 7// 2001;108(7):1323-1327.
97. Healy DP, Holland EJ, Nordlund ML, et al. Concentrations of levofloxacin, ofloxacin, and ciprofloxacin in human corneal stromal tissue and aqueous humor after topical administration. *Cornea*. 2004;23(3):255-263.
98. Dash TK, Konkimalla VB. Poly-ε-caprolactone based formulations for drug delivery and tissue engineering: A review. *Journal of Controlled Release*. 2/28/ 2012;158(1):15-33.
99. Woodruff MA, Hutmacher DW. The return of a forgotten polymer— Polycaprolactone in the 21st century. *Progress in Polymer Science*. 10// 2010;35(10):1217-1256.

100. Dash TK, Konkimalla VB. Polymeric Modification and Its Implication in Drug Delivery: Poly- $\epsilon$ -caprolactone (PCL) as a Model Polymer. *Molecular Pharmaceutics*. 2012/09/04 2012;9(9):2365-2379.
101. Lee BJ, Smith SD, Jeng BH. Suture-related corneal infections after clear corneal cataract surgery. *J Cataract Refract Surg*. May 2009;35(5):939-942.
102. Wagoner MD, Welder JD, Goins KM, Greiner MA. Microbial Keratitis and Endophthalmitis After the Boston Type 1 Keratoprosthesis. *Cornea*. Apr 2016;35(4):486-493.
103. Wong S-C, Baji A, Leng S. Effect of fiber diameter on tensile properties of electrospun poly( $\epsilon$ -caprolactone). *Polymer*. 10/6/ 2008;49(21):4713-4722.
104. Zhang S, Liu X, Barreto-Ortiz SF, et al. Creating Polymer Hydrogel Microfibres with Internal Alignment via Electrical and Mechanical Stretching. *Biomaterials*. 01/15 2014;35(10):3243-3251.
105. Chen WL, Wu CY, Hu FR, Wang IJ. Therapeutic penetrating keratoplasty for microbial keratitis in Taiwan from 1987 to 2001. *Am J Ophthalmol*. Apr 2004;137(4):736-743.
106. Callegan MC, Engelbert M, Parke DW, 2nd, Jett BD, Gilmore MS. Bacterial endophthalmitis: epidemiology, therapeutics, and bacterium-host interactions. *Clinical microbiology reviews*. Jan 2002;15(1):111-124.
107. Fay A, Nallasamy N, Bernardini F, et al. Multinational comparison of prophylactic antibiotic use for eyelid surgery. *JAMA Ophthalmology*. 2015;133(7):778-784.

108. Kellar CA. Solid organ transplantation overview and delection criteria. *The American journal of managed care*. Jan 2015;21(1 Suppl):S4-11.
109. Goodney PP, Beck AW, Nagle J, Welch HG, Zwolak RM. National trends in lower extremity bypass surgery, endovascular interventions, and major amputations. *Journal of Vascular Surgery*. 7// 2009;50(1):54-60.
110. Abu-Omar Y, Taggart DP. Coronary artery bypass surgery. *Medicine*. 9// 2014;42(9):527-531.
111. Lok CE, Foley R. Vascular Access Morbidity and Mortality: Trends of the Last Decade. *Clinical Journal of the American Society of Nephrology*. July 3, 2013 2013;8(7):1213-1219.
112. Browning MB, Dempsey D, Guiza V, et al. Multilayer vascular grafts based on collagen-mimetic proteins. *Acta Biomaterialia*. 3// 2012;8(3):1010-1021.
113. Zeebregts CJ. Non-penetrating Clips for Vascular Anastomosis. *European Journal of Vascular and Endovascular Surgery*. 2005;30(3):288-290.
114. Marx SO, Totary-Jain H, Marks AR. Vascular smooth muscle cell proliferation in restenosis. *Circulation. Cardiovascular interventions*. Feb 01 2011;4(1):104-111.
115. Han J, Lelkes PI. Drug-Eluting Vascular Grafts. In: Domb AJ, Khan W, eds. *Focal Controlled Drug Delivery*. Boston, MA: Springer US; 2014:405-427.
116. Towbin AJ, Towbin RB, Di Lorenzo C, Grifka RG. Interventional Radiology in the Treatment of the Complications of Organ Transplant in the Pediatric Population—Part 1: The Kidneys, Heart, Lungs, and Intestines. *Seminars in Interventional Radiology*. 2004;21(4):309-320.

- 117.** Pantelias K, Grapsa E. Vascular access today. *World Journal of Nephrology*.  
06/06  
11/20/received  
05/23/revised  
06/01/accepted 2012;1(3):69-78.
- 118.** Li L, Terry CM, Shiu Y-TE, Cheung AK. Neointimal hyperplasia associated with synthetic hemodialysis grafts. *Kidney international*. 07/30 2008;74(10):1247-1261.
- 119.** Schachner T, Zou Y, Oberhuber A, et al. Local application of rapamycin inhibits neointimal hyperplasia in experimental vein grafts. *The Annals of Thoracic Surgery*. 5// 2004;77(5):1580-1585.
- 120.** Paulson WD, Kipshidze N, Kipiani K, et al. Safety and efficacy of local periadventitial delivery of sirolimus for improving hemodialysis graft patency: first human experience with a sirolimus-eluting collagen membrane (Coll-R). *Nephrology Dialysis Transplantation*. 2012;27(3):1219-1224.
- 121.** Manson RJ, Ebner A, Gallo S, et al. Arteriovenous Fistula Creation Using the Optiflow Vascular Anastomosis Device: A First in Man Pilot Study. *Seminars in Dialysis*. 2013;26(1):97-99.
- 122.** Kawatsu S, Oda K, Saiki Y, Tabata Y, Tabayashi K. External application of rapamycin-eluting film at anastomotic sites inhibits neointimal hyperplasia in a canine model. *Ann Thorac Surg*. Aug 2007;84(2):560-567; discussion 567.
- 123.** Chang EI, Galvez MG, Glotzbach JP, et al. Vascular anastomosis using controlled phase transitions in poloxamer gels. *Nat Med*. 2011;17(9):1147-1152.

124. Mutsuga M, Narita Y, Yamawaki A, et al. Development of novel drug-eluting biodegradable nano-fiber for prevention of postoperative pulmonary venous obstruction. *Interactive CardioVascular and Thoracic Surgery*. April 1, 2009 2009;8(4):402-407.
125. Takenaka H, Esato K, Ohara M, Zempo N. Sutureless anastomosis of blood vessels using cyanoacrylate adhesives. *Surg Today*. 1992;22(1):46-54.
126. Chang DW, Chan A, Forse RA, Abbott WM. Enabling sutureless vascular bypass grafting with the exovascular sleeve anastomosis. *J Vasc Surg*. Sep 2000;32(3):524-530.
127. Colombo A, Orlic D, Stankovic G, et al. Preliminary observations regarding angiographic pattern of restenosis after rapamycin-eluting stent implantation. *Circulation*. 2003;107(17):2178-2180.
128. Toutouzas K, Di Mario C, Falotico R, et al. Sirolimus-eluting stents: a review of experimental and clinical findings. *Z Kardiol*. 2002;91 Suppl 3:49-57.
129. Suzuki T, Kopia G, Hayashi S, et al. Stent-based delivery of sirolimus reduces neointimal formation in a porcine coronary model. *Circulation*. Sep 4 2001;104(10):1188-1193.
130. Rodriguez AE, Granada JF, Rodriguez-Alemparte M, et al. Oral rapamycin after coronary bare-metal stent implantation to prevent restenosis: the Prospective, Randomized Oral Rapamycin in Argentina (ORAR II) Study. *J Am Coll Cardiol*. Apr 18 2006;47(8):1522-1529.



131. Stojkovic S, Ostojic M, Nedeljkovic M, et al. Systemic rapamycin without loading dose for restenosis prevention after coronary bare metal stent implantation. *Catheter Cardiovasc Interv.* Feb 15 2010;75(3):317-325.
132. Gershlick AH. Is there any place for oral anti-restenotic treatment in the era of drug eluting stents? *Heart.* 2005;91(11):1377-1379.
133. *The United States Pharmacopeial Convention. USP 29-NF 24.*  
. Rockville, MD: The United States Pharmacopeial Convention, January 1, 2006:2052.
134. Fingar DC, Richardson CJ, Tee AR, Cheatham L, Tsou C, Blenis J. mTOR controls cell cycle progression through its cell growth effectors S6K1 and 4E-BP1/eukaryotic translation initiation factor 4E. *Molecular and cellular biology.* Jan 2004;24(1):200-216.
135. Okeke CO, Quigley HA, Jampel HD, et al. Adherence with topical glaucoma medication monitored electronically the Travatan Dosing Aid study. *Ophthalmology.* Feb 2009;116(2):191-199.
136. Ramulu PY, Corcoran KJ, Corcoran SL, Robin AL. Utilization of various glaucoma surgeries and procedures in Medicare beneficiaries from 1995 to 2004. *Ophthalmology.* Dec 2007;114(12):2265-2270.
137. Arora KS, Robin AL, Corcoran KJ, Corcoran SL, Ramulu PY. Use of Various Glaucoma Surgeries and Procedures in Medicare Beneficiaries from 1994 to 2012. *Ophthalmology.* Aug 2015;122(8):1615-1624.
138. Saeedi OJ, Jefferys JL, Solus JF, Jampel HD, Quigley HA. Risk factors for adverse consequences of low intraocular pressure after trabeculectomy. *J Glaucoma.* Jan 2014;23(1):e60-68.

139. Patel S, Pasquale LR. Glaucoma drainage devices: a review of the past, present, and future. *Semin Ophthalmol*. Sep-Nov 2010;25(5-6):265-270.
140. Breckenridge RR, Bartholomew LR, Crosson CE, Kent AR. Outflow resistance of the Baerveldt glaucoma drainage implant and modifications for early postoperative intraocular pressure control. *J Glaucoma*. Oct 2004;13(5):396-399.
141. Gilbert DD, Bond B. Intraluminal pressure response in Baerveldt tube shunts: a comparison of modification techniques. *J Glaucoma*. Jan 2007;16(1):62-67.
142. Jones E, Alaghband P, Cheng J, Beltran-Agullo L, Sheng Lim K. Preimplantation Flow Testing of Ahmed Glaucoma Valve and the Early Postoperative Clinical Outcome. *J Curr Glaucoma Pract*. Jan-Apr 2013;7(1):1-5.
143. Sheybani A, Reitsamer H, Ahmed, II. Fluid Dynamics of a Novel Micro-Fistula Implant for the Surgical Treatment of Glaucoma. *Invest Ophthalmol Vis Sci*. Jul 2015;56(8):4789-4795.
144. Sheybani A, Lenzhofer M, Hohensinn M, Reitsamer H, Ahmed, II. Phacoemulsification combined with a new ab interno gel stent to treat open-angle glaucoma: Pilot study. *J Cataract Refract Surg*. Sep 2015;41(9):1905-1909.
145. Sheybani A. Ab Interno Gelatin Stent With Mitomycin-C Combined With Cataract Surgery for Treatment of Open-Angle Glaucoma: 1-Year Results. *American Society of Cataract & Refractive Surgery*. San Diego, CA2015.
146. Battle JF, Fantes F, Riss I, et al. Three-Year Follow-up of a Novel Aqueous Humor MicroShunt. *J Glaucoma*. Feb 2016;25(2):e58-65.

147. Pinchuk L, Riss I, Battle JF, et al. The development of a micro-shunt made from poly(styrene-block-isobutylene-block-styrene) to treat glaucoma. *J Biomed Mater Res B Appl Biomater*. Sep 18 2015.
148. Ayyala RS, Michelini-Norris B, Flores A, Haller E, Margo CE. Comparison of different biomaterials for glaucoma drainage devices: part 2. *Arch Ophthalmol*. Aug 2000;118(8):1081-1084.
149. Sheybani A, Dick B, Ahmed, II. Early Clinical Results of a Novel Ab Interno Gel Stent for the Surgical Treatment of Open-angle Glaucoma. *J Glaucoma*. Nov 10 2015.
150. Agarwal S, Wendorff JH, Greiner A. Use of electrospinning technique for biomedical applications. *Polymer*. 12/8/ 2008;49(26):5603-5621.
151. Lavoisier A, Schlaeppi JM. Early developability screen of therapeutic antibody candidates using Taylor dispersion analysis and UV area imaging detection. *MAbs*. 2015;7(1):77-83.
152. Fu J, Sun F, Liu W, et al. Subconjunctival Delivery of Dorzolamide-Loaded Poly(ether-anhydride) Microparticles Produces Sustained Lowering of Intraocular Pressure in Rabbits. *Molecular Pharmaceutics*. 2016/09/06 2016;13(9):2987-2995.
153. Saheb H, Ahmed, II. Micro-invasive glaucoma surgery: current perspectives and future directions. *Curr Opin Ophthalmol*. Mar 2012;23(2):96-104.
154. Ayyala RS, Duarte JL, Sahiner N. Glaucoma drainage devices: state of the art. *Expert Rev Med Devices*. Jul 2006;3(4):509-521.

155. Pham QP, Sharma U, Mikos AG. Electrospun Poly( $\epsilon$ -caprolactone) Microfiber and Multilayer Nanofiber/Microfiber Scaffolds: Characterization of Scaffolds and Measurement of Cellular Infiltration. *Biomacromolecules*. 2006/10/01 2006;7(10):2796-2805.
156. Yao J, Bastiaansen C, Peijs T. High Strength and High Modulus Electrospun Nanofibers. *Fibers*. 2014;2(2):158.
157. Giovingo M. Complications of glaucoma drainage device surgery: a review. *Semin Ophthalmol*. Sep-Nov 2014;29(5-6):397-402.
158. Khan W, Muntimadugu E, Jaffe M, Domb AJ. Implantable Medical Devices. In: Domb JA, Khan W, eds. *Focal Controlled Drug Delivery*. Boston, MA: Springer US; 2014:33-59.
159. Richter GM, Coleman AL. Minimally invasive glaucoma surgery: current status and future prospects. *Clin Ophthalmol*. 2016;10:189-206.
160. Sharp KV, Adrian RJ. Transition from laminar to turbulent flow in liquid filled microtubes. *Experiments in Fluids*. 2004;36(5):741-747.
161. Echavez M, Agulto M, Imelda Veloso M. Intravitreal Bevacizumab as Adjunctive Therapy for Bleb Survival in Trabeculectomy in Rabbit Eyes. *Philipp J Ophthalmol*. 6/ 2012;37(1):45-51.
162. Acosta AC, Espana EM, Yamamoto H, et al. A newly designed glaucoma drainage implant made of poly(styrene-b-isobutylene-b-styrene): Biocompatibility and function in normal rabbit eyes. *Archives of Ophthalmology*. 2006;124(12):1742-1749.

- 163.** Battle JF, Fantes F, Riss I, et al. Three-Year Follow-up of a Novel Aqueous Humor MicroShunt. *Journal of Glaucoma*. 2016;25(2):e58-e65.

## Curriculum Vitae

### PERSONAL INFORMATION

Date of Birth July 19, 1990  
Location of Birth Columbus, Ohio

### EDUCATION

2017 Ph.D., Biomedical Engineering, The Johns Hopkins University (JHU)  
2012 B.S., Chemical and Biomolecular Engineering; minors: political science, entrepreneurship, The Ohio State University (OSU), *magna cum laude* with honors and research distinction

### EXPERIENCE

#### *Academic Positions*

2012 – 2017 PhD Candidate (Advisors: Dr. Justin Hanes and Dr. Youseph Yazdi)  
Dept. of Biomedical Engineering, JHU  
2014 Instructor, Dept. of Biomedical Engineering, JHU  
2010 – 2012 Undergraduate Research Scholar (Advisor: Dr. Jessica Winter)  
Dept. of Chemical and Biomolecular Engineering, OSU  
2008 – 2010 Undergraduate Research Assistant (Advisor: Dr. Jessica Winter)  
Dept. of Chemical and Biomolecular Engineering, OSU

#### *Industry Positions*

2015 – Present Co-Founder, President, Access HEARS (affordable, accessible delivery of amplification devices to older adults with hearing loss)  
2012 – Present Executive Director (2012-2014), Advisor (2014-Present), Social Innovation Lab at Johns Hopkins University (social enterprise incubator)  
2012 – Present Co-Founder, CEO (2012), Director (2012-2014), Core Quantum Technologies, Inc. (“MultiDot” platform for cancer detection)  
2011 – 2012 College Ambassador, Help Remedies, Inc. (consumer health & pharmaceutical company; acquired by Remedies, LLC in 2013)  
2010 – 2012 Co-Founder, President, Dollars 4 Change (fundraising for impactful community organizations)

#### *Other Professional Positions*

2016 – Present National Fellowships Selection Committee, JHU  
2014 – Present Judge, JHU Business Plan Competition  
2013 – Present Advisor, Technology Commercialization and Research Center, Nanjing University, China  
2014 – 2016 Community Advisory Board, JHU Center for AIDS Research  
2013 – 2014 Internal Advisory Board, BME EDGE (Extramural Development in Graduate Education), JHU  
2013 – 2014 Co-President, Biomedical Engineering PhD Council, JHU  
2011 – 2012 Founder, President, Students for a Healthy Campus (successfully advocated for OSU to become tobacco-free)  
2010 – 2012 Co-Chair, Undergraduate Research Office Student Advisory Committee, OSU

## SELECTED HONORS AND AWARDS

2016	The Center for Nanomedicine Award for Research Excellence, Center for Nanomedicine at the Wilmer Eye Institute, JHU
2016	Hive Global Leader, Hive Global Leaders Program
2015	One of fifty Leaders of Tomorrow for the Mid-Atlantic bioeconomy
2014	One of three US delegates invited to advise the Italian government on using social enterprise to advance the economy and public welfare
2014 – 2017	Roche Scholar of the ARCS Foundation, ARCS Foundation Metro Washington
2013 – 2016	Graduate Research Fellowship, National Science Foundation
2013	Thomas J. Kelly and Mary L. Kelly Young Scholar Award, JHU
2012	Outstanding Undergraduate Student Award, American Institute of Chemists
2012	Outstanding Senior Award (conferred to less than 0.3% of graduating seniors), OSU
2012	Finalist, Student Innovator of the Year, OSU
2012	1 <sup>st</sup> Place, Ohio State University Business Plan Competition, OSU
2011, 2012	Spirit of Ohio State Award (only recipient to receive the award twice), OSU
2010	Honors & Scholars Summer Research Fellowship, OSU
2010	Donald F. Othmer Academic Excellence Award, American Institute of Chemical Engineers
2009	2nd Place, Nanotechnology Design Competition, OSU
2008	Morrill Excellence Scholar, OSU
2008	National Merit Scholar
2008	Valedictorian, Reynoldsburg High School

## PATENTS

1. **Parikh, K.**, Patel, H., Hanes, J. Process and apparatus for making twisted electrospun fibers and devices (*PCT patent pending*).
2. **Parikh, K.**, Ensign, L., Hanes, J. Ultra-thin, high strength, drug-loaded sutures and coatings thereof (*PCT patent pending*).
3. **Parikh, K.**, Pitha, I., Hanes, J. Partially degradable stents for controlled reduction of intraocular pressure (*PCT patent pending*).

## PUBLICATIONS

<sup>†</sup>*Co-first author*

### **Peer reviewed**

1. Kashiwabuchi, F.<sup>†</sup>, **Parikh, K.S.**<sup>†</sup>, Omiadze, R., Zhang, S., Luo, L., Patel, H., Xu, Q., Ensign, L.M., Mao, H.Q., Hanes, J., McDonnell, P.J. (2017) Development of absorbable, antibiotic-eluting sutures for ophthalmic surgery, *Translational Vision & Science Technology*, 2017; 6(1):1-8. *Cover article*.
2. Han, N., Bradley, P., Johnson, J., **Parikh, K.S.**, Hissong, A., Calhoun, M.A., Lannutti, J.J., Winter, J.O. (2013) Effects of hydrophobicity and mat thickness on release from hydrogel-electrospun fiber mat composites, *Journal of Biomaterials Science, Polymer Edition*, 24(17): 2018-2030.

3. **Parikh, K.S.**, Rao, S.S., Ansari, H.M., Zimmerman, L.B., Lee, L.J., Akbar, S.A., Winter, J.O. (2012) Ceramic nanopatterned surfaces to explore the effects of nanotopography on cell attachment, *Materials Science and Engineering: C*, 32(8): 2469-2475.
4. Han, N., Johnson, J., Bradley, P., **Parikh, K.S.**, Lannutti, J.J., Winter, J.O. (2012) Cell attachment to hydrogel-electrospun fiber mat composite materials, *Journal of Functional Biomaterials*, 3(3): 497-513.
5. Han, N., Rao, S.S., Johnson, J., **Parikh, K.S.**, Bradley, P., Lannutti, J.J., Winter, J.O. (2011) Hydrogel-electrospun fiber mat composite coatings for neural prostheses, *Frontiers in Neuroengineering*, 4(2). doi:10.3389/fneng.2011.00002.
6. Winter, J.O., Han, N., Owens, M., Larison, J., Wheasler, J., **Parikh, K.S.**, Siers, L. (2008) Polymer hydrogel thin film coatings for acute drug delivery from neural prostheses, *PMSE Preprints*, 99: 801-802.

### ***In preparation***

7. **Parikh, K.S.**, Josyula, A., Ahn, J.Y., Omiadze, R., Ensign, L.M., Kiely, A.K., Hanes, J., Pitha, I. (2017) Reduction of intraocular pressure in rabbits via a nano-structured glaucoma drainage implant, *in preparation*.
8. **Parikh, K.S.**, Omiadze, R., Josyula, A., Shi, R., Anders, N.M., He, P., Al-Towerki, A.E., Yazdi, Y., McDonnell, P.J., Ensign, L.M., Hanes, J. (2017) Ultra-thin, high strength, antibiotic-eluting sutures for prevention of ophthalmic Infection, *in preparation*.
9. Yang, J. †, **Parikh, K.S.** †, Duncan, G.A., Ensign, L.M., Hanes, J., Xu, Q. (2017) Inhibition of corneal neovascularization through sustained release of sunitinib from absorbable thin films, *in preparation*.
10. **Parikh, K.S.**, Zhang, H., Fukunishi, T., Josyula, A., Omiadze, R., Hanes, J., Ensign, L.M., Hibino, N. (2017) Rapamycin-eluting, nanofiber-coated sutures for inhibition of neointimal hyperplasia following vascular anastomosis procedures, *in preparation*.
11. Omiadze, R. †, Date, A. †, **Parikh, K.S.**, Josyula, A., Kanvinde, P., Ensign, L.M., Hanes, J. (2017) Moxifloxacin nanosuspensions developed through hydrophobic ion-pairing provide more efficient treatment of ocular infection, *in preparation*.

### **CONFERENCE ABSTRACTS AND PROCEEDINGS**

\* *indicates podium presentation*

1. **Parikh, K.S.**, Josyula, A., Ahn, J.Y., Omiadze, R., Ensign, L.M., Kiely, A.K., Hanes, J., Pitha, I. (2017) Development and characterization of a nano-structured glaucoma shunt. Association for Research in Vision and Ophthalmology: Baltimore, MD.
2. **Parikh, K.S.**, Omiadze, R., Josyula, A., Shi, R., Al-Towerki, A.E., Yazdi, Y., McDonnell, P.J., Ensign, L.M., Hanes, J. (2016) A new method to produce nano-structured, high strength, drug-eluting sutures. Biomedical Engineering Society: Minneapolis, MN.
3. **Parikh, K.S.**, Omiadze, R., Josyula, A., Shi, R., Al-Towerki, A.E., Yazdi, Y., McDonnell, P.J., Ensign, L.M., Hanes, J. (2016) Nano-structured, antibiotic-eluting sutures for prevention of ophthalmic infection. NanoDDS: Baltimore, MD.
4. **Parikh, K.S.\***, Omiadze, R., Josyula, A., Shi, R. Yazdi, Y., McDonnell, P.J., Ensign, L.M., Hanes, J. (2016) Absorbable, high strength, antibiotic-eluting sutures for



prevention of ophthalmic infection. Wilmer Research Meeting: Baltimore, MD. 1<sup>st</sup> place, oral presentation.

5. **Parikh, K.S.\***, Yazdi, Y., Rice, E.M. (2015) Innovating within universities: a guide to navigating the university environment to build impactful programming, initiatives, and organizations. Venturewell Open: Washington, D.C.
6. **Parikh, K.S.\***, Herscovitch, P., Wollensak, A., Purcell, V., Davis, L. (2014) Why size doesn't matter: enabling entrepreneurship, innovation and invention in small private design and liberal arts colleges. Venturewell Open: San Jose, CA
7. **Parikh, K.S.** and Winter, J.O. (2012) A novel approach to the design of cellular nanoenvironments. Denman Research Forum: Columbus, OH. 3<sup>rd</sup> place, poster presentation.
8. Han, N., Johnson, J., **Parikh, K.S.**, Bradley, P., Hissong, A., Lannutti, J., Winter, J.O. (2010) Electrospun fiber-hydrogel controlled release composites. Biomedical Engineering Society: Austin, TX.
9. **Parikh, K.S.\***, Rao, S., Zimmerman, L.B., Ansari, H., Lee, L.J., Akbar, A., Winter, J.O. (2010) Innovative, Inexpensive Surfaces to Investigate the Effect of Nanotopography on Cells. Central Regional Meeting of American Chemical Society: Dayton, OH.
10. **Parikh, K.S.** and Winter, J.O. (2010) Nanopatterned surfaces for wound healing. Institute of Materials Research Forum: Columbus, OH.
11. **Parikh, K.S.\***, Rao, S.S., Zimmerman, L.B., Winter, J.O. (2009) A Novel, Low Cost Method for Investigating the Effect of Nanotopography on Biomaterials. American Institute of Chemical Engineers: Nashville, TN.

## TEACHING EXPERIENCE

2016	Graduate Teaching Assistant, <i>Molecules and Cells</i> (EN.580.221.01, Biomedical Engineering), JHU
2014	Course Creator and Instructor, <i>Biotechnology Entrepreneurship</i> (EN.580.122.13, Biomedical Engineering), JHU Enrollment: 30; Rating (out of 5.0): Course: 4.67; Instructor: 4.72
2014	Guest Lecture, <i>Seminar on Public Health and Well-being in Baltimore</i> (AS.280.320, Sociology), JHU
2014	Guest Lecture, <i>Introduction to Biomedical Engineering</i> (Biomedical Engineering), Nanjing University, China
2013	Guest Lecture, <i>Nanoparticles for Drug Delivery and Application in Medicine</i> (EN.580.106.41, Biomedical Engineering), JHU
2013	Guest Lecture, <i>B'more Innovative: Studying Change through Charm City</i> (AS.230.116.31, Sociology), JHU

## CONTACT INFORMATION

### ***Current***

#### Address:

19 S. Exeter St.  
Baltimore, MD 21202  
Email: ksp@jhu.edu

### ***Permanent***

#### Address:

7973 Slate Park Avenue  
Reynoldsburg, OH  
Email: kunal.parikh.71@gmail.com